12-2011

Time-Interval Analysis for Radiation Monitoring

Peng Luo
Clemson University, pengl@clemson.edu

TIME-INTERVAL ANALYSIS FOR RADIATION MONITORING

A Dissertation
Presented to
the Graduate School of
Clemson University

In Partial Fulfillment
of the Requirements for the Degree
Doctor of Philosophy
Environmental Engineering and Earth Sciences

---

by
Peng Luo
December 2011

Accepted by:
Dr. Timothy A. DeVol, Committee Chair
Dr. Robert A. Fjeld
Dr. Brian A. Powell
Dr. Julia L. Sharp

ABSTRACT

On-line radiation monitoring is essential to the U.S. Department of Energy (DOE) Environmental Management Science Program for assessing the impact of contaminated media at DOE sites. The goal of on-line radiation monitoring is to quickly detect small or abrupt changes in activity levels in the presence of a significant ambient background. The focus of this research is on developing effective statistical algorithms to meet the goal of on-line monitoring based on time-interval (time-difference between two consecutive radiation pulses) data. Compared to the more commonly used count data which are registered in a fixed count time, time-interval data possess the potential to reduce the sampling time required to obtain statistically sufficient information to detect changes in radiation levels. This dissertation has been formulated into three sections based on three statistical methods: sequential probability ratio test (SPRT), Bayesian statistics, and cumulative sum (CUSUM) control chart. In each section, time-interval analysis based on one of the three statistical methods was investigated and compared to conventional analyses based on count data in terms of average run length (ARL or average time to detect a change in radiation levels) and detection probability with both experimental and simulated data. The experimental data were acquired with a DGF-4C (XIA, Inc) system in list mode. Simulated data were obtained by using Monte Carlo techniques to obtain a random sampling of a Poisson process. Statistical algorithms were developed using the statistical software package R and the programming function built in the data analysis environment IGOR Pro. 4.03.

Overall, the results showed that the statistical analyses based on time-interval data provided similar or higher detection probabilities relative to other statistical analyses based on count data, but were able to make a quicker detection with fewer pulses at relatively higher radiation levels. To increase the detection probability and further reduce the time needed to detect a change in radiation levels for time-interval analyses, modifications or adjustments were proposed for each of the three chosen statistical methods. Parameter adjustment to the preset background level in the SPRT test could reduce the average time to detect a source by 50%. Enhanced reset modification and moving prior modification proposed for the Bayesian analysis of time-intervals resulted in a higher detection probability than the Bayesian analysis without modifications, and were independent of the amount of background data registered before a radioactive source was present. The robust CUSUM control chart coupled with a modified runs rule showed the ability to further reduce the ARL to respond to changes in radiation levels, and keep the false positive rate at a required level, e.g., about 40% shorter than the standard time-interval CUSUM control chart at 10.0cps relative to a background count rate of 2.0cps.

The developed statistical algorithms for time-interval data analyses demonstrate the feasibility and versatility for on-line radiation monitoring. The special properties of time-interval information provide an alternative for low-level radiation monitoring. These findings establish an important base for future on-line monitoring applications when time-interval data are registered.

DEDICATION

This dissertation is dedicated to my wife, Xing Gao, and our son, Gaoxu (David) Luo. It is also dedicated to my parents, Hongchang Luo and Deling Xue. Their extraordinary love, encouragement and support have made this dream a reality.

ACKNOWLEDGEMENTS

I would like to express my gratitude to all people who have contributed a lot to this work. Without their help, this work could not have been completed.

First, I would like to thank my advisor Dr. Timothy A. DeVol, who offered me the great opportunity to pursue my Ph.D. degree in his research group. The support, guidance and encouragement from Dr. DeVol are absolutely necessary for me to successfully perform this research. With his generous financial support, I got many chances to present my work at national and international conferences. Invaluable comments and suggestions received at the conferences are very helpful to perfect my research plan and make a great progress.

I would like express my special gratitude to Dr. Julia L. Sharp for serving on my advisory committee. With her sincere instructions, I have learned a lot in complex statistical methods and successfully applied them to my research. She was fully involved in my research projects and put a lot time and efforts on helping me to prepare my technical presentations, revise papers for publications. I am also indebted to Dr. Robert A. Fjeld and Dr. Brian A. Powell who served on my advisory committee for reviewing my work, bringing many thoughts to the work, and broadening my knowledge in nuclear field.

Special thanks go to Dr. Hui Tan, a former Ph.D. student in Dr. DeVol's group, for his detailed instructions on DGF-4C manipulation and help on modifying the DGF-4C firmware to meet my needs for this study. I also would like to thank my lab mates and

friends, Kelly, Amy, Kirk, Aurelie, and Thompson, and all my fellow students, who added something special to my stay in Clemson.

In addition, I would like to thank Jan, Mary, Patsy, Betty and Anne who are working for the EE&ES department. Their sincere helps have contributed significantly to this work and to my education.

Finally, I would like to thank my family for their understanding and support. Special thanks go to my wife Xing Gao, whose love and support are essential for me to get through the long road to finish this work; and to my parents, Hongchang Luo and Deling Xue, who gave me unselfish love and understanding to pursue my dream.

The following research works were conducted in part with funding from the U.S. Department of Energy, under the Environmental Management Science Program # DE-FG02-07ER64411 grant.

TABLE OF CONTENTS

Table of Contents (Continued)

Page

Table of Contents (Continued)

Page

Table of Contents (Continued)

Page

LIST OF TABLES

LIST OF FIGURES

List of Figures (Continued)

Figure Page

List of Figures (Continued)

Figure Page

List of Figures (Continued)

Figure Page

LIST OF SYMBOLS AND ABBREVIATIONS

Symbols

r	count rate (cps)
s	seconds
t	time (s)
α	false positive rate
β	false negative rate
h	CUSUM decision interval value
h_{cnt}	CUSUM decision interval value for count data
h_{ti}	CUSUM decision interval value for time-interval data
k_{α}	critical value corresponding to the probability of α
k_{β}	critical value corresponding to the probability of β
k	CUSUM reference value
k_{cnt}	CUSUM reference value for count data
k_{ti}	CUSUM reference value for time-interval data
r_0	background level
r_1	alarm level
r_a	acceptable mean count rate
r_d	out-of-control mean count rate
A	SPRT upper threshold
B	SPRT lower threshold
H_0	Null hypothesis

List of Symbols and Abbreviations (Continued)

H_1	Alternative hypothesis
L_c	detection limit
L_D	*a priori* limit of detection
N_{max}	maximum observations for SPRT

Abbreviations

ARL	Average run length
cps	count per second
CUSUM	Cumulative Sum
$FIRCUSUM_{cnt}$	Poisson CUSUM with fast initial response feature
$FIRCUSUM_{ti}$	Time-interval CUSUM with fast initial response feature
$rCUSUM_{ti}$	Time-interval CUSUM coupled with two-in-a-row rule
$mrCUSUM_{ti}$	Time-interval CUSUM couple with modified two-in-a-row rule
DOE	Department of Energy
keV	kilo electron volts
ROI	region of interest
SIT	Single interval test
SPRT	Sequential probability ratio test

CHAPTER 1

INTRODUCTION

In the United States, radioactive contamination at Department of Energy (DOE) sites is a persistent health and safety issue. During World War II and the Cold War, the United States developed a complex of nuclear industrial facilities which were located at over 100 sites across 30 states and territories. Most activities conducted by DOE and its predecessor agencies (the Atomic Energy Commission, and Energy Research and Development Administration) in these sites have been related to production and testing of nuclear weapons. As the result of nuclear weapon-related activities, hazardous and radioactive contaminants were introduced into the environment through a variety of pathways, such as the release of process effluents to seepage basins, accidental spills, and leaks from storage tanks and waste transfer lines. (Young and MacDonell 1999; Palmisano and Hazen 2003).

With the end of the Cold War in the early 1990s and subsequent shutdown of nuclear weapon production reactors, the DOE mission changed markedly to remediation, decommissioning and decontamination of contaminated media (including soil, sediment, groundwater and surface water) on and around DOE sites. In 1989, the DOE's environmental management science program was created by the 104th Congress to reduce threats to health and safety posed by the contaminants at DOE sites (Young and MacDonell 1999; Palmisano and Hazen 2003; U.S. DOE 1997, 2000).

Environmental radiation monitoring at DOE sites is essential to the environmental management program. In the processes of cleaning up contaminated media, especially the subsurface contamination, monitoring is used to support the development of conceptual and predictive models of contaminant behavior, to demonstrate the effectiveness of remediation actions, and to gain regulatory approval. In addition, such monitoring information can be employed to understand the contaminant fate and transport, and can be used to validate and revise conceptual and predictive models. Therefore efficient and effective on-line or in-situ monitoring systems over the long term are required (U.S. DOE 2000, 2004).

Generally, the detection decision whether a radioactive source is present is made based on a specific statistical method. The ideal goal of radiation monitoring is to make a decision with a zero false positive rate (α) or a zero false negative rate (β), but this is unrealistic. It is well recognized that radioactive decay is a random process which is commonly characterized as a Poisson process when the number of nuclei is large and the observation time is short compared with the half-life of the radioactive species. Consequently, any radiation measurement is subject to some degree of statistical uncertainty. The inherent uncertainty in measurement results, together with short count time, long distance from source to detector, and attenuation effects cause unavoidable error rates in any final decision. In practice, a proper statistical method or technique is chosen to minimize both types of error rate (Knoll 2010; DeVol et al. 2009). Many statistical methods have been used for radiation monitoring. Among them, the single interval test (SIT) which is in a form of the Shewhart control chart is the most commonly

employed radiation monitoring procedure (Montgomery 2001). In the case of detecting small changes in the background radiation level, other relatively more sophisticated methods, such as the cumulative sum (CUSUM), Bayesian statistics, and sequential probability ratio test (SPRT) are used (Montgomery 2001; Hughes and DeVol 2008; Attardo 2007; Jarman et al. 2004). The focus of this research is on developing effective statistical algorithms for the analysis of time-interval information, which can be applied to the long-term on-line radiation monitoring.

Statistical Methods for On-Line Radiation Monitoring

Single Interval Test (SIT)

For a single interval test (SIT), radiation pulses are collected in a fixed-length count time regardless of the strength of the radiation level. Then the result of the observation--- the total or net number of pulses in this case --- is compared to a single critical level (detection limit) to decide whether a radiation source is detected. For the comparison of net number of pulses, a commonly used detection limit L_c popularized by Currie (1968) is given by

$$L_C = k_\alpha \sigma_0 \ , \qquad (1.\ 1)$$

where k_α is the 1-α percentile of the standardized normal distribution corresponding to the probability of α, and σ_0 is the standard deviation of the net signal. For example, if α=0.05, then $k_\alpha \approx 1.65$ is the 95^{th} percentile.

If the total number of pulses is used, the detection limit is given by

$$L_C' = N_0 + L_C \ , \qquad (1.\ 2)$$

where N_0 is the total number of pulses coming from the background radiation level (Jarman et al. 2004).

For on-line radiation monitoring, SIT is often performed in terms of the Shewhart control chart on which each observed result is plotted and compared with control limits. The chart has a center line representing the background radiation level, an upper control limit which is equal to L_C or L_C', and a lower control limit if it is necessary. One major disadvantage of the SIT method is that only the information contained in the most recent data point is considered, and the information contained in previous data points is disregarded. As a result, the SIT method is relatively insensitive to small changes in radiation levels while it readily detects large shifts (Montgomery 2001; Attardo 2007; Walpole and Myers 1997).

Sequential Probability Ratio Test (SPRT)

The sequential probability ratio test (SPRT) is a specific method of sequential analysis, developed by Abraham Wald (1952). A distinctive feature of SPRT is that the number of observations required by the test procedure is not determined in advance. When it is applied to statistical hypothesis testing, SPRT requires a substantially fewer number of observations than an equally reliable testing based on a predetermined number of observations (Wald 1952).

With a traditional hypothesis testing, such as the SIT method, after an observation is obtained, one of two possible actions is made: accept the null hypotheses H_0 or accept the alternative hypothesis H_1. In other words, a final decision has to be made on the observation no matter if the evidence is strong or ambiguous. Unlike traditional hypothesis testing, there is a third possible action for SPRT: additional observations are taken until the evidence can strongly support one of the two hypotheses (Ghosh and Sen 1991).

In low-level radioactivity monitoring, a simple hypothesis test is often designed as: the null hypothesis (H_0) that a sequence of measurements is from the background level r_0 against the alternative hypothesis (H_1) that the measurements are from an alarm level (background plus source) r_1. For this hypothesis testing the sequential probability ratio test is defined as follows: let $f(x, r_i)$ denote the distribution of the measurement variable x (counts or time-interval) under a certain process (r_0 or r_1). For a sequence of independent observations, $x_1, x_2, \ldots x_n$, the probability that the n observations are obtained when H_1 is true is given by

$$p_{1n} = f(x_1, r_1) f(x_2, r_1) \ldots f(x_n, r_1) \quad . \tag{1. 3}$$

And the probability for the n observations obtained under H_0 is given by

$$p_{0n} = f(x_1, r_0) f(x_2, r_0) \ldots f(x_n, r_0) \quad . \tag{1. 4}$$

At each stage of the experiment, the probability ratio p_{1n}/p_{0n} is computed and compared to thresholds to make a decision. For purpose of practical computation, the natural

logarithm of the probability ratio is commonly calculated, so that the individual ratios are additive.

$$\ln\left(\frac{p_{1n}}{p_{0n}}\right)=\ln\left(\frac{f(x_1,r_1)}{f(x_1,r_0)}\right)+\ln\left(\frac{f(x_2,r_1)}{f(x_2,r_0)}\right)+\ldots+\ln\left(\frac{f(x_n,r_1)}{f(x_n,r_0)}\right). \quad (1.5)$$

Let z_i denote the i^{th} term of the ratio,

$$z_i=\ln\left(\frac{f(x_i,r_1)}{f(x_i,r_0)}\right). \quad (1.6)$$

Then the sum of the ratios, $\lambda_n=\sum_{i=1}^{n} z_i$ is compared to two thresholds, A and B, where $B<A$, to make a decision.

If $\lambda_n \geq A$, H_0 is rejected (H_1 is accepted),

if $\lambda_n \leq B$, H_0 is accepted,

and if $B<\lambda_n<A$, the test continues by taking additional observations until a decision can be made or the maximum observations, N_{max} is reached.

A and B are related to the desired false positive rate, α_0, and false negative rate, β_0 by the following inequalities,

$$A\leq\ln\left(\frac{1-\beta_0}{\alpha_0}\right)$$

$$B\geq\ln\left(\frac{\beta_0}{1-\alpha_0}\right). \quad (1.7)$$

These two inequalities give an upper limit for *A* and a lower limit for *B*, and these limits are commonly used as thresholds in practice. Using these thresholds, the actual error rates α and β are not identical to the desired error rates α_0 and β_0. Since the desired error rates α_0 and β_0 are normally small in practical application, the actual error rates will be very close to desired values (Wald 1952).

Implemented in the 1980s, the SPRT method has been applied to radiation monitoring of vehicles, personnel and packages for nuclear safeguards and homeland security. SPRT has been shown to be an effective statistical method for detecting illicit nuclear materials, such as special nuclear materials (SNM) that may be used for terrorisms (Jarman et al. 2004; York and Fehlau 1997; Fehlau et al. 1983; Fehlau 1993; Coop 1985). In these applications, SPRT has shown the ability to shorten decision times and improve detection probabilities. Yuan and Kernan (2006) suggested that SPRT is a promising algorithm for quick determination of field radiation levels. With this method, the sample size for high radiation region is reduced and therefore the exposure to field radiation surveyors could be reduced. In addition, Humenik and Gross (1990, 1991) examined the properties of SPRT for rapid surveillance of off-normal operations of nuclear plant components.

Bayesian Statistics

In the 18th century, a Presbyterian minister, Thomas Bayes first discovered the theorem that now bears his name (Bolstad 2007). Now Bayes' theorem is experiencing a renaissance in fields of science ranging from astrophysics to genomics and in real-world

applications such as the change-point detection in quality control system and testing of new drugs (Malakoff 1999).

Bayesian probability statement about the underlying parameter *r* (mean count rate in this case) given the data *x* begins with a model providing a joint probability distribution for *r* and *x*, $p(r, x)$ (Gelman 2004; Ellison 1996). The joint probability mass or density function can be written as a product of two probabilities,

$$p(x)\,p(r \mid x) = p(r, x) = p(r)\,p(x \mid r)\,. \tag{1. 8}$$

Rearranging terms in equation (1. 8) yields an expression for $p(r \mid x)$, the posterior probability (*conditional probability*) of obtaining the parameter *r* given the data *x* is

$$p(r \mid x) = \frac{p(x \mid r) \cdot p(r)}{p(x)}\,. \tag{1. 9}$$

This expression is known as Bayes' theorem. In this expression, $p(r)$ is the prior probability of observing *r* that is expected by the investigator before the experiment is conducted. It is the quantitative description of what the investigator believes based on previous experience and knowledge. The distribution $p(x \mid r)$ is the likelihood function (*conditional probability*) which defines the probability to obtain a measurement *x* given *r*. The denominator $p(x)$ is referred to as the marginal distribution of the data. In the case of discrete *r*, $p(x) = \sum_r p(r)\,p(x \mid r)$, and for continuous *r*, $p(x) = \int p(r)\,p(x \mid r)dr$. The denominator $p(x)$ acts as a scaling constant that normalizes the sum or integral of the area

under the posterior probability distribution. Since the denominator contains no information about *r* and is a constant, it is enough to think of Bayes' theorem in its proportional form as

$$p(r \mid x) \propto p(x \mid r) \cdot p(r). \tag{1. 10}$$

And the conceptual form of Bayes' theorem is

$$posterior\ probability \propto likelihood \times prior\ probability.$$

The posterior probability is the goal of a Bayesian analysis. It summarizes the investigator's knowledge of the parameter given the prior belief and the subsequent data (Cherry et al. 2002).

In the case of a series of independent measurements, Bayesian analysis can be conducted sequentially (Bolstad 2007; Bochud et al. 2007). Using an appropriate likelihood and prior probability, the posterior probability is calculated for the first observation. For subsequent measurements, the existing posterior is used as a prior and a new posterior is computed from the Bayes' theorem. In this way, the Bayesian inference incorporates the new information at each measurement to update our state of knowledge of the parameter. The result of the sequential estimation is equivalent to the outcome of the Bayesian estimate with one data containing the whole information for all sequential measurements. For both estimations, the prior has a fundamental role since it can potentially bias the whole Bayesian analysis process (Bolstad 2007; Lee 2004).

Statistical inference can be conducted either through a classical approach which is often referred to as the frequentist approach, or through the Bayesian approach. The primary differences between the two methods of statistic inference lie in their interpretations of concepts of probability, data, parameter, confidence/credible intervals and conclusions.

Different viewpoints of probability are the fundamental distinction between the two approaches. Frequentist probability is always interpreted as long-run relative frequency: the probability of an event is the proportion of times it would occur if the experiment was repeated an infinite number of repetitions under identical conditions. Therefore, probability is calculated based on all possible random samples that could have occurred, not based on the actual sample that did occur (Bolstad 2007). In contrast, probability statements made in Bayesian framework must be interpreted as "degree of belief" based on the actual occurring data. Bayesian approach allows the state of knowledge about anything unknown to be described in the prior by a probability distribution. Our belief about parameters is updated through Bayes' theorem after the data have been acquired (Bolstad 2007; Gelman 2004). The second major difference between the two methods is about the numerical characteristics of the population parameters. In frequentist statistics, parameters are assumed to be fixed but unknown constants (Bolstad 2007). The statistical inference by frequentist methods is based on the statistic of random samples. For example, the mean of a sampling distribution is used as an unbiased estimator for the true parameter value. On the contrary, the Bayesian approach treats parameters as unknown random variables, and the Bayesian posterior

distribution is calculated based on the sample data that actually occurred (Bolstad 2007). Therefore, probability statements are allowed to be associated directly with parameters, which give the relative weights to each possible parameter value. Table 1.1 summarizes the differences between frequentist and Bayesian statistics.

Table 1.1 Fundamental differences between frequentist and Bayesian statistical inferences. (adapted from Ellison 1996 and Moshirpour 1997)

concept/term	Frequentist Statistics	Bayesian Statistics
Probability	1.) Probability of an event: result of an infinite series of trials under identical conditions 2.) A subjective prior is not allowed	1.) Probability statement: the degree of belief about parameter(s) in light of the data 2.) A subjective prior is allowed
Parameter(s)	Fixed unknown constant(s)	Random unknown variable(s)
Data	Random (representative) sample	Fixed
k % interval	Confidence interval: include the true value of a given parameter in *k*% of all possible sample intervals	Credible interval: *k*% of the possible parameter values will fall within the interval
Treatment of nuisance parameters	Conditions on sufficient statistics or maximum likelihood estimate	Integrates over all possible values
Conclusion	$p(x\|\theta)$	$p(\theta\|x)$

note: x is the data of a measurement, θ is the underlying true parameter(s) and k is a real number.

A prior distribution that gives our belief about the possible values of parameters is needed before any data are collected. There are basically three methods to assign the prior distribution, namely, “noninformative” prior, “natural conjugate” prior and “empirical Bayes” prior (Lee 2004). The “noninformative” prior is used when we don’t have any information and experience about the system under investigation (Bolstad 2007). The rationale for using noninformative prior distributions is to let the data speak

for themselves (Gelman 2004). The second method of defining the prior probability is from the natural conjugate family. Bayes' theorem defines that the posterior distribution is the product of the likelihood function and the prior probability. If the posterior distribution has the same parametric form as the prior distribution, this property is called conjugacy. A prior from the conjugate family makes the estimation of the posterior distribution mathematically tractable and convenient in that the posterior distribution follows a known parametric form (Gelman 2004). With this method, some estimation about the posterior inference, such as the mean and the standard deviation for a given problem, can be calculated directly (Lee 2004). "Empirical Bayes" prior is the third method of determining the prior distribution. An empirical prior combines any prior information and the data from previous experiments (Lee 2004). The advantage of this method is its flexibility in using methods such as probability plotting and goodness-of-fit tests to define the prior distribution.

Bayesian statistics has been discussed in health physics literature especially in the past two decades. A common problem in health physics is to decide whether a measurement differs from background when the activity of interest is low in the presence of dominant background. This type of decision can be made based on different rules (Strom and MacLellan 2001). Bayesian statistics, which allows for the inclusion of prior knowledge, provides a promising solution to this problem. Little (1982) first investigated the use of Bayesian theorem in health physics. He considered a counting situation where the net count rate can be negative using frequentist statistics because of random fluctuations, but the true result should be non-negative. Using a prior distribution with

zero probability for negative results, Bayesian analysis gave positive estimates of net rates and probability intervals which are coherent and meaningful (Little 1982). At the Los Alamos National Laboratory (LANL), innovative work employing Bayes' theorem has been undertaken by Guthrie Miller, Harry Martz and others (Strom 1998). Miller et al (2002) extended the work of Little (1982) using exact marginalized Poisson likelihood functions for counting measurement processes involving a background subtraction. With an empirical marginalized likelihood function containing more information of the measurement, Bayesian analysis produced a higher quality result and avoided the work dealing with problems associate with a negative net count (Miller et al. 2002). In addition, Miller et al. (1993) recommended a new analysis method based on the principles of Bayesian inference to determine whether a bioassay measurement should be interpreted as "positive" or "zero". They investigated the effects of the prior distribution on the estimates and interpretations of internal dosimetry and proposed some models for determining appropriate priors according to the availability of prior knowledge (Miller et al. 1993, 2001).

As in the field of health physics, Bayesian statistics has been exploited in other nuclear fields. Bayesian statistics has been applied to the measurement of activities of radioactive samples (Laedermann et al. 2005; Groer and Lo 1996). Groer and Lo (1996) discussed the derivation of the posterior density for the airborne ^{218}Po concentration based on Bayes' theorem. From this posterior density, the mean and variance of the airborne ^{218}Po concentration were calculated. In the study, they used the Poisson distribution to characterize the buildup and decay of ^{218}Po on a filter paper. Laedermann

et al. (2005) analyzed the measurements of radioactive samples using a prior determined by assuming that the number of radiation particles emitted and detected follows the Poisson distribution. The result from the Bayesian approach is always positive and a credible interval can be easily calculated from the whole distribution of the parameter. In addition, the result showed that the Bayesian and classical estimates were practically indistinguishable at higher activities. Bochud et al. (2007) illustrated the use of Bayesian statistics in estimating the activity of a decaying nuclide with short half-life. Bayesian statistics can produce coherent estimates and confidence intervals with less number of measurements. In contrast, the activity estimated by the conventional method has higher uncertainty and is less meaningful.

Because of the ability of taking into account all sources of uncertainty, such as random and systematic effects, Bayesian statistics has been used to give more accurate estimates of uncertainties of radiation measurements (Bergin and Milford 2000; Kaeker and Jones 2003; Weise et al. 2006). Using Bayesian Monte Carlo analysis, Bergin and Milford (2000) analyzed the data of ozone concentration in their case studies and showed that the estimated uncertainty at the peak concentration was effectively reduced. Based on Bayes' theorem, Weise et al. (2006) calculated Bayesian characteristic limits such as the detection limit and the decision threshold, which took into account all sources of uncertainty. They suggested a revision of some parts of ISO (International Organization for Standardization) guide in which characteristic limits are currently determined based on frequentist statistics. For the expression of uncertainty of measurements in the ISO

guide, Kacker and Jones (2003) proposed new evaluation methods from Bayesian viewpoint to make the expression of uncertainty consistent.

Bayesian techniques have also been applied for reducing false positive rates in low-level radioactivity measurements (DeVol et al. 2009; Strom and MacLellan 2001). Strom and MacLellan (2001) evaluated the actual false positive rates for eight decision rules as a function of *a priori* false positive rate and background mean. The results indicated that Currie's decision rule gives the poorest result and the Bayesian rule works much better. DeVol et al. (2009) compared false positive and false negative rates of radiological data for the classical and Bayesian statistical process control chart techniques. The results showed that the Bayesian method, Shiryayev-Roberts (S-R) control chart (Kenett and Pollak 1996), was the best method for controlling the number of false positives (DeVol et al. 2009).

Additionally, Bayesian techniques have been used for radiological source detection and estimation (Morelande and Ristic 2009). Morelande and Ristic proposed an algorithm based on Bayes' theorem that can detect and accurately estimate the parameters such as location and intensity of up to four sources.

Cumulative Sum (CUSUM) Control Chart

The CUSUM control chart was first introduced by Page (1954) as an alternative to the Shewhart chart for quality control and improvement in manufacturing processes. Instead of considering the most recent data point, the CUSUM chart incorporates all the information contained in the sequence of data points by accumulating deviations of data

points over time. For this reason, the CUSUM chart is more effective than Shewhart control chart to detect small process shifts (Montgomery 2001).

The CUSUM control chart is often calculated and plotted in form of the tabular (or algorithmic) CUSUM, which is called the two-sided CUSUM control chart. The tabular CUSUM works by adding up deviations from a target value that are above target with a statistic, C^+, and adding up deviations from a target value that are below target with another statistic, C^-. The statistic C^+ is called one-sided upper CUSUM statistic and C^- is called one-sided lower CUSUM statistic. For a process, let x_i be the i^{th} observation that has a mean value r_a when the process is in control. The mean value r_a is often referred to the target value. The statistics C^+ and C^- are given by

$$C_i^+ = \max[0, x_i - k + C_{i-1}^+] \tag{1. 11}$$

$$C_i^- = \max[0, k - x_i + C_{i-1}^-] \tag{1. 12}$$

where the starting values for the standard CUSUM control chart are $C_0^+ = C_0^- = 0$, k is the reference value and is also called the allowance or slack value (Montgomery 2001). The reference value k is chosen carefully to optimize the response to a shift from an in-control mean value r_a to an out-of-control mean value r_d (Attardo 2007; Holdbrook 2001). For the case of normally distributed observations, it is often chosen about the halfway between r_a and r_d:

$$k = \frac{|r_d - r_a|}{2} \tag{1. 13}$$

At each observation, after calculating the C_i^+ and C_i^-, a decision interval value, *h*, is needed to make a decision whether the process is out of control. If either C_i^+ or C_i^- exceeds *h*, the process is considered to be out of control (Montgomery 2001).

In practice, people prefer to standardize the variable x_i by $x_i' = \frac{x_i - r_a}{\sigma}$ where σ is the standard deviation of the process.

$$C_i^+ = \max[0, x_i' - k' + C_{i-1}^+] \quad (1.\ 14)$$

$$C_i^- = \max[0, k' - x_i' + C_{i-1}^-] \quad (1.\ 15)$$

where k' is the reference value for the standardized CUSUM. The relationship between k' and *k* is $k' = k / \sigma$. Here, the decision interval value is defined to be h', and $h' = h / \sigma$.

For radiation monitoring, the most commonly used applications is the detection of an increase in count rate or the detection of a decrease of time-interval. Thus, a one-sided CUSUM control chart is often employed. The CUSUM control chart is usually evaluated by calculating its average run length (ARL), which is the average number of observations taken before an out-of-control signal is triggered. Ideally, the ARL should be long when the process is in control and short when the process is out of control (Lucas 1985).

Because of its effectiveness to detect small shifts, particularly for sample size of n=1, and relative simplicity, the CUSUM control chart is a good candidate for environmental monitoring. For instance, it has been applied to well or reservoir monitoring for chemical contaminants in groundwater and surface water (Gibbons 1999; Manly and MacKenzie 2000). In 1977, Marshall suggested the use of cumulative sum

charts for monitoring the background radiation level from a radiochemical counter. According to the study, the CUSUM charts could detect abrupt changes in the count rate of the order of one standard deviation (Marshall 1977). For count data such as the number of radiation interactions registered in a detector, Lucas (1985) provided more detailed information about the implementation of the CUSUM control chart. In his paper, a Poisson CUSUM in which the number of counts per sampling interval is modeled by the Poisson distribution, and time-between-events CUSUM were discussed in terms of determining the *k* and *h* values for general scenarios. He suggested that time-between-events CUSUM could be used when it is possible to record the occurrence time for each event (Lucas 1985). Most recently, the CUSUM chart has been exploited for on-line radiation monitoring of low level radioactivity in environmental solutions, and unauthorized nuclear materials for homeland security (Hughes and DeVol 2008; Attardo 2007). To improve the sensitivity of the CUSUM for the process that an out-of-control situation occurs at start-up, Lucas and Crosier (1982a) devised the fast initial response (FIR) CUSUM. The FIR CUSUM sets C_0 equal to some nonzero value instead of zero in the standard CUSUM (Lucas and Crosier 1982a). In addition, Lucas and Crosier (1982b) proposed the robust CUSUM by using the two-in-a-row rule to account for the extreme observations obtained in count data (Lucas and Crosier 1982b).

Time-Interval Distribution

The Poisson distribution characterizes the random nature of radioactive decay when the probability of decay of a single atom during observation is much less than one.

For a Poisson process, the probability *P(m)* for observing *m* decays (*m*=0, 1, 2, …) in a time interval *t* is given by (Evans 1955; ICRU 1994)

$$P(m) = \frac{(rt)^m}{m!} e^{-rt} \quad . \tag{1. 15}$$

The term 'time-interval' refers to the time difference between two consecutive pulses. In time-interval distribution analysis the time-interval density, *f(t)*, is usually employed to characterize the distribution. The probability of the next event taking place in *dt* after a delay of time *t* since the last event is denoted as *f(t)dt*. For the Poisson distribution, the probability for the next event to occur in *dt* is:

$$f(t)dt = re^{-rt}dt \tag{1. 16}$$

where e^{-rt} is the probability of no events during time from time 0 to t for $t \geq 0$ (ICRU 1994). By taking the effect of dead time into account, a theoretical expression of the time-interval density for non-paralysable spectrometer with a stationary source has been established,

$$f(t)dt = U(t-\tau)re^{-r(t-\tau)}dt \tag{1. 17}$$

in which $U(t)$ is a unit step function, and τ is the dead time (Pomme 1999).

From equation (1. 16), the average time interval is,

$$\bar{t} = \frac{\int_0^\infty tf(t)dt}{\int_0^\infty f(t)dt} = \frac{\int_0^\infty tre^{-rt}dt}{1} = \frac{1}{r} \qquad (1.\ 18)$$

As expected, the average time interval is equal to the reciprocal of the count rate. Shown in Figure 1.1 are three theoretical time-interval densities for different mean count rates, *r*. We note that short time-interval has a higher probability than that of relatively long time-interval and a higher count rate results in a higher probability of short time intervals. The short time-interval results in a larger difference in time-interval densities between two count rates.

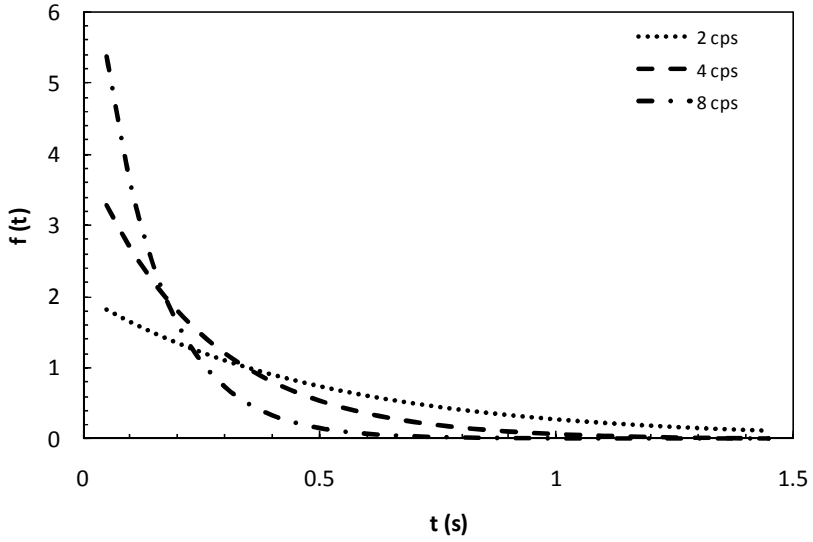

Figure 1.1. Theoretical time-interval densities (eq. 1.16) of three counting processes, 2 cps, 4cps and 8 cps.

From equation (1. 16), time-interval probability $p(t)$ for the Poisson distribution is derived. The distribution $p(t)$ gives the probability of a time-interval t in which one or more radiation pulses can be observed:

$$p(t) = 1 - e^{-rt}. \tag{1. 19}$$

Figure 1.2 shows the theoretical time-interval probabilities for three different count rates. We can see that time-interval distribution patterns are similar to those shown in Figure 1.1. The probability of short time-intervals is higher than that of long time intervals for all counting processes.

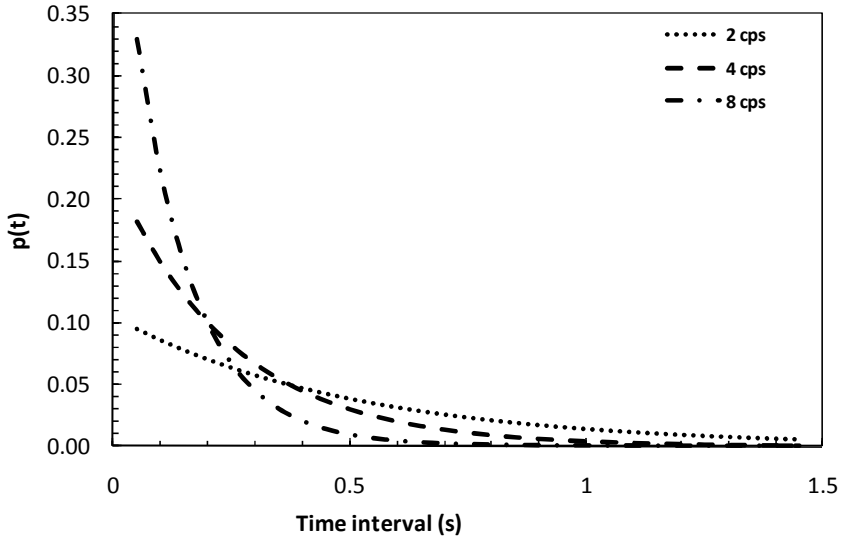

Figure 1.2. Theoretical time-interval probability distributions (eq. 1.19) of three counting processes, 2cps, 4cps and 8cps.

When a digital "scaler" is employed to produce one output pulse only after N input pulses have been registered, the time-interval between two scaled output pulses is

called a “scaled” time-interval. The distribution of scaled time-intervals for the Possion process is

$$I_N(t)\cdot dt = \frac{(rt)^{N-1}e^{-rt}}{(N-1)!}r\cdot dt\,, \qquad (1.\ 20)$$

in which N is the number of input pulses in the time interval and t is the time needed to record these pulses (Evans 1955). Figure 1.3 shows an example of the distributions of scaled time-intervals.

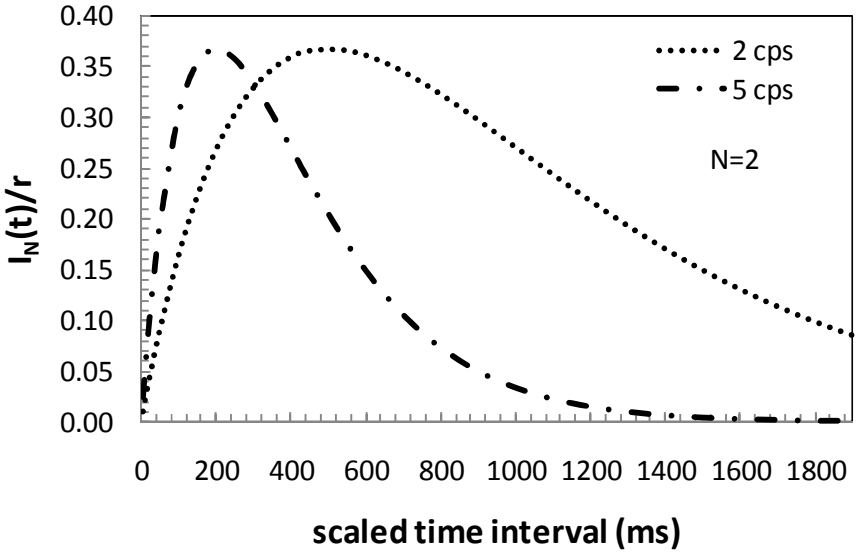

Figure 1.3. The scaled time-interval distribution with N=2 for count rate 2cps and 5cps, respectively.

In radiation monitoring, data can be collected either by integrating the number of pulses registered by the detector during a given count interval or by recording the arrival time stamp of each registered pulse. The former method is widely used because of its simplicity.

When a radioactive source is present, it would result in a significant change in the time-interval distribution at the background level, especially for short time-intervals. This special property of time-interval distribution has been applied to several problems. By limiting time-intervals to a pre-assigned range, Arandjelovic et al. (2002) developed an algorithm for preset count digital-rate meter to suppress statistical fluctuations of mean count rate measurements. Baeten et al. (1998) applied time-interval analysis to neutron multiplicity measurements which offers high sensitivity for the assay of Pu-bearing waste drums. Dowdy et al. (1978) devised a neutron detector suitcase based on S-fold time-interval measurements to detect transients of neutron-emitting radioactive materials.

In our research, we focus on using time-interval information derived from the arrival times of each registered pulse for radiation monitoring. Three statistical methods, SPRT, Bayesian statistics, and CUSUM, are applied for time-interval analyses. Advantages and disadvantages of the three time-interval methods will be compared to the commonly used count information in a fixed count time. In addition, the performances of the three methods based on time-interval data are compared to the classical SIT method in terms of ARL, false positive and false negative rates.

Research Objectives

The overall objective of this research project is to develop time-interval based statistical methods and techniques for on-line radiation monitoring. Registering time-interval data possesses the potential to reduce the sampling time required to obtain sufficient information to detect abrupt changes in radiation levels. The research proposed

herein is divided into three sections. Based on the fundamental experimental study of the time-interval distribution, three statistical methods (SPRT, Bayesian statistics, and CUSUM) are applied to time-interval data analyses for radiation monitoring. The three methods for time-interval analyses are chosen based on their common characteristics of incorporating previous information into the decision-making. The potential advantages of collecting time-interval information for radiation monitoring will be evaluated for the three methods and compared to a conventional statistical method. The details for each section are listed as following.

Objective 1: Apply the sequential probability ratio (SPRT) test to on-line radiation monitoring by using the scaled time-interval as an independent variable, and evaluate its advantages/disadvantages relative to conventional SPRT in which observations are obtained in a fixed count time.

Utilization of scaled time-interval in SPRT is investigated as an alternative to conventional fixed count time analysis with experimental and simulated data. SPRT is used as the decision-making algorithm because of its well-known property to minimize the average sampling size (i.e. decision time) for sequentially acquired observations. The performance of the scaled time-interval based SPRT is evaluated in terms of estimated time to decision and detection probability ($1-\beta$) against commonly used single-interval test (SIT) and SPRT with a fixed count time. Furthermore, adjustments of parameters in SPRT are investigated to give better performance at meeting the specified statistical requirements.

Objective 2: Analyze time-interval observations using Bayesian techniques and investigate advantages of time-interval information for distinguishing small changes in the background radiation level for on-line monitoring.

Bayesian statistics is fundamentally different from the frequentist statistics. Bayesian inference treats parameters as random unknown variables, and uses a probability density to reflect the state of knowledge about plausible parameter values. Bayesian approach allows *a priori* information about the parameter, such as the net count rate and background, to be included in statistical inference. Data are collected to update or modify the prior distribution to obtain the posterior distribution for the unknown parameter based Bayes' theorem. By analyzing time-intervals of on-line monitoring data, it is expected that a change in the background can be detected with low false positive rate.

Objective 3: Use the cumulative sum (CUSUM) method to analyze time-interval data for on-line radiation monitoring and compare its advantages to those of CUSUM with count data and Shewhart control chart.

The CUSUM method is a classical technique that is widely used for industrial quality control. The major property of the CUSUM method is the ability to incorporate information contained in a previous sequence of observations. The CUSUM tracks cumulative sums of the deviations of the observations from a target value (the background, for example) to detect an abrupt change in the background. This method is promising for low-level radiation monitoring in which a small and steady increase in radiation level happens in the presence of a significant ambient background.

Overview

Time-interval analyses based on each of the three chosen statistical methods were investigated with experimental data and simulated data. The results are presented in the next three chapters as individual papers and the order of presentation follows the order of the research objectives. In chapter 2, the study on sequential probability ratio test (SPRT) of scaled time-interval data are summarized. A paper titled "Sequential probability ratio test using scaled time-intervals for environmental radiation monitoring" by P. Luo, T. A. DeVol, and J. L. Sharp has been published in the *IEEE Transactions on Nuclear Science*, vol. 57, No. 3 (2010) 1556-1562. Chapter 3 presents the results of Bayesian analysis of time-interval data. A paper titled "Bayesian analysis of time-interval data for environmental radiation monitoring" by P. Luo, J. L. Sharp, and T. A. DeVol has been submitted to *IEEE Transactions on Nuclear Science* for review. Chapter 4 summarizes the results of cumulative sum (CUSUM) analyses of time-interval data for radiation monitoring. A paper titled "CUSUM analysis of time-interval data for on-line radiation monitoring" by P. Luo, T. A. DeVol, and J. L. Sharp has been submitted to the Health Physics Journal. Finally, a brief summary of the major findings in this research is provided in chapter 5 with a prospective plan of future work on time-interval analyses. Other results that are not included in the main body of the dissertation are given in the appendices, as well as experimental data relative to experimental results and a part of important computer code developed for this research.

CHAPTER 2

SEQUENTIAL PROBABILITY RATIO TEST USING SCALED TIME-INTERVALS FOR ENVIRONMENTAL RADIATION MONITORING

Abstract

Sequential probability ratio test (SPRT) of scaled time-interval data (time to record *N* radiation pulses), SPRT_scaled, was evaluated against commonly used single-interval test (SIT) and SPRT with a fixed counting interval, SPRT_fixed, on experimental and simulated data. Experimental data were acquired with a DGF-4C (XIA, Inc) system in list mode. Simulated time-interval data were obtained using Monte Carlo techniques to perform a random radiation sampling of the Poisson distribution. The three methods (SIT, SPRT_fixed and SPRT_scaled) were compared in terms of detection probability and average time to make a decision regarding the source of radiation. For both experimental and simulated data, SPRT_scaled provided similar detection probabilities as other tests, but was able to make a quicker decision with fewer pulses at relatively higher radiation levels. SPRT_scaled has a provision for varying the sampling time depending on the radiation level, which could further shorten the time needed for radiation monitoring. Parameter adjustments to the SPRT_scaled method for increased detection probability are discussed.

Introduction

Subsurface contamination by anthropogenic radionuclides at United States Department of Energy (DOE) sites is a persistent and vexing problem for the DOE's Environmental Management Science Program. As an integrated component, on-line environmental radiation monitoring is essential to the environmental management program. In the processes of cleaning up contaminated media, long-term environmental radiation monitoring is required to support the development of conceptual and predictive models of contaminant behavior, to demonstrate the effectiveness of remediation actions, and to gain regulatory approval (U.S. DOE 2000, 2004). The goal of on-line environmental radiation monitoring is to quickly detect small changes in activity levels in the presence of a significant ambient background. By sensing the gradual or abrupt change in the radiation level, a final decision will be made to conclude whether a radiation source is present. Ideally, we want to make a decision with no false positives (Type I error) or false negatives (Type II error), but this is unrealistic. It is well recognized that radioactive decay is a random process which is commonly characterized by the Poisson distribution or Gaussian distribution. Consequently, the inherent uncertainty in measurement causes unavoidable error rates in any final decision (Knoll 2010; ICRU 1994). In practice, a proper statistical method or technique is chosen to minimize both Type I and Type II errors.

A typical statistical method used in radiation monitoring is the single-interval test (SIT) (Jarman et al. 2004). SIT accumulates radiation counts over a fixed-length counting interval, and compares the resulting counts or count rates to a single critical level. SIT

can be conducted easily, but it is relatively insensitive to small changes in radiation levels. Therefore, more sophisticated statistical methods or techniques have been developed and adopted to detect small changes in radiation levels. For example, Marshall suggested the use of cumulative sum control charts (CUSUM) for monitoring the background radiation level from a radiochemical counter (Marshall 1977). Apostolopoulos employed maximum likelihood techniques as an on-line statistical processing method to improve the response of radiation rate meters (Apostolopoulos 2008). Fehlau, Jarman and Coop applied the sequential probability ratio test (SPRT) in portal monitors (Jarman et al. 2004; York and Fehlau 1997; Coop 1985).

SPRT is a specific statistical method of sequential analysis developed by Abraham Wald. A distinctive feature of SPRT is that the number of observations required by the test procedure is not determined in advance. When SPRT is applied to statistical hypothesis testing, SPRT requires a substantially fewer number of observations than an equally reliable test based on a predetermined number of observations (Wald 1952). Implemented in the 1980s, SPRT has been applied to radiation monitoring of vehicles, personnel and packages for nuclear safeguards and homeland security. SPRT is an effective statistical method for detecting illicit nuclear materials, such as special nuclear materials (SNM) (Jarman et al. 2004; York and Fehlau 1997; Fehlau et al. 1983; Fehlau 1993; Coop 1985). In these applications, SPRT has been shown to have the ability to shorten decision times and improve detection probabilities. Yuan and Kernan suggested that SPRT is a promising algorithm for quick determination of radiation levels in the field (Yuan and Kernan 2006). With this method, the sample size for high radiation region is

reduced and therefore the exposure to field radiation surveyors could be reduced. In addition, Humenik and Gross examined SPRT for rapid surveillance of off-normal operations of nuclear plant components (Humenik and Gross 1990; Gross and Humenik 1991).

When applying a statistical method to analyze radiation data from a detector system, there are two distinct ways to look at the data: either the radiation counts registered in a fixed counting interval or the time difference between adjacent pulses (time-interval) is used for the analysis. The former method is technically easier to handle and it is the most common way to analyze radiation data. Time-interval distribution has been applied to several problems. By limiting time-intervals to a pre-assigned range, Arandjelovic et al. developed an algorithm for preset count digital-rate meters to suppress statistical fluctuations of mean count rate measurements (Arandjelovic et al. 2002). Baeten et al. applied time-interval analysis to neutron multiplicity measurements which offered high sensitivity for the assay of Pu-bearing waste drums (Baeten et al. 1998). Dowdy et al. devised a neutron detection system based on S-fold time-interval measurements to detect transients of neutron-emitting radioactive materials (Fehlau et al. 1983; Dowdy et al. 1978).

Registering counts in a fixed counting interval and registering time-intervals provide us with two different data sampling methods. The time needed to record a statistically significant number of pulses could be shorter than counting for a fixed counting interval. Therefore, registering time-intervals possesses the potential to reduce the sampling time required to obtain sufficient information to detect abrupt changes in

radiation levels. In this study, we investigate the characteristics of time-interval distributions, and use time-interval information to conduct the SPRT of on-line radiation monitoring data. In addition, we evaluate advantages and disadvantages of the time-interval based SPRT (SPRT_scaled) compared to the commonly used SIT and traditional SPRT with a fixed counting interval (SPRT_fixed).

Theory and Methods

Time-interval Distribution

The Poisson distribution characterizes the random nature of radioactive decay when the probability of decay of a single atom during observation is much less than one. For a Poisson process, the probability *P(m)* for observing *m* decays (*m*=0, 1, 2, …) in a time interval *t* is given by

$$P(m) = \frac{(rt)^m}{m!} e^{-rt} \quad , \tag{2. 1}$$

where *r* is the mean count rate (Knoll 2010; ICRU 1994).

The term ‘time-interval’ refers to the time difference between two consecutive pulses. In time-interval distribution analysis the time-interval density, *f(t),* is usually employed to characterize the distribution. The probability of the next event taking place in *dt* after a delay of time *t* since the last event is denoted as $f(t) \cdot dt$. For the Poisson distribution, the probability for the next event to occur in *dt* is:

$$f(t)dt = re^{-rt}dt \quad , \tag{2. 2}$$

where e^{-rt} is the probability of no events from time 0 to *t*, and *r*, $t \geq 0$ (Knoll 2010; ICRU report 52 1994).

When a digital "scaler" is employed to produce one output pulse only after *N* input pulses have been registered, the time-interval between two scaled output pulses is called a "scaled" time-interval. The distribution of scaled time-intervals for the Possion process is,

$$I_N(t) \cdot dt = \frac{(rt)^{N-1} e^{-rt}}{(N-1)!} r \cdot dt \quad , \tag{2. 3}$$

in which *N* is the number of the input pulses in the time interval and *t* is the time needed to record these pulses (Knoll 2010). Figure 2.1 shows an example of the distributions of scaled time-intervals.

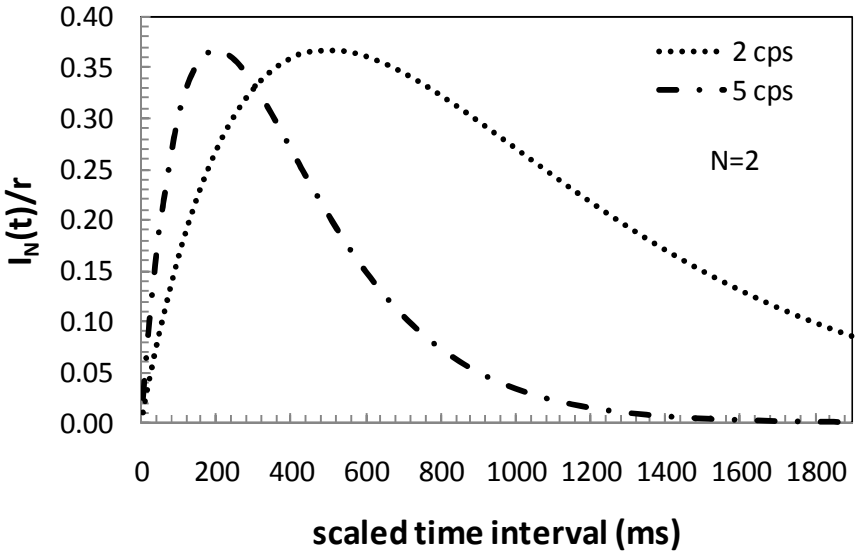

Figure 2.1. The scaled time-interval distribution with *N*=2 input pulses for mean count rate 2 cps and 5 cps, respectively.

Single Interval Test

Single interval test (SIT) is a typical method used in radiation detection. For SIT, radiation pulses are collected in a fixed counting interval regardless of the strength of the radiation level. The result of the observation--- the total or net number of pulses --- is compared to a single critical level to decide whether a radiation source is detected. If the net number of radiation pulses is used for the decision-making, the critical level is given as:

$$L_c = k_\alpha \sigma_0 \quad , \tag{2. 4}$$

where k_α is the 1-α percentile of the standardized normal distribution corresponding to probability α, and σ_0 is the standard deviation of the net signal. If the total number of pulses is used, the critical level is given by

$$L_c' = N_0 + L_c \quad , \tag{2. 5}$$

where N_0 is the total number of radiation pulses coming from the background level (Jarman et al. 2004). In this study, the desired false positive rate α_0 is set at 0.05. Thus, $k_{\alpha_0} \approx 1.645$.

For on-line radiation monitoring, SIT is often performed in terms of the Shewhart control chart on which each observed result is plotted and compared with control limits. The chart has a line representing the background radiation level, an upper control limit at L_c', and a lower control limit if necessary. One major disadvantage of the Shewhart chart is that only the information contained in the most recent data point is considered, and the information contained in previous data points is disregarded. As a result, the SIT method

is relatively insensitive to small changes in radiation levels while it readily detects large shifts (Montgomery 2001).

Sequential Probability Ratio Test (SPRT)

With traditional hypothesis testing, such as the SIT method, after an observation is obtained, one of two possible actions is made: accept the null hypotheses (H_0) or accept the alternative hypothesis (H_1). In other words, a final decision is made on the observation no matter if the evidence is strong or ambiguous. Unlike traditional hypothesis testing, there is a third possible action for the SPRT: additional observations will be taken until the evidence can strongly support one of the two hypotheses (Ghosh and Sen 1991). The sequential probability ratio test is defined as follows. Let x_i represent the result (counts in a fixed counting time, for example) for the i^{th} observation, and $f_j(x_i)$ denote the probability density of the variable x_i ($f_j(x_i) = P(k)$ as given in equation (2.1), for example) under the hypotheses H_j, j=0 or 1 (background vs. alarm, for example). At each observation, a probability ratio $f_1(x_i)/ f_0(x_i)$ is calculated. The sum of the probability ratios from previous observations is compared to two thresholds to make a decision. For simplicity, a natural logarithm of the probability ratio is commonly calculated for the tested quantity, so that the individual ratios are additive. Let z_i denote the natural logarithm of the ratio,

$$z_i = \ln\left(\frac{f_1(x_i)}{f_0(x_i)}\right). \qquad (2.6)$$

Then the sum of the ratios, $\lambda_n = \sum_{i=1}^{n} z_i$ is compared to two thresholds, *A* and *B*, where *B*<*A*, to make a decision.

If $\lambda_n \geq A$, H_0 is rejected.

If $\lambda_n \leq B$, H_0 is accepted.

If $B < \lambda_n < A$, the test continues by taking additional observations until a decision can be made or the maximum observations, N_{max}, is reached.

Thresholds *A* and *B* are related to the desired false positive rate α_0 and false negative rate β_0 (Wald 1952). They are given by

$$\begin{aligned} A &\leq \ln\left(\frac{1-\beta_0}{\alpha_0}\right) \\ B &\geq \ln\left(\frac{\beta_0}{1-\alpha_0}\right). \end{aligned} \quad . \qquad (2.7)$$

These two inequalities give an upper limit for *A* and a lower limit for *B*, and these limits are commonly used as thresholds in practice. Using the limits as the thresholds, the actual error rates α and β are not identical to the desired error rates α_0 and β_0, but they are very close to the desired values (Wald 1952).

In radiation monitoring, SPRT tests the hypothesis (H_0) that a sequence of measurements is from the background level r_0 only against the hypothesis (H_1) that the measurement sequence is from an alarm level r_1, which indicates the presence of a radiation source. Here, the alarm level is set at a level that the false negative rate is β_0, which is given by (2.5) based on the desired α_0 and β_0. When SPRT_fixed is conducted,

the observation is the count of registered radiation pulses, c_i, in a fixed counting interval. Thus, the natural logarithm of the ratio z_i is calculated by

$$z_i = c_i \cdot \ln(r_1/r_0) + (r_0 - r_1)t \quad , \tag{2. 8}$$

where t is the length of the counting interval for each observation.

When scaled time-intervals are used for SPRT_scaled, the observation is the time-interval, t_i, for observing N input radiation pulses. Consequently, z_i is given by

$$z_i = (N-1)\ln(r_1/r_0) + (r_0 - r_1) \cdot t_i \, . \quad . \tag{2. 9}$$

Compared to (2.8), the difference in calculating the probability ratios at each observation is that the observable variation is different for the two sequential tests. Single interval test (SIT) is a typical quantification method used in radiation measurements.

Experimental Instruments and Simulation

Figure 2.2 shows the schematic diagram of the radiation acquisition system used for experimental data. Beta radiation from a $^{90}Sr/^{90}Y$ source (~3700 Bq each, E_{max}=0.55MeV/2.3 MeV) was detected using a G-M detector. The output from an amplifier (ORTEC model 572) was sent to a DGF-4C module (XIA, Inc) where it was digitized at a rate of 40 MHz with 16-bit precision. The DGF-4C module was connected to a Pentium IV, 2.3 GHz host computer through a Jorway 73A crate controller and controlled through a graphical user interface, DGF-4C viewer 3.05. The DGF-4C viewer 3.05 runs specifically under an interactive programming and data analysis environment,

IGOR Pro. 4.03 (XIA 2004; Chandrikamohan and DeVol 2007; Skulski and Momayezi 2001). Using list mode, a binary output file containing time stamp information was prepared by the DGF-4C module for off-line analysis. The time resolution is 25ns. Based on a special built-in function in the IGOR Pro., the absolute time stamp of each input pulse was extracted from the list mode data. Time-intervals or scaled time-intervals were obtained to conduct SPRT. By adjusting the distance from the source to the detector, experimental data for low level radiation (2-10cps) were acquired. At each radiation level, about 25,000 radiation pulses were registered to provide for a good general comparison among the methods.

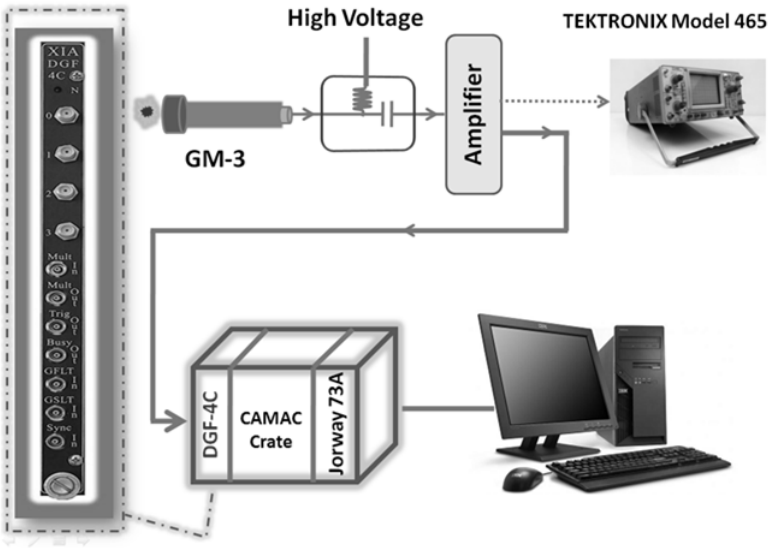

Figure 2.2. Schematic diagram of CAMAC module based time-interval acquisition system.

In addition, a Monte Carlo method was employed to simulate a random radiation sampling based on the density function of time-interval distributions. The simulation is

conducted through a program written in IGOR Pro. In the simulation, the arriving time of each pulse is a random process governed by the time interval distribution described in (2.2). According to the arriving time information, simulated scaled time-intervals were extracted for the SPRT test. At each radiation level, 10^6 random pulses were simulated. Compared to experimental acquisition, simulation is a rapid and convenient means to compare the three methods. To register 10^6 radiation pulses at low count rate levels, the simulation can be done within a few minutes, while the experimental data collection takes hours to days depending on the count rate.

The same experimental and simulated data sets were used to evaluate the SIT, SPRT_fixed, and SPRT_scaled methods. The fixed counting interval is 6s for SIT and 1s for SPRT_fixed. The performances of the three methods were evaluated in terms of estimated time to decision and detection probability (1- β), where β is the actual false negative rate. It should be noted that the fixed counting time for SIT and SPRT_fixed are arbitrary. A proper fixed counting time should be determined based on a real application. Since time-intervals and counts in a fixed counting interval provide two distinct ways for radiation data analyses, a fair comparison between SPRT_scaled and SPRT_fixed is not practical. In this study, we provide insight on the advantages and disadvantages of these two methods.

Results and Discussion

Experimental results were used to study the characteristics of scaled time-intervals and the SPRT with scaled time-intervals while the simulated radiation data were

used to investigate the possibilities and effects of parameter adjustments on the results from the SPRT_scaled method.

Experimental SPRT Results

The experimental detection probabilities (1- β) for different radiation levels are shown in Figure 2.3. The average background count rate is 2.0cps. The probabilities α_0 and β_0 are set at 0.05. Correspondingly, the alarm radiation level for the SPRT testing is 4.35cps. Based on (2.7), A=2.94 and B=-2.94 are used for the two thresholds. N_{max}=16 for both types of SPRT methods. Unless otherwise specified, these are the parameters used in all analyses presented in this paper. For the scaled time-interval based SPRT test, N=4 and 6 input pulses are presented.

Generally, SPRT_scaled has similar performance to that of SIT and SPRT_fixed. For radiation levels around the background level, SPRT_scaled results in a very low detection probability relative to other methods. For example, at the mean count rate of about 2cps, the detection probability is about 12.0% for SIT, 3.3% for SPRT_fixed, and 0.04% for SPRT_scaled. At greater than 2.5 times the background count rate, all three methods have essentially the same detection probabilities. For a count rate between the background and 2.5 times the background, the detection probability of SPRT_scaled is relatively lower than that of others.

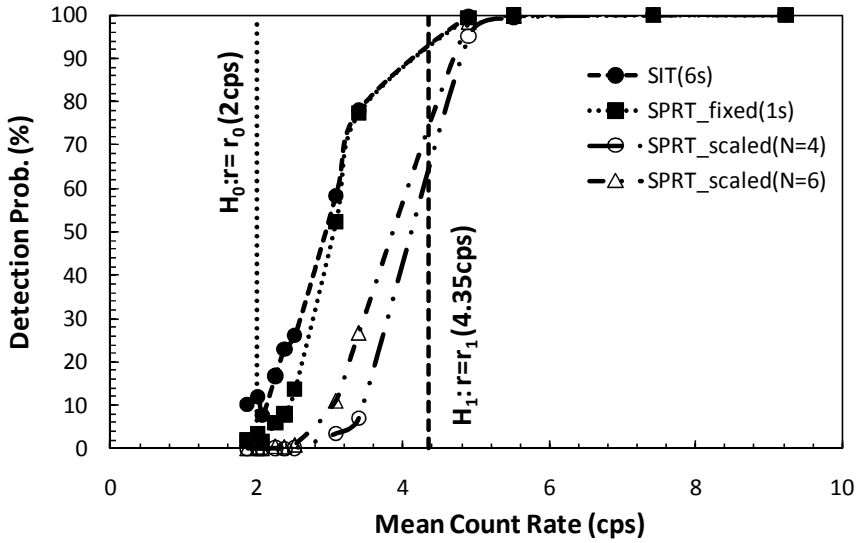

Figure 2.3. Detection probability for experimental data. Each point is obtained by analyzing about 25,000 registered pulses.

Figure 2.4 shows the average time to make a decision using SPRT_fixed and SPRT_scaled. This time is fixed at 6s for the SIT method. For a low radiation level, SPRT_scaled needs more time than that of SPRT_fixed to make a decision. As the radiation level reaches a higher level, the average decision time needed for SPRT_scaled is close to that of SPRT_fixed. In addition, the average decision time varies with the size of scaled pulses, *N*. In the low radiation range, more time is needed to make a detection decision for higher *N*.

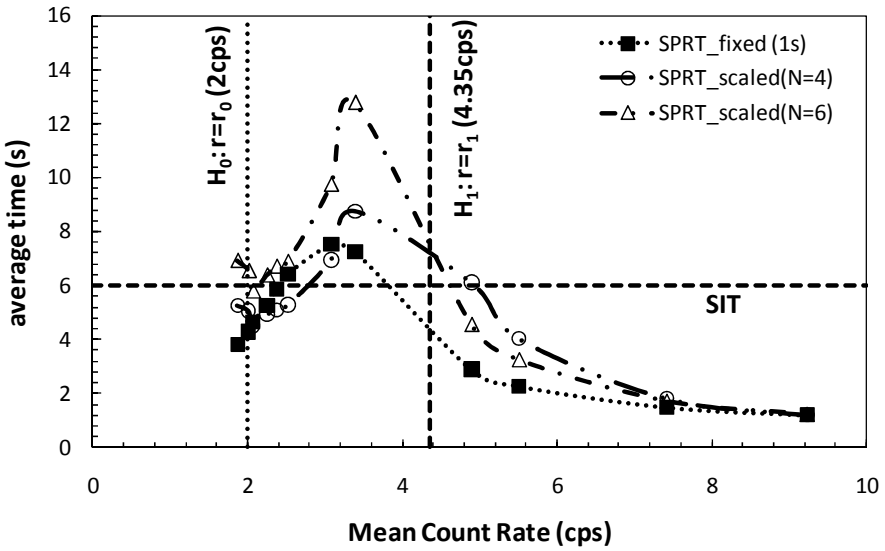

Figure 2.4. Average decision time for experimental data. The decision time for SIT is always 6s in this case.

Simulated SPRT Results

Figure 2.5 and Figure 2.6 illustrate the detection probability and average decision time obtained from simulated data. Results from simulated data are consistent with the results from the experimental data. The simulated detection probability results presented in Figure 2.5 indicate that simulation is a reasonable way to study the sensitivity of scaled time-intervals for radiation monitoring. In Figure 2.6, when the radiation level reaches a certain high level (>10 cps with this data), the average decision time for SPRT_scaled becomes less than that of SPRT_fixed.

In the study of parameter adjustments, we use simulated data to investigate the effects of N_{max}, A, and B on the detection probability and the average time to make a decision focusing on the SPRT_scaled method. No adjustment is performed for

SPRT_fixed. SPRT_fixed is used as a reference to visualize the effects of parameter adjustments to SPRT_scaled.

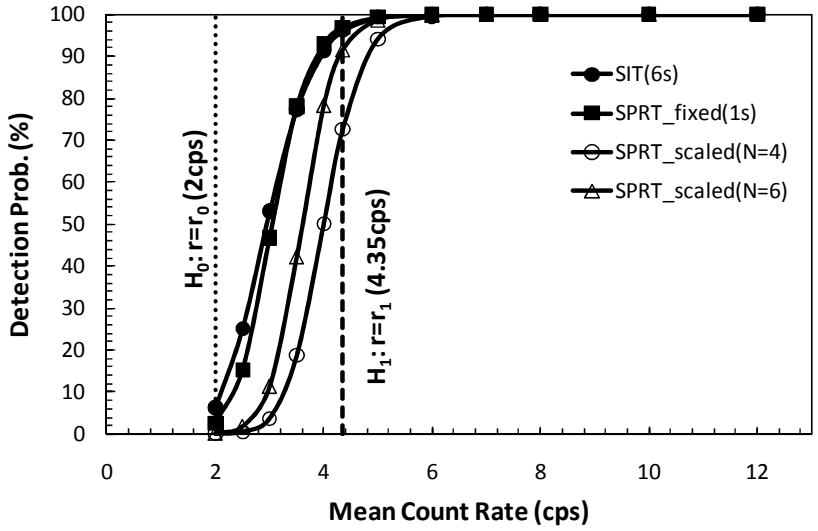

Figure 2.5. Detection probability for simulated data. Each point is obtained by analyzing 10^6 simulated registered pulses.

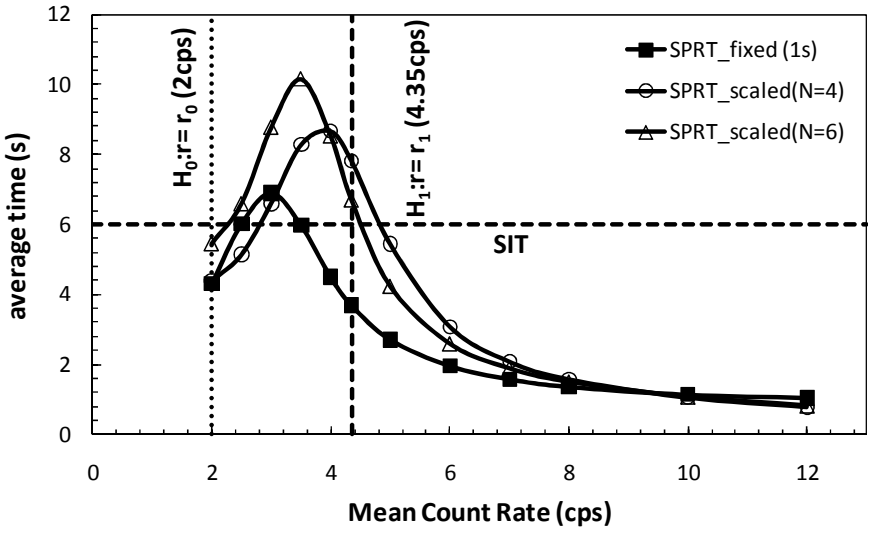

Figure 2.6. Average decision time for simulated data. The decision time for SIT is always 6s in this case.

Parameter Adjustments

Figures 2.4 and 2.6 show that the average decision time for radiation levels between the background and the alarm level of the SPRT_scaled method is longer than that of SPRT_fixed and SIT methods. And the detection probabilities in this range are lower than that of SIT and SPRT_fixed. For the cases in which higher detection probabilities and shorter decision times are the primary concerns, an improvement is needed.

In the practice of the SPRT testing, a truncation strategy is commonly used to reduce the average decision time. That is, the decision using SPRT is forced when the test has not reached a decision by a given time or given number of observations, N_{max} (Jarman et al. 2004). The choice of a proper N_{max} depends on the time limit that can be tolerated in the practice.

Figure 2.7 gives the results of the truncation strategy by setting the maximum observations, N_{max}, at 4. N_{max}=4 is less than the average number of observations needed for SPRT method to make a decision at a radiation level between the background and the alarm level. In previous results, N_{max} was set at 16. Compared to Figure 2.6, it is obvious that the average time to make a decision is reduced, especially in the range of low radiation levels. However, the detection probabilities cannot be drastically improved as shown in Figure 2.8.

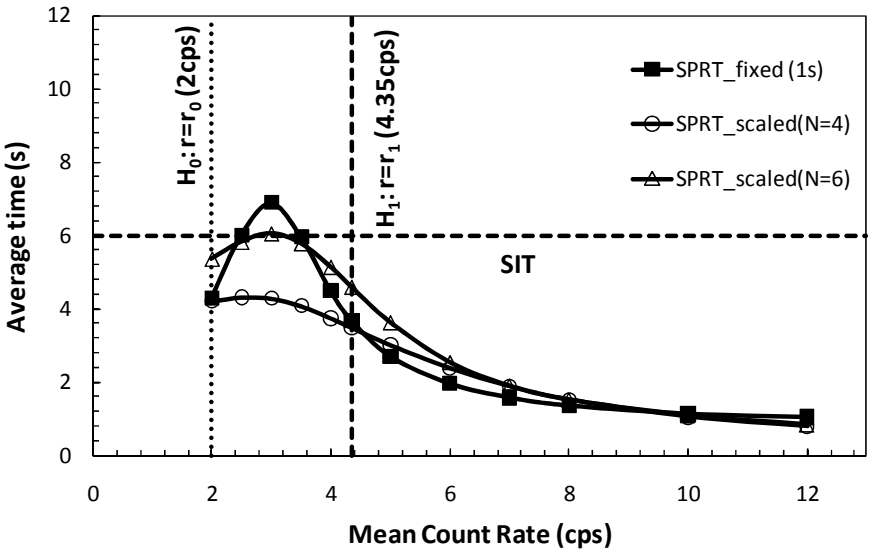

Figure 2.7. Average detection time for truncation strategy when N_{max}=4. SPRT_fixed is the same as in Figure 2.6 and it is used as a reference.

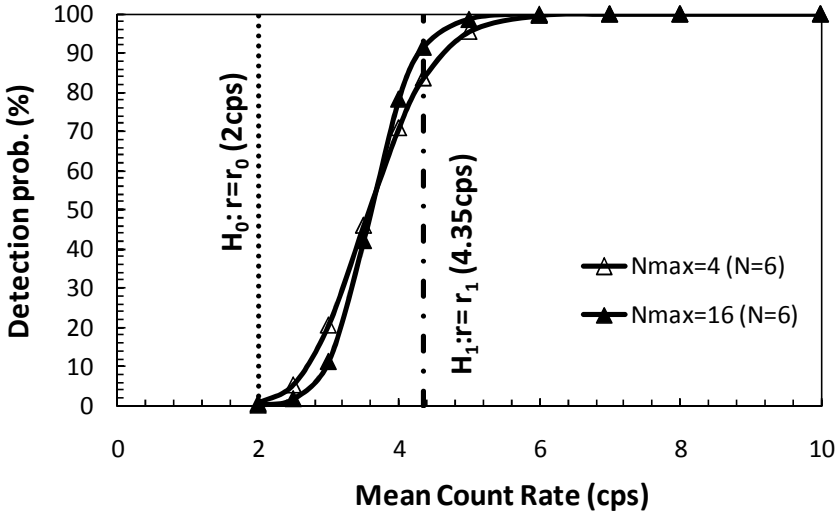

Figure 2.8. Average decision time of SPRT_scaled with N=6 input pulses for two different maximum observations: N_{max}=4 and N_{max}=16.

Thresholds A and B can be adjusted to give desired error rates, but the exact determination of thresholds is usually laborious (Wald 1952). Figure 2.9 shows an example

of the detection probability for adjusting threshold *A*. With a smaller *A* value, the actual error rate β at the alarm level is reduced while the actual error rate α at the ground level is increased. Even though the detection probability is increased, the detection probability of SPRT_scaled is still lower than that of SIT and SPRT_fixed. On the contrary, when a larger *B* value is used as the threshold, the actual β at the alarm level is increased while the actual rate α at the background level is reduced.

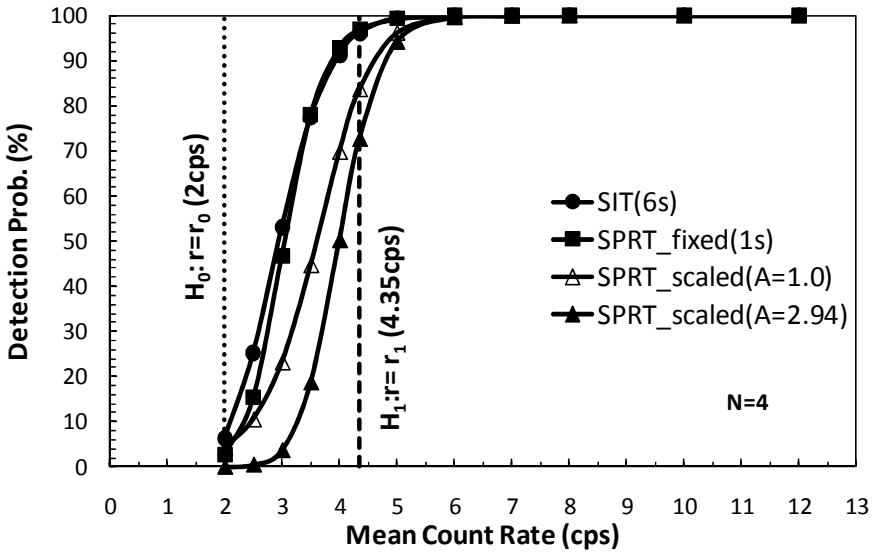

Figure 2.9. Detection probability for the adjustment of A from 2.9 to 1.0 (*N*= 4 input pulses). SIT and SPRT_fixed are the same as in Figure 2.5, and they are used as references.

An adjustment of r_0 (2.9) was investigated to consider the change of the detection probability and the average decision time. Here r_0 is treated as a parameter only in the SPRT algorithm, not a variable in a real experiment. Figures 2.10 and 2.11 illustrate an example of the adjustment of the preset background level (r_0). The hypothesis is that if one

can shift the detection probability curve to the left the detection probability will increase. With r_0=2 cps, α was much lower than expected while β was higher than expected. Figure 2.10 shows the effect of the r_0 adjustment with different values for N= 6 input pulses. With a smaller r_0' value to replace the preset r_0, the detection probability curve is further shifted to the left. This means that the detection probability is higher, especially for relatively low radiation levels. Figure 2.11 shows the average decision time for SPRT_scaled with different N when r_0'=1.0 cps is used to replace the preset background, r_0=2.0 cps. Except for the radiation level around the background, the average decision time for SPRT_scaled is less than that of SPRT_fixed. As shown in Figure 2.10, the error rate α for this adjustment is also increased with the shift of the detection curve. This implies that there is a compromise between the amount of the shift and the tolerable error rates. Thus, α and β can be made closer to the expected value of 0.05 by the adjustment of r_0 in the SPRT algorithm.

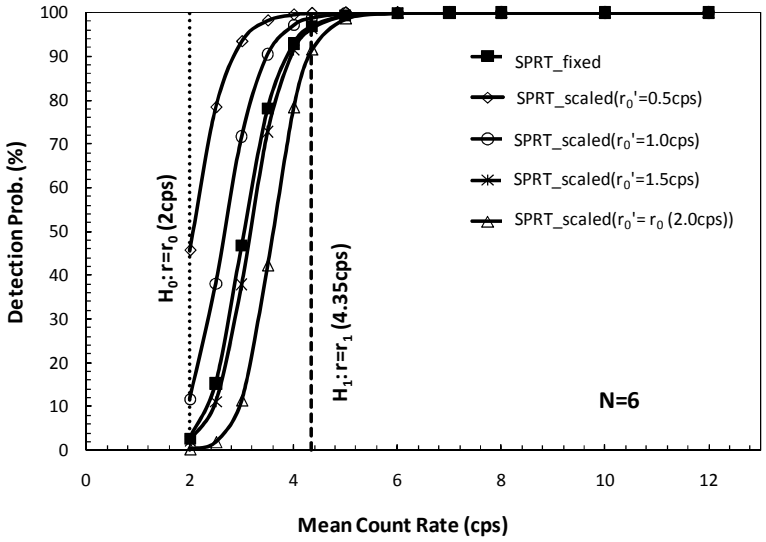

Figure 2.10. Detection probabilities of the adjustments of r_0 in the SPRT algorithm for ratio calculations when r_0' = 0.5 cps, 1.0 cps and 1.5 cps, respectively (N= 6). The SPRT_fixed method is the same as in Figure 2.5.

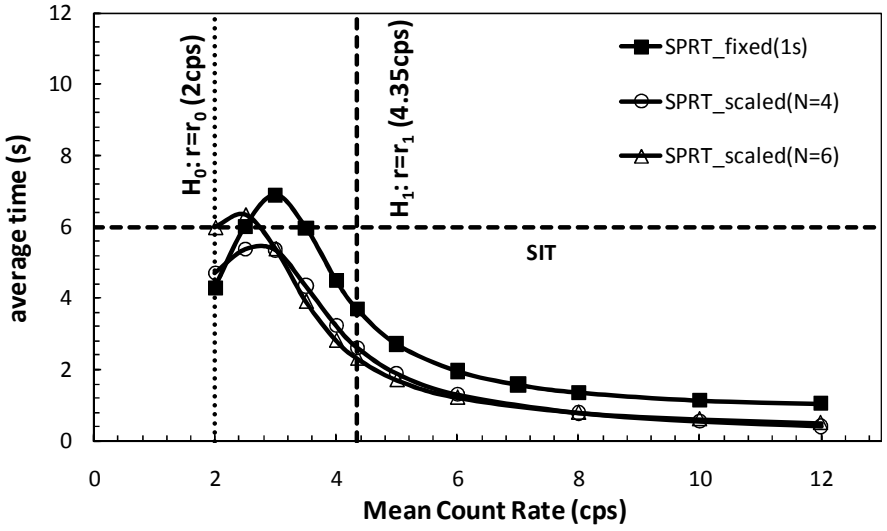

Figure 2.11. Average time with r_0' = 1.0 cps in the ratio calculation for SPRT_scaled with N=4 and 6 input pulses.

Conclusion

For radiation monitoring in which radiation data are obtained sequentially, the time difference between two consecutive pulses or scaled outputs can be extracted easily. The specific features of time-interval distribution provide an alternative way to analyze on-line sequential data. With a proper statistical method, time-interval information can provide another effective way for on-line radiation monitoring. According to this study, the SPRT with scaled time-interval information had similar performance to SIT and the SPRT with a fixed counting interval at lower count rates, but delivered a faster response when the count rate reached a certain high level. In addition, parameters in SPRT are able to be adjusted for different specifications. Continued investigation of the use of the time-interval distribution by applying other statistical methods or techniques is valuable.

References

Apostolopoulos, G. 2008. On-line statistical processing of radiation detector pulse trains with time-varying count rates. *Nuclear Instruments & Methods in Physics Research Section A-Accelerators Spectrometers Detectors and Associated Equipment* 595, (2) (OCT): 464-73.

Arandjelovic, V., A. Koturovic, and R. Vukanovic. 2002. A software method for suppressing statistical fluctuations in preset count digital-rate meter algorithms. *IEEE Transactions on Nuclear Science* 49, (5 Part 3): 2561-6.

Baeten, P., M. Bruggeman, R. Carchon, and W. De Boeck. 1998. Neutron multiplicity measurements on 2201 waste drums containing Pu in the range 0.1-1 g Pu-240(eff) with the time interval analysis method. *Nuclear Instruments & Methods in Physics Research Section A-Accelerators Spectrometers Detectors and Associated Equipment* 413, (2-3) (AUG 21): 333-40.

Chandrikamohan, P., and T. A. DeVol. 2007. Comparison of pulse shape discrimination methods for phoswich and CsI :T1 detectors. *IEEE Transactions on Nuclear Science* 54, (2) (APR): 398-403.

Coop, K. L. 1985. Monte-carlo simulation of the sequential probability ratio test for radiation monitoring. *IEEE Transactions on Nuclear Science* 32, (1): 934-8.

Dowdy, E. J., C. N. Henry, R. D. Hastings, and S. W. France. 1978. Neutron detector suitcase for the nuclear emergency search team. *Los Alamos Scientific Lab.Report LA*-7108.

Fehlau, P. E., J. C. Pratt, J. T. Markin, and T. Scurry Jr. 1983. Smarter radiation monitors for safeguards and security. Proceedings of the 24th Annual Meeting of the Institute of Nuclear Materials Management, Vail, Colorado, 1983, pp. 122-8.

Fehlau, P. E. 1993. Comparing a recursive digital-filter with the moving-average and sequential probability-ratio detection methods for snm portal monitors. *IEEE Transactions on Nuclear Science* 40, (2) (APR): 143-6.

Ghosh, B. K., and P. K. Sen. 1991. *Handbook of sequential analysis.* New York: Marcel Dekker.

Gross, K. C., and K. E. Humenik. 1991. Sequential probability ratio test for nuclear-plant component surveillance. *Nuclear Technology* 93, (2) (FEB): 131-7.

Humenik, K., and K. C. Gross. 1990. Sequential probability ratio tests for reactor signal validation and sensor surveillance applications. *Nuclear Science and Engineering* 105, (4) (AUG): 383-90.

ICRU report 52. 1994. *Particle counting in radioactivity measurements.*

Jarman, K. D., L. E. Smith, and D. K. Carlson. 2004. Sequential probability ratio test for long-term radiation monitoring. *IEEE Transactions on Nuclear Science* 51, (4) (AUG): 1662-6.

Knoll, G. F. 2010. *Radiation detection and measurement*. 4th ed. New Jersey: John Wiley & Sons Inc.

Marshall, R. A. G. 1977. Cumulative sum charts for monitoring of radioactivity background count rates. *Analytical Chemistry* 49, (14): 2193-6.

Montgomery, D. C. 2001. *Introduction to statistical quality control.* New York: John Wiley & Sons.

Skulski, W., and M. Momayezi. 2001. Particle identification in CsI(tl) using digital pulse shape analysis. *Nuclear Instruments & Methods in Physics Research Section A-Accelerators Spectrometers Detectors and Associated Equipment* 458, (3) (FEB): 759-71.

U.S. Department of Energy. 2004. *Transport of contaminants in subsurface environments at DOE sites.* DE-FG01-05ER05-12.

———. 2000. *Research needs in subsurface science.* ISBN: 0-309-51437-1. http://www.nap.edu/catalog/9793.html.

Wald, A. 1952. *Sequential analysis.* New York: John Wiley & Sons.

XIA. 2004. *User's manual digital gamma finder (DGF) DGF-4C*. Newark, CA: X-Ray Instrumentation Associates.

York, R. L., and P. E. Fehlau. 1997. *1997 update for the applications guide to vehicle SNM monitors.* LA-13247-MS.

Yuan, D., and W. Kernan. 2006. Sequential probability ratio test (SPRT) for dynamic radiation level Determination–Preliminary assessment. *Computational Science–ICCS 2006*: 179-87.

CHAPTER 3

BAYESIAN ANALYSIS OF TIME-INTERVAL DATA FOR ENVIRONMENTAL RADIATION MONITORING

Abstract

Time-interval (time difference between two consecutive pulses) analysis based on the principles of Bayesian inference was compared with frequentist methods to determine the method with the highest detection probability and the best average run length. Using experimental and simulated data, Bayesian analysis of time-intervals (Bayesian (ti)) was compared with Bayesian and frequentist analyses of counts in a fixed count time (Bayesian (cnt) and 1.65σ, respectively). Experimental data were acquired with DGF-4C (XIA, Inc) system in list mode. Simulated data were obtained using Monte Carlo techniques to obtain a random sampling of the Poisson distribution. All statistical algorithms were developed using R (R Core Development Team, 2010). Detection probabilities and average run lengths for the three methods were compared. Bayesian analysis of time-interval information provided a similar detection probability as Bayesian analysis of count information, but was able to make a decision with fewer pulses at relatively higher radiation levels. In addition, for the cases with very short presence of the source (< count time), time-interval information is more sensitive to detect a change than count information since the source data is averaged by the background data in the entire count time. The relationships of the source time, change points and modifications to the Bayesian approach for increasing detection probability are presented.

Introduction

On-line environmental radiation monitoring is essential to the U.S. Department of Energy (DOE) Environmental Management Science Program for cleaning up contaminated media at DOE sites (U.S. DOE 2004). Radiation monitoring also plays an important role in monitoring the presence of unauthorized nuclear materials and locating a lost or stolen radioactive source (Panofsky 2003). The goal of on-line radiation monitoring is to quickly detect small or abrupt changes in activity levels in the presence of significant ambient background. An on-line radiation monitoring system should satisfy the following basic requirements: i) perform routine monitoring properly in the long-term with the least number of false positives; ii) quickly detect changes in radiation levels with the least number of false negatives; iii) have a long average run length (ARL) when the radiation level is at the background level and a short ARL when the radiation level changes to an elevated level. In the case of low-level radioactivity, two factors make distinguishing between a radioactive source and natural background particularly difficult. First, because of the random nature of the radioactive decay, the number of emitted particles and the number of particles registered in a detector follows the Poisson distribution, resulting in inherent uncertainty in the number of recorded counts. Second, radiation monitoring is usually performed in a nature background that also involves counts from natural radionuclide in the environment and cosmic radiation (Laedermann et al. 2005). Radiation monitoring becomes even more complex as a radioactive source is contained in a moving medium, shielded by non-radioactive materials, or occurs at a relatively long distance away from the detector. Consequently, there is a finite probability

that unavoidable errors are associated with any detection decision. In practice, a proper statistical method or technique is chosen to minimize the rates of each type of error.

A conventional radiation monitoring method based on classical statistics involves setting a decision level (*DL*) for a given false positive rate (α). A monitoring result (counts or count rate) is then compared to the decision level. If the value of the result is greater than the decision level, then one makes the decision that there is activity present above the background. Strom and MacLellan (2001) discussed eight different rules for setting a decision level. They evaluated the actual false positive rates for eight decision rules as a function of *a priori* false positive rate and background mean. A commonly used decision level developed by Currie (1968) is given as $DL=k_\alpha\sigma_0$, where k_α is the 1-α percentile of the standardized normal distribution with corresponding probability α (e.g. for a false positive rate α =5%, $k_\alpha\approx1.645$), and σ_0 is the standard deviation of the background counts. The conventional monitoring method can be conducted easily, but one major disadvantage is that only information contained in the latest data point is exploited, and the information contained by the entire sequence of data points is disregarded. Therefore, more sophisticated statistical methods or techniques have been developed and adopted in the field of health physics to make a more reliable and coherent radiation monitoring decision. Among them, Bayesian methods provide a promising framework for making a more accurate decision in low-level activity monitoring by providing direct probability statements about the underlying parameter (e.g. mean count rate, *r*) based on prior information and actual data.

Unlike classical statistical procedures (often referred to as frequentist statistics), Bayesian statistical methods permit the formal incorporation of prior subjective knowledge, belief and information beyond that contained in the observed data in the inference process via Bayes' theorem. As in other fields of physical sciences, Bayesian statistics has been discussed in health physics literature as an alternative to classical statistical methods for analyzing low-level radioactivity in the presence of background counts. Little (1982) first investigated the use of Bayes' theorem in health physics to address the situation where estimates of net rates of activity can be negative when frequentist statistics are used. Using a prior distribution with zero probability for negative values, Bayesian analyses give meaningful positive estimates of net rates. Miller et al. (1993, 2001, 2002) extended Little's work in estimates and interpretations of internal dosimetry and environmental monitoring applications. Bayesian techniques have also been applied to estimate the low-level activities of decaying nuclides with short half-lives (Bochud et al. 2007; Groer and Lo 1996). Because of the ability to take into account sources of uncertainty, Bayesian statistics have been used to give more accurate estimates of uncertainty of radiation measurements. Weise et al. (2006) calculated Bayesian characteristic limits such as the detection limit and the decision threshold by taking into account sources of uncertainty. Weise et al (2006) suggested a revision of some parts of the ISO (International Organization for Standardization) guide in which characteristic limits are currently determined based on frequentist statistics. Kacker and Jones (2003) proposed new evaluation methods for the expression of uncertainty of measurements in the ISO guide from a Bayesian viewpoint to make it consistent. Additionally, Bayesian

techniques have been applied for reducing false positive rates in low-level radioactivity monitoring (DeVol et al. 2009; Strom and MacLellan 2001). DeVol et al. (2009) compared false positive and false negative rates (β) of time series radiological data for classical control chart and Bayesian statistical process control chart known as the Shiryayev-Roberts (S-R) control chart. The results showed that the Bayesian method was the best for controlling the false positive rates relative to the Shewhart (3-σ) and the cumulative sum (CUSUM) control charts.

There are two distinct ways to record the radiation data: either the radiation counts registered in a fixed count time or the arrival time of each registered pulse. According to the arrival time, the time difference (time-interval) between two consecutive pulses can be extracted. The former method is technically easier to handle and it is the most common way to analyze radiation data. Utilization of time-interval information in radiation measurements has been discussed by several authors. By limiting time intervals to a pre-assigned range, Arandjelovic et al. developed an algorithm for preset count digital-rate meters to suppress statistical fluctuations of mean count rate measurements (Arandjelovic et al. 2002). Dowdy et al. devised a portable neutron detection system to search for neutron-emitting radioactive materials based on S-fold time-interval measurements (Dowdy et al. 1978).

The time needed to record a statistically significant number of pulses could be shorter than counting for a fixed count time. Therefore, registering time-intervals possesses the potential to reduce the sampling time required to obtain sufficient information to detect abrupt changes in radiation levels, and avoids the work of

determining an appropriate fixed count time. Time-interval information can result in a quick response to the change in radiation levels and keep the false positive rate at a low level. In this study, we investigate the characteristics of time-interval distributions, and apply Bayesian statistics to the analysis of time-interval data from on-line radiation monitoring. In addition, we evaluate advantages and disadvantages of the time-interval based Bayesian analysis (Bayesian (ti)) compared to the frequentist method (1.65σ) and traditional Bayesian analysis with a fixed count time (Bayesian (cnt)). We also modify the updating of the prior distribution with previous information to reduce the effect of the background, which can improve the performance of the Bayesian analysis.

Theory and Methods

Time-interval Distribution

The random nature of radioactive decay is characterized as a Poisson process when the number of nuclei is large and the observation time is short compared with the half-life of the radioactive species. The probability *P(m)* for observing *m* decays (*m*=0, 1, 2, …) in a time interval *t* is given by the Poisson distribution,

$$P(m) = \frac{(rt)^m}{m!} e^{-rt} \quad , \tag{3. 1}$$

where *r* is the mean count rate.

The time-interval density, *f(t)*, is usually employed to characterize the time-interval distribution. The probability of the next event taking place in *dt* after a delay of

time *t* since the last event is denoted as *f(t)dt.* For the Poisson process, the probability for the next event to occur in *dt* is:

$$f(t)dt = re^{-rt}dt \quad , \tag{3. 2}$$

where e^{-rt} is the probability of no events from time 0 to t, and r, $t \geq 0$. The density function expressed in (3.2) is commonly referred to as the exponential distribution (Knoll 2010).

Bayes' Theorem

Let us consider a radioactive decay process described by an underlying mean count rate, *r*, and let *x* denote the observed value (e.g., time-interval) in radiation measurements. The mathematical form of Bayes' theorem is defined as

$$p(r \mid x) = \frac{p(x \mid r)\, p(r)}{p(x)} \quad , \tag{3. 3}$$

where *p(r|x)* is the posterior probability distribution of the unknown parameter *r* given the data *x* and *p(x|r)* is the likelihood function which is given by a chosen probability model, such as the Poisson distribution and the exponential distribution (Bolstad 2007; Gelman 2004). The prior probability distribution of *r* is given as *p(r);* this is a quantitative description of our belief about *r* based on previous experience and knowledge before the experiment is conducted. The denominator *p(x)* is referred to as the marginal distribution of the data which normalizes the posterior probability distribution.

The goal of a Bayesian analysis is to obtain the posterior probability which summarizes our knowledge of the parameter, *r*, given the prior belief and the observed data, *x*.

In the case of a series of independent measurements obtained over time in radiation monitoring, Bayesian analysis can be conducted sequentially (Bolstad 2007). Using a designated initial prior probability and likelihood function, the posterior probability is calculated for the first observation. For a subsequent measurement, the existing posterior probability is used as a new prior in combination with the newly available data to give an updated posterior. In this way, the Bayesian estimate of the parameter *r* incorporates the new information at each measurement to update our state of knowledge about *r*.

A prior probability that gives our belief about the possible values of parameters is needed before data collection. A prior from a conjugate family can make the estimation of the posterior mathematically tractable and convenient in that the posterior will follow the same parametric form as the prior (Gelman 2004). In this study, a conjugate distribution known as the Gamma distribution is assigned to be the prior in both the count data (Bayesian (cnt)) and time-interval data (Bayesian (ti)) Bayesian analyses. For the likelihood that is given by the Poisson distribution and the exponential distribution, the Gamma distribution is used to assign a conjugate prior (Gelman 2004). Therefore, the posterior probability can also be expressed in the form of the Gamma distribution. The general probability density function of the Gamma distribution, *Gamma (a, b)*, is given by

$$Gamma(a,b) = \frac{b^a}{\Gamma(a)} r^{a-1} e^{-br} \ , \qquad (3.\ 4)$$

where a is the shape parameter, b is the reverse scale parameter, and $\Gamma(a)$ is the Gamma function. The parameter r is the true count rate of the process that can be estimated based on the measured count rate.

For the count information in a fixed count time obtained in n independent observations, $c=(c_1, c_2, \ldots c_n)$, the likelihood is given by $\prod_i \frac{(rt_c)^{c_i}}{c_i!} e^{-rt_c}$, where t_c is the fixed count time for each observation. In this study, the fixed count time was set at 1 second. Based on Bayes' theorem, the posterior probability of r is given as

$$p(r \mid c) \propto p(c \mid r)\, p(r) = Gamma(a + \sum_i c_i, b + nt_c) \ . \qquad (3.\ 5)$$

When the time-intervals obtained in n independent observations, $t=(t_1, t_2, \ldots t_n)$, are used for Bayesian inference, the likelihood is given by: $\prod_i re^{-rt_i}$. Accordingly, the posterior distribution is given by

$$p(r \mid t) \propto p(t \mid r)\, p(r) = Gamma(a + n, b + \sum_i t_i) \ . \qquad (3.\ 6)$$

For the time-interval information, an assumption is made that the time information of each registered radiation pulse is read out one at a time, and the run time of a radiation detection system is the sum of the time-intervals that are incorporated into the Bayesian inference.

In the situation of on-line radiation monitoring, the first posterior is calculated for the first available data point (counts in a fixed count time or a time-interval) by assigning an initial prior. From the posterior probability distribution, the probability that the true parameter r is above the predetermined background r_0 can be inferred. Using a similar method as that in frequentist statistics, a detection limit can be set to the outcome from the posterior probability distribution. For example, a detection limit is set at 95% for the posterior probability distribution. A detection decision is made when the outcome r from the posterior probability distribution is 95% or higher to be above the r_0. If the decision regarding the presence of a source cannot be made, a new data point will be acquired to update the posterior by using the current posterior as a new prior. In this way, the Bayesian inference incorporates the new information at each observation to update our state of knowledge of the parameter until a detection decision is made or a sequence of observations is terminated. All statistical algorithms for the Bayesian inference were developed using R (R Development Core Team 2010).

Modifications to Bayesian Analysis

In the Bayesian analysis described above, the prior is updated passively whenever a new data point is available. When an excessive amount of data from the background level are included in the prior, a potential drawback for the prior update is to delay the detection or fail to detect change if the change occurs over a limited time. To quantify the amount of background data that are incorporated in Bayesian inference, we borrow the term “change point” that is common in statistical literature (Kenett and Zacks 1998).

A change point is the length of time that the background is counted before the count rate changes to an elevated level.

In this study, two modifications, enhanced reset and moving prior, were proposed to address the effect of the change point in the Bayesian analyses. Figure 3.1 shows the methodology of the enhanced reset modification. The principle of the enhanced reset method is to discard the previous information when the posterior shows a distribution that is consistent with the background. The enhanced reset modification sets a two-stage limit for the maximum number of data points used for the Bayesian inference and sets a discriminator to determine whether the existing posterior probability distribution is consistent with the background. The discriminator is established at a given probability that the parameter *r* from the posterior distribution is above the background level. When the number of data points in the current posterior probability reaches the first stage of the limit (e.g. 10 pulses), the discriminator will be used to determine whether the previous data are combined into the next step of the Bayesian inference. If the current posterior shows that the true *r* has a higher probability than the discriminator to be above the background, the information contained in the posterior will be incorporated into the next step of the Bayesian inference. Our knowledge regarding *r* is continuously updated by combining new data points until a final detection decision is made or the total number of data points included in the latest posterior probability reaches the second stage of the limit (e.g., 20 pulses). Otherwise, the process will start over from a new observation with the designated initial prior.

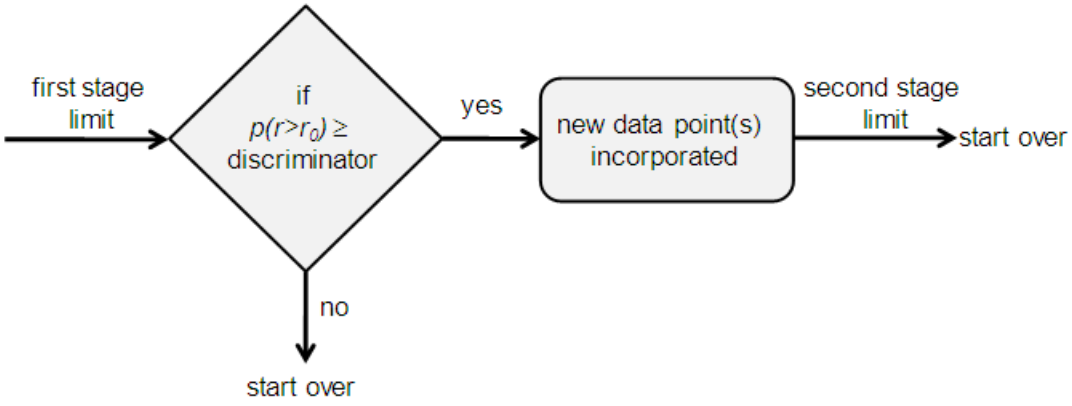

Figure 3.1. The methodology of the enhanced reset modification.

The moving prior modification relies on the latest information to calculate the posterior probability by updating the prior probability with each new data point. A fixed length for the vector of data is set for the maximum number of data points contained in the prior probability distribution. Starting from the first data point, the prior accumulates information one data point at a time. When a fixed length of data is accumulated, the prior will keep the same length of data (e.g., 10 pulses) and shift forward to update its information with new data points.

Experimental Instruments and Simulation

Figure 3.2 shows the schematic diagram of the radiation acquisition system used for experimental data. Gamma radiation (E_γ = 1173.2 keV and 1332.5 keV) from a ^{60}Co source (~14,000 Bq) was detected using a NaI(Tl) scintillation detector. The output from a preamplifier (ORTEC model 113) was sent to a DGF-4C module (XIA, Inc) where it was digitized at a rate of 40 MHz with 16-bit precision. The DGF-4C module was

controlled through a graphical user interface, DGF-4C viewer 3.05, which runs under an interactive programming and data analysis environment, IGOR Pro. 4.03 (XIA 2004; Luo et al. 2010). Using list mode, a binary output file containing time stamp information was prepared by the DGF-4C module for off-line analyses. The time resolution is 25 ns. Based on a program written in IGOR Pro., time-intervals were extracted from the list mode data for Bayesian analyses. By adjusting the distance from the source to the detector, experimental data for low-level radiation (2-10 cps for the 1332.5 keV peak) were acquired. At each level, about 10^5 radiation pulses were registered to provide for a good general comparison among the methods. For experimental data analysis, three regions of interest (ROI) were set to look at pulses within a specific energy range. One ROI was set to include both cobalt-60 full energy peaks, and the other two ROIs were set for each full energy peak, respectively.

In addition, a Monte Carlo method was employed to simulate a random radiation sampling based on the time-interval density function given in (3.2). The simulation was conducted in IGOR Pro. At each radiation level, 10^6 random pulses were simulated.

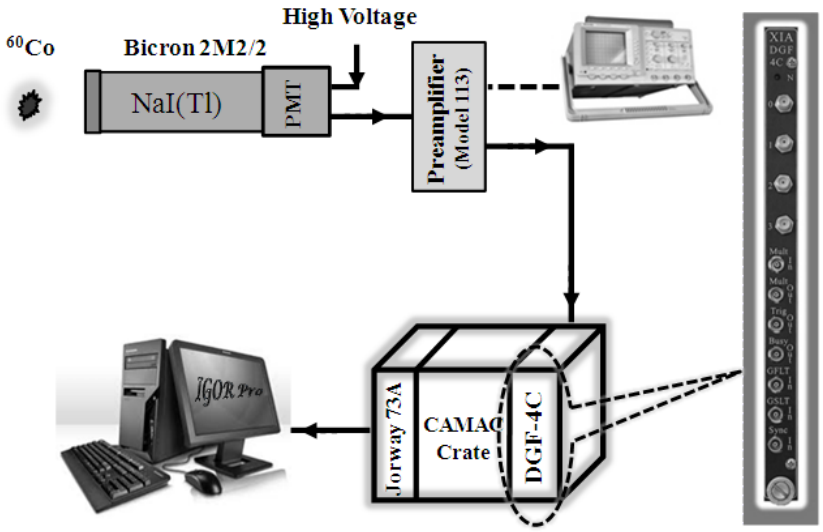

Figure 3.2. Schematic diagram of CAMAC module based time-interval acquisition system.

The same experimental and simulated data sets were used to evaluate the Bayesian (cnt), Bayesian (ti) and the frequentist method, 1.65σ. A fixed count time (1s) was used for both Bayesian (cnt) and 1.65σ methods which analyze count information. The performances of the three methods were evaluated in terms of average run length (ARL) and detection probability (1- β). To compare the three methods easily, ARL is defined here as the average time needed to issue an alarm following an increased signal. One thing to be noted is that the detection probability at the background level is the false positive rate. For radiation levels above the background, a higher detection probability is equivalent to a lower false negative rate. ARL was calculated based on a sequence of 10^5 experimental pulses or 10^6 simulated pulses at each radiation level. Detection probabilities were calculated for several detection scenarios that were fabricated based on experimental or simulated data. The most used scenario was simulated in the following

manner: after a detector system registered 5s background data, a ^{60}Co source was placed at a predetermined count rate (distance) for 5s, then the source was removed and the detector continued another 5s background counting. Using the same manner, 10^4 trials were tested at each level. In this study, we provide insight to the advantages and disadvantages of Bayesian analyses relative to the frequentist method for two distinct ways for radiation data analyses – time-intervals and counts in a fixed count time.

Results and Discussion

Experimental data were used to study the characteristics of time-intervals in a specified ROI of gamma spectrum, while the simulated data were used to investigate the effects of possible factors and modifications to Bayesian approaches for improving detection probabilities.

Bayesian Analysis without Modifications

In the analysis of experimental data, three ROIs were set to look at radiation pulses from the ^{60}Co source. Average run lengths were calculated for radiation levels within each ROI. Figure 3.3 shows the ARLs of the three methods for radiation pulses within the 1332.5 keV ROI. The frequentist detection limit was set at a level which gave α=0.05. The detection limit for both Bayesian analyses was set at a level where the parameter r from the posterior probability distribution had 95% or higher probability to be above the preset background level. Based on previous background measurements ($r_0 \sim$ 2 cps within the 1332.5 keV ROI in this case), the initial prior probability was assigned as

Gamma (2, 1) which is equivalent to 2 counts observed in 1s count time. Thus, this prior distribution provides 1s of information for the Bayesian analysis. Gamma (2, 1) was always used as the initial prior for the first data point in a sequence of observations through the study. After that, the prior was updated based on the newly available data. The rationale for using a prior with less information is to let the actual, most recent data dictate the prior distribution. Based on our study, experimental data from all the three ROIs resulted in similar results.

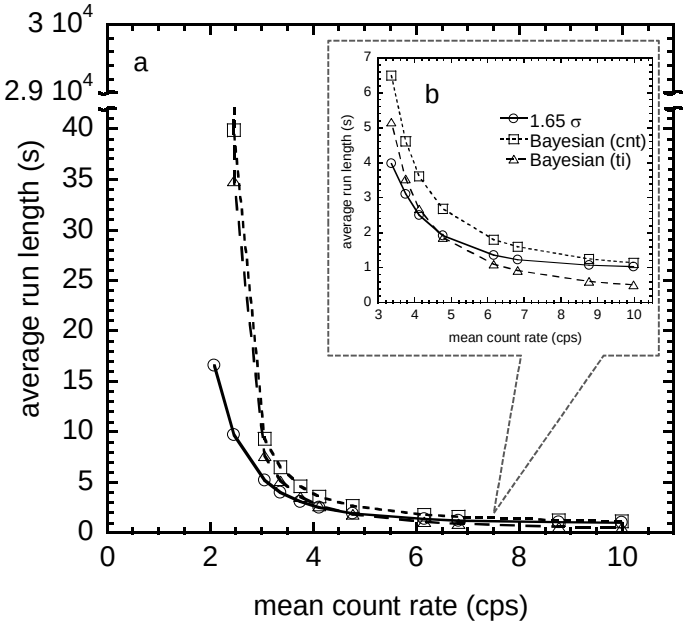

Figure 3.3. Experimental average run lengths (ARL) of the three methods for the radiation pulses within the 1332.5 keV ROI of ^{60}Co. ARLs for the radiation levels between 3.5 cps to 10 cps are zoomed in (b). Gamma (2, 1) is assigned for the initial prior in the Bayesian analyses for both types of data. Standard deviations are smaller than the symbols.

At the background level, no detection decision was made for either Bayesian method based on 2.9×10^4 seconds of data, which indicates that the Bayesian approach has

much longer ARLs than the frequentist method. A longer ARL when there is no source present implies a lower false positive rate. For frequentist statistics, the false positive rate can be calculated by $\alpha = 1/ARL$ (Montgomery 2001). When the radiation level increases, the ARLs for the Bayesian methods decrease quickly and are close to that of the frequentist method. At relatively higher radiation levels (> 4.5cps), Bayesian (ti) has a shorter ARL than other methods. Therefore, time-interval information has the ability to quickly detect a change of radiation levels. The shorter ARL implies that the Bayesian analysis with time-interval information is more sensitive to a change in radiation levels than the Bayesian analysis with count information and the frequentist method.

In Figure 3.4, the detection probability (1- β) for a scenario based on experimental data in the 1332.5 keV ROI (5s background + 5s source + 5s background) is shown. The manner to simulate the scenario is the same as explained in section III. Overall, Bayesian analyses for both count data and time-intervals result in a similar detection probability. At the background level (2.0cps), both types of Bayesian analyses have lower detection probabilities. In other words, the Bayesian method could have lower false positive rates than the frequentist method. When radiation levels are higher (~7.0 cps), the three methods show similar detection probabilities. For radiation levels between the background and the higher level, Bayesian analysis has a lower detection probability than the frequentist method. The reason for this is that Bayesian analysis incorporates the background data and prior information into its decision while the frequentist method only considers the information in the latest data point.

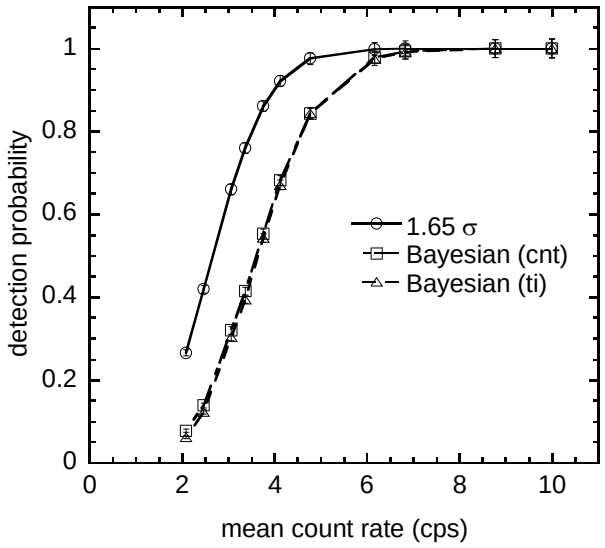

Figure 3.4. Experimental detection probabilities of the three methods for the scenario (5s background + 5s source + 5s background) using the radiation pulses within the 1332.5 keV ROI.

Figure 3.5 illustrates the average run length and detection probability obtained from simulated data. To be consistent with the background level of the experimental observation in the 1332.5 keV ROI, the background level of simulated data was set at 2.0cps throughout the study. At the background level, only one decision was made for both types of Bayesian analyses in 5.0×10^5 seconds of simulated data. The Bayesian (cnt) method made a decision at 9453 second, and Bayesian (ti) method made a decision after 8961 seconds of data. This indicates that Bayesian analyses have a long ARL at the background level. Results from simulated data are consistent with results from the experimental data. Therefore, simulation is a reasonable way to conduct a general study on the properties of Bayesian analysis. Our current study focuses on developing an algorithm to use time-interval information from a specific ROI or a full spectrum with a low count rate.

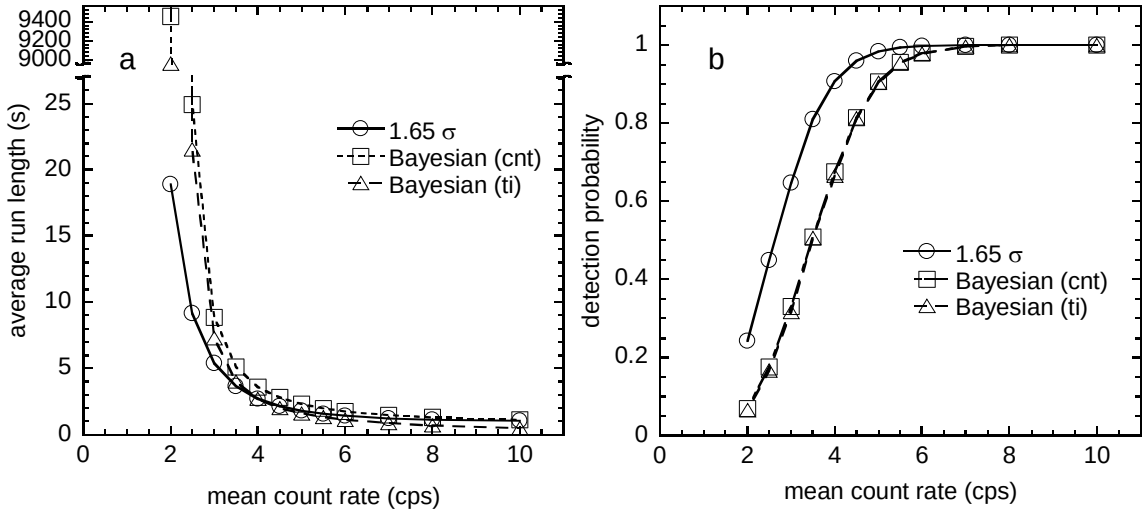

Figure 3.5. Average run length (a) and detection probability (b) of the scenario (5s background + 5s source + 5s background) for the three methods from simulated data. The background level is 2.0 cps. The same detection limits and initial prior were used. Standard deviations are smaller than the symbols.

Factors Affecting Detection Decisions

Based on simulated data, three factors, source time, detection limit, and change point, are investigated to find possible effective ways to improve detection decisions for on-line radiation monitoring. Source time is defined here as the length of time the source produces the prescribed count rate in the detector.

In Figure 3.6, the detection probabilities of the three methods for a special scenario with only 0.5s source time is shown. Since the fixed count time is 1s for the frequentist and Bayesian (cnt) methods, the 0.5s source data is followed by 0.5s background data to make it comparable to a measurement obtained in one second. As indicated in the average run length estimate, time-interval information shows its

advantage in radiation detection when radiation levels reach a higher level. When source time is limited (< count time), Bayesian (ti) could result in a higher detection probability than Bayesian (cnt) since the time-interval method needs less time to collect sufficient data to make a detection than other methods at relatively high radiation levels. For counting in a fixed count time, even radiation pulses from the source are registered at a significant count rate during its prompt presence (< count time), the overall count information obtained in the entire fixed count time is not significantly different from the background. As the result, the detector system fails to detect the source.

Figure 3.7 shows the relationship of the source time and the detection probability for four different source times: 2s, 5s, 20s and 50s. The background counts are still 5s before and after the presence of the source. With more source data available, probabilities that rise with source intensity for both types of Bayesian analyses approach the probabilities found with the frequentist method. This indicates that Bayesian analysis has the ability to reduce the false negative rate β when more data from the source are included into the decision while still keeping the false positive rate α at a low level. With more data from the source, the weight of the prior probability and the background counts on the posterior probability are diminished. On the other hand, when the amount of source data is less than that of background data (Figure 3.7(a)), the posterior is dominantly determined by the background information. As a result, the detection probabilities of both Bayesian analyses are reduced. In addition, for the cases in which a large amount of source data are available, the advantage of time-interval information to respond to the change quickly becomes less important, but it is still the better option than

count information when the time to make the detection is one of the concerns for radiation monitoring.

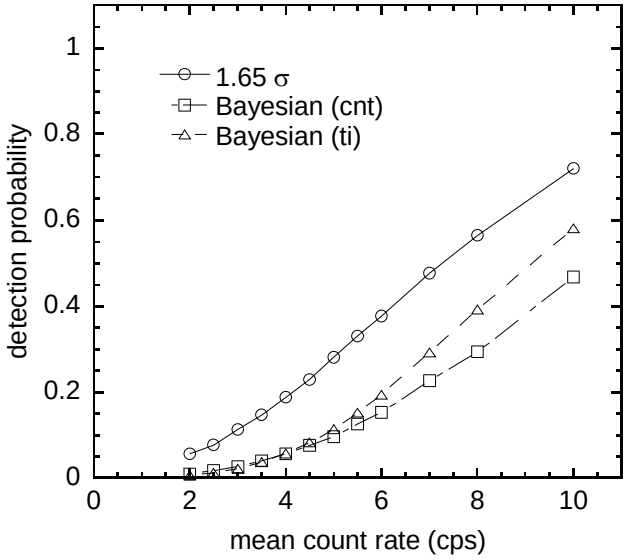

Figure 3.6. Detection probabilities of the three methods for the scenario with only 0.5s source time. After the source count, 0.5s background count is followed to make it as a 1s measurement. Standard deviations are smaller than the symbols.

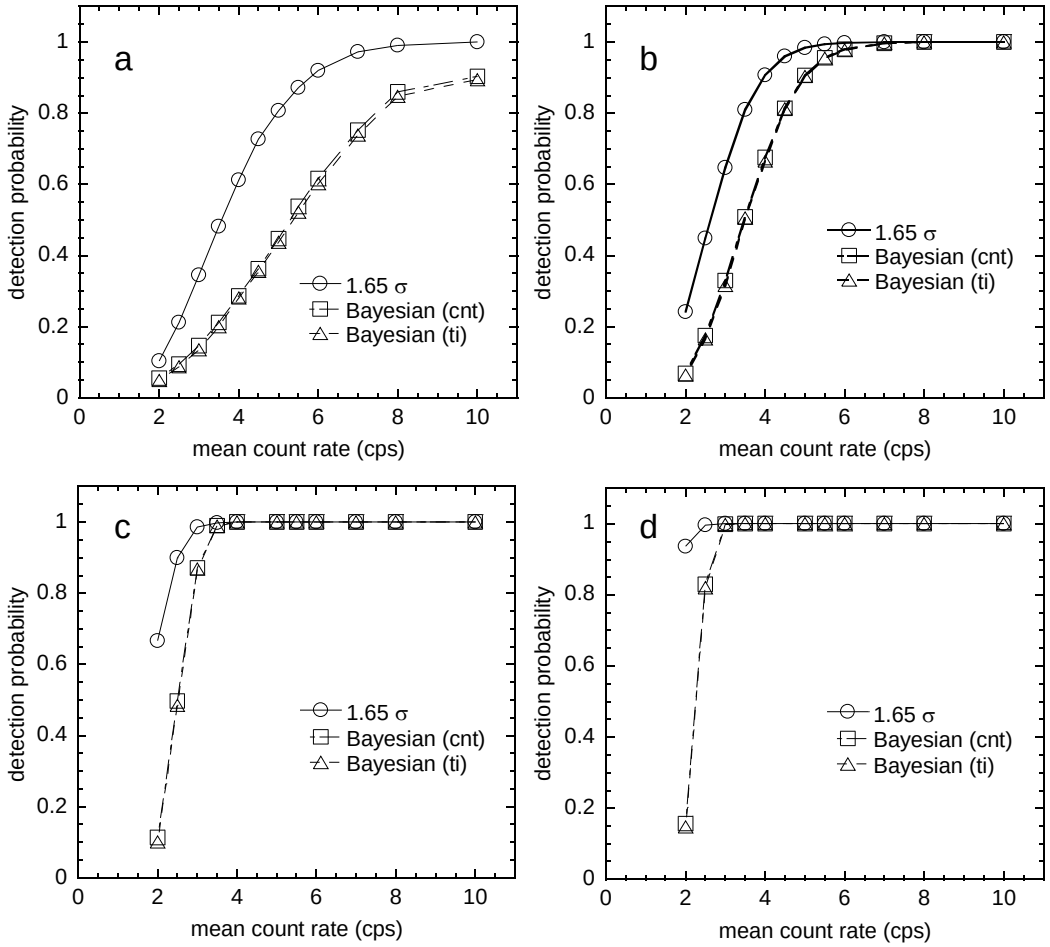

Figure 3.7. Detection probabilities of the three methods for scenarios: (a) 2s, (b) 5s, (c) 20s, and (d) 50s source time. Background counts are 5s before and after the designated source time. Standard deviations are smaller than the symbols.

One example illustrating the effect of detection limit is shown in Figure 3.8 when the detection limit for the Bayesian analyses was changed from 95% to 60%. The scenario being analyzed is the same as that corresponding with the data being presented in Figure 3.7(c). Compared to the result shown in Figure 3.7(c), the performance of Bayesian analyses are improved by adjusting the detection limit to a lower level. With the

new detection limit, Bayesian analyses have the same false negative rates as the frequentist method but with lower false positive rates than the frequentist method. When 60% detection limit was used, the ARL for the Bayesian methods was an order of magnitude greater than the frequentist method at the background level. For the elevated radiation levels above the background, the ARL of the Bayesian methods is below that for the frequentist method. The choice of the detection limit to adjust the false positive rate and false negative rate is based on people's preference or special needs for the radiation monitoring.

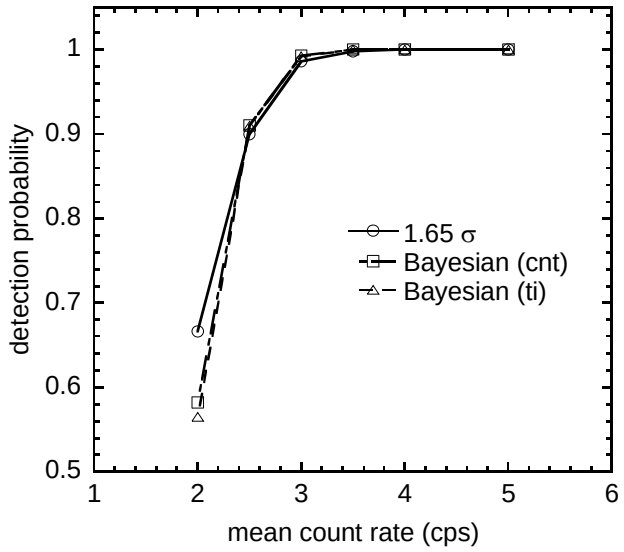

Figure 3.8. Detection probabilities of the three methods for scenario with 20s source data (5s background + 20s source + 5s background) when the detection limit for Bayesian analyses was set at a level where the parameter *r* from the posterior probability distribution was 60% or more to be above the preset background. Standard deviations are smaller than the symbols.

The effect of the change point was investigated at the radiation level of 4.0 cps and shown in Figure 3.9. The level of 4.0 cps is the median level between the background level and the level where the three methods will have the same detection probabilities.

The scenario consists of an amount of background data (from 0s to 20s) followed by 5s of source data at 4.0 cps, then followed by another 5s background. The change point determines the amount of background data that will be included in Bayesian inferences. The greater contribution of the background data is on the detection decision when more background data are incorporated. When source data are abundant, the effect of the change point can be eventually diminished, but the detection decision would be delayed. For the cases where source data are limited, the detection decision will be deteriorated. Therefore, a modification to the Bayesian analysis is needed to alleviate the effect of the change point.

Modified Bayesian Analysis

Using the modified method described in the theory section to update the prior, the detection probabilities of modified Bayesian analyses for the same scenarios in Figure 3.9 are shown in Figure 3.10 and Figure 3.11. Figure 3.10 shows the results for Bayesian analyses of count information and Figure 3.11 shows the results for Bayesian analyses of time-interval information. The detection limit for both modified Bayesian analyses was again set at 95%. The two-stage limit is set as 5 s/10 s for count information, and 10 pulses/20 pulses for time-interval information. The discriminator is established at 70% for both types of data. For the scenario with 5s background data (2.0 cps), there are about 20% of trials with the parameter from the posterior distribution having more than 70% to be above the preset background level. In contrast, the scenario with 5.0s of 2.5 cps data, 50% of trials pass the discriminator. The fixed length of data for the moving prior method is set at 5 s for count data and 10 pulses for time-interval data.

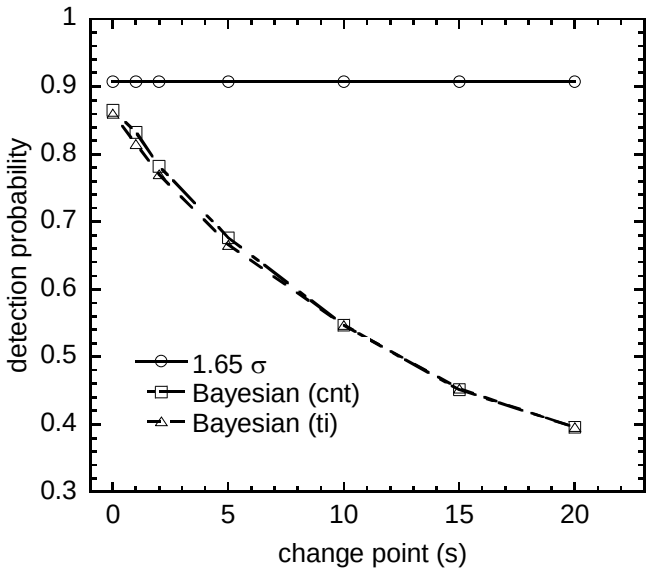

Figure 3.9. Detection probabilities of the three methods for scenarios with different change points. The source time for the scenarios is 5s at 4.0cps, followed by 5s background count. Standard deviations are smaller than the symbols.

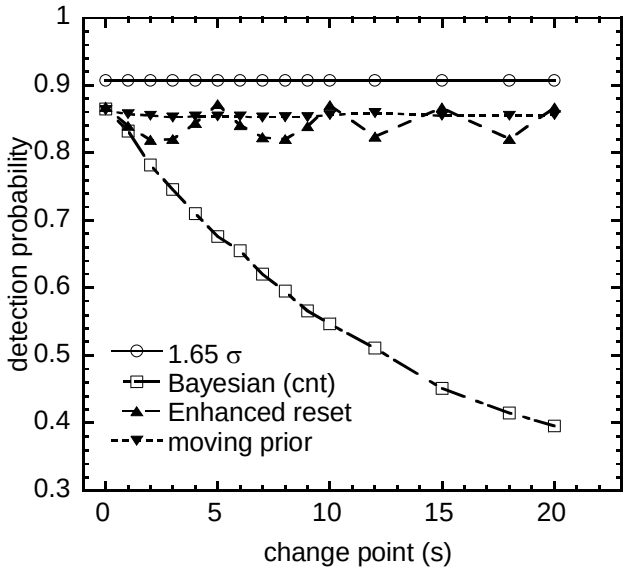

Figure 3.10. Detection probabilities of the modified Bayesian analyses with count information for scenarios with different change points for 4.0 cps level. Standard deviations are smaller than the symbols.

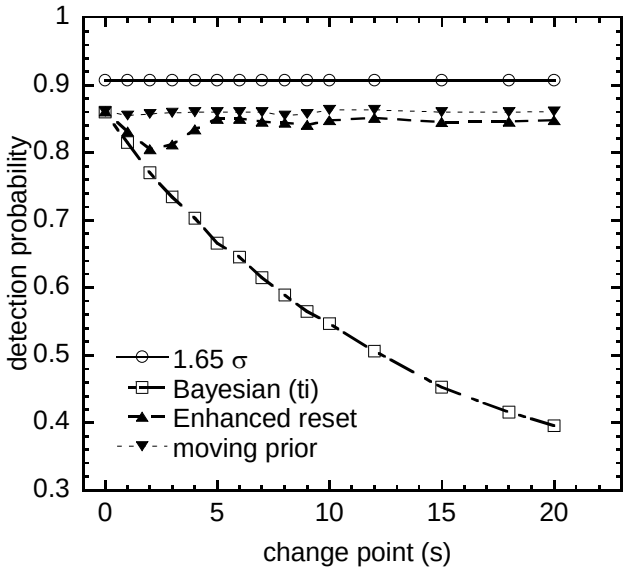

Figure 3.11. Detection probabilities of the modified Bayesian analyses with time-interval information for scenarios with different change points for 4.0 cps level. Standard deviations are smaller than the symbols.

As designed, both modified Bayesian analysis methods resulted in a higher detection probability (lower false negative rates) than the Bayesian analyses without modifications. The performances of the two modified methods are independent of the change point relative to the Bayesian analyses without modifications. The detection probability of the enhanced reset method shows a periodical fluctuation when count information is utilized. In contrast, the fluctuation only shows up at the beginning when the change point happens earlier for time-interval data. This difference results from the different settings of the two-stage limit and different random number of data points between count data and time-interval data.

Conclusion

Bayesian analysis has the ability to include previous data into detection decisions, which results in lower false positive rate than the frequentist method, and has the possibility to reduce false negative rate with more data collected. The main difficulties that could discourage people to use Bayesian statistics are the conceptual understanding, and the complexity and heavy load of the computation. The special features of time-intervals provide an alternative for low-level radiation monitoring. When Bayesian methods are applied for on-line time series data, time-interval information shows a similar performance as count information. In the situation where the source data are limited (source time < count time), time-interval information is more sensitive to detect the change than the count information acquired in an entire count time. Without considering other factors (e.g. detection system and analyzing process) that may affect the time needed for detection decision, time-interval information has the potential to respond quickly at relatively higher radiation levels. The proposed modified Bayesian analyses are relatively independent of the change point at which the radiation level is changed from the background to an elevated level. Time-interval information is preferred if other factors are the same.

Acknowledgement

We would like to thank DOE Environmental Management Science Program (Grant no. DE-FG02-07ER64411) for financial support. And we thank Hui Tan from XIA Inc. for the valuable instruction to DGF-4C manipulation and help on modifying the DGF-4C firmware to register radiation pulses within a specified ROI.

References

Arandjelovic, V., A. Koturovic, and R. Vukanovic. 2002. A software method for suppressing statistical fluctuations in preset count digital-rate meter algorithms. *IEEE Transactions on Nuclear Science* 49, (5 Part 3): 2561-6.

Bochud, F. O., C. J. Bailat, and J. P. Laedermann. 2007. Bayesian statistics in radionuclide metrology: Measurement of a decaying source. *Metrologia* 44, (4) (AUG): S95-S101.

Bolstad, W. M. 2007. *Introduction to Bayesian statistics.* New Jersey: Wiley-IEEE.

Currie, L. A. 1968. Limits for qualitative detection and quantitative determination - application to radiochemistry. *Analytical Chemistry* 40, (3): 586-93.

DeVol, T. A., A. A. Gohres, and C. L. Williams. 2009. Application of classical versus Bayesian statistical control charts to on-line radiological monitoring. *Journal of Radioanalytical and Nuclear Chemistry* 282, (3) (DEC): 933-8.

Dowdy, E. J., C. N. Henry, R. D. Hastings, and S. W. France. 1978. Neutron detector suitcase for the nuclear emergency search team. *Los Alamos Scientific Lab. Report LA*-7108.

Gelman, A. 2004. *Bayesian data analysis.* New York: CRC press.

Groer, P. G., and Y. Lo. 1996. Measurement of airborne Po-218 - A Bayesian approach. *Health Physics* 71, (6) (DEC): 951-5.

Kaeker, R., and A. Jones. 2003. On use of Bayesian statistics to make the guide to the expression of uncertainty in measurement consistent. *Metrologia* 40, (5): 235-48.

Kenett, R., and S. Zacks. 1998. *Modern industrial statistics: Design and control of quality and reliability.* California: Duxbury Press.

Knoll, G. F. 2010. *Radiation detection and measurement*. 4th ed. New Jersey: John Wiley & Sons Inc.

Laedermann, J. P., J. F. Valley, and F. O. Bochud. 2005. Measurement of radioactive samples: Application of the Bayesian statistical decision theory. *Metrologia* 42, (5) (OCT): 442-8.

Little, R. J. A. 1982. The statistical-analysis of low-level radioactivity in the presence of background counts. *Health Physics* 43, (5): 693-703.

Luo, P., T. A. DeVol, and J. L. Sharp. 2010. Sequential probability ratio test using scaled time-intervals for environmental radiation monitoring. *IEEE Transactions on Nuclear Science* 57, (3): 1556-62.

Miller, G., W. C. Inkret, T. T. Little, H. F. Martz, and M. E. Schillaci. 2001. Bayesian prior probability distributions for internal dosimetry. *Radiation Protection Dosimetry* 94, (4): 347-52.

Miller, G., W. C. Inkret, and H. F. Martz. 1993. Bayesian detection analysis for radiation exposure. *Radiation Protection Dosimetry* 48, (3): 251-6.

Miller, G., H. F. Martz, T. T. Little, and R. Guilmette. 2002. Using exact poisson likelihood functions in Bayesian interpretation of counting measurements. *Health Physics* 83, (4) (OCT): 512-8.

Montgomery, D. C. 2001. *Introduction to statistical quality control.* New York: John Wiley & Sons.

Panofsky, W. K. H. 2003. Nuclear proliferation risks, new and old. *Issues in Science and Technology* 19, (4): 73-4.

R Development Core Team. 2010. The R project for statistical computing. http://www.r-project.org/.

Strom, D. J., and J. A. MacLellan. 2001. Evaluation of eight decision rules for low-level radioactivity counting. *Health Physics* 81, (1) (JUL): 27-34.

U.S. Department of Energy. 2004. *Transport of contaminants in subsurface environments at DOE sites.* DE-FG01-05ER05-12.

Weise, K., K. Huebel, E. Rose, M. Schlaeger, D. Schrammel, M. Taeschner, and R. Michel. 2006. Bayesian decision threshold, detection limit and confidence limits in ionizing-radiation measurement. *Radiation Protection Dosimetry* 121, (1) (DEC): 52-63.

XIA. 2004. *User's manual digital gamma finder (DGF) DGF-4C*. Newark, CA: X-Ray Instrumentation Associates.

CHAPTER 4

CUSUM ANALYSIS OF TIME-INTERVAL DATA FOR ON-LINE RADIATION MONITORING

Abstract

Three statistical control charts methods were investigated to determine the one with the highest detection probability and the best average run length (ARL). The three control charts include: the Shewhart control chart of count data, cumulative sum (CUSUM) analysis of count data (Poisson CUSUM) and CUSUM analysis of time-interval (time difference between two consecutive radiation pulses) data (time-interval CUSUM). The time-interval CUSUM control chart was compared with the Poisson CUSUM and the Shewhart control charts with experimental and simulated data. The experimental data were acquired with a DGF-4C (XIA, Inc) system in list mode. Simulated data were obtained by using Monte Carlo techniques to obtain a random sampling of a Poisson process. All statistical algorithms were developed using R (R Core Development Team, 2010). Detection probabilities and ARLs for the three methods were compared. The time-interval CUSUM control chart resulted in a similar detection probability as that of the Poisson CUSUM control chart, but had the shortest ARL at relatively higher radiation levels, e.g., about 40% shorter than the Poisson CUSUM at 10.0cps. Both CUSUM control charts resulted in a higher detection probability than that of the Shewhart control chart, e.g., 100% greater than the Shewhart control method at 4.0cps. In addition, when time-interval information was used, the CUSUM control chart

coupled with a modified runs rule ($mrCUSUM_{ti}$) showed the ability to further reduce the time needed to respond to changes in radiation levels, and keep the false positive rate at a required level.

Introduction

On-line radiation monitoring is essential to the U.S. Department of Energy (DOE) Environmental Management Science Program for cleaning up media contaminated with anthropogenic radionuclides (U.S. DOE 2004). The goal of on-line radiation monitoring is to quickly detect small changes in radioactivity levels in the presence of a significant ambient background. In the case of low-level or background-dominant radioactivity, two factors make it difficult to distinguish between a radioactive source and natural background. First, the random nature of radioactive decay results in an inherent uncertainty in the number of registered radiation particles in a detector. It is well recognized that the number of emitted particles and the number of particles registered in a detector are Poisson distributed. Second, radiation from natural radionuclides in the environment and cosmic radiation are involved into the gross counts registered by the detector (Laedermann et al. 2005). Generally, the decision regarding whether or not a radioactive source is present is made based on a specific statistical method. In practice, a proper statistical method is chosen to minimize the false negative rate β (or maximize the detection probability, 1- β) while holding the false positive rate α at a desired level.

The Shewhart control chart is a classical statistical method that is commonly used in radiation monitoring. It is also referred to as the single-interval-test (Jarman et al.

2004). The Shewhart control chart monitors the mean radiation level based on the radiation counts registered in a fixed-length count time and a detection limit (*DL*) that is set for a given false positive rate. One major disadvantage of the Shewhart method is that only the information contained in the latest data point is exploited, and the information contained by the entire sequence of data points is disregarded. As a result, the Shewhart method is relatively insensitive to small changes in radiation levels while it readily detects large shifts (Montgomery 2001). Therefore, more sophisticated statistical methods have been developed and adopted to detect small changes in radiation levels. The cumulative sum (CUSUM) control chart is one of the most effective charts for detecting small shifts in radiation levels since the CUSUM chart has a shorter average run length (ARL) than the standard Shewhart control chart (Kenett and Zacks 1998). ARL is generally defined as the average number of observations taken before a shift is detected and an out-of-control alarm is issued.

The CUSUM control chart was first introduced by Page (1954) as an alternative to the Shewhart control chart for quality control and improvement in manufacturing processes. Instead of considering the most recent data point, the CUSUM control chart incorporates all of the information contained in a sequence of data points by accumulating deviations of data points over time. For this reason, the CUSUM chart is more effective than the Shewhart control chart to detect small shifts (Montgomery 2001). Because of its effectiveness to detect small shifts, the CUSUM control chart is a good candidate for environmental radiation monitoring (DeVol et al. 2009; Hughes and DeVol 2008; Marshall 1977). Marshall (1977) suggested the use of the CUSUM control chart for

monitoring the background radiation level from a radiochemical counter. According to Marshall's study, the CUSUM control chart could detect abrupt changes of the order of one standard deviation. Hughes and DeVol (2008) evaluated the performance of the CUSUM control chart compared to the 3-sigma Shewhart and the exponentially weighted moving average (EWMA) control charts. The comparison was conducted based on time series radiation counter data from flow cells. The results showed that the CUSUM method was suitable to detect the radioactivity by requiring less solution volume and gave the best estimation of sample concentration. In addition, the study by DeVol et al. (2009) showed that the CUSUM control chart had overall comparable performance to control the false negative rate relative to the Shiryayev-Roberts control chart.

For count data such as the number of radiation pulses registered in a detector, Lucas (1985) provided detailed descriptions about the design and implementation procedures of the CUSUM control chart. In his study, the Poisson CUSUM control chart and the "time-between-events CUSUM" control chart were discussed in terms of determining the reference value k and the decision interval value h. For the Poisson CUSUM method, the number of counts recorded in a sampling interval is modeled by the Poisson distribution. Accordingly, the time between two consecutive events of concern follows the exponential distribution. In the radiation monitoring and measurement process, 'event' is a radiation interaction registered in a detector, and 'time' is the time difference (time-interval) between two consecutive radiation pulses. In this study, the time-between-events CUSUM control chart is referred to as the "time-interval CUSUM" control chart. To improve the sensitivity of the CUSUM control chart for the process that

an out-of-control situation occurs at start-up, Lucas and Crosier (1982a) devised the fast initial response (FIR) CUSUM (FIRCUSUM). In addition, Lucas and Crosier (1982b) proposed the robust CUSUM (rCUSUM) by coupling the basic CUSUM with a runs rule (two-in-a-row rule whereby two observations in a row occur outside of a preset control limit) to guard against an out-of-control signal occurring for reasons other than a true process shift. Recently, time-between-events CUSUM control charts have drawn increasing interest as an alternative to traditional control charts for monitoring the occurrence rate of rare events, such as the occurrence of industrial accidents and congenital malformations (Vardeman and Ray 1985; Liu et al. 2006; Cheng and Chen 2010; Xie et al. 2010)). The general measure of effectiveness for a control chart is the average run length (ARL) where the ARL is as the average time needed to make a decision to alarm following a change point. The performances of the Poisson CUSUM control chart and the time-interval CUSUM control chart are evaluated on the basis of ARL.

In radiation detection and monitoring, count information in a fixed count time is commonly recorded for further analyses since it is technically easier to handle. Utilization of time-interval information in radiation measurements has been discussed by several authors. By limiting time-intervals to a pre-assigned range, Arandjelovic et al. (2002) developed an algorithm for preset count digital-rate meters to suppress statistical fluctuations of mean count rate measurements. Dowdy et al. (1978) devised a portable neutron detection system to search for neutron-emitting radioactive materials based on S-fold time-interval measurements. Sakaue et al. (2007) assembled a portable system to

monitor artificial radionuclides in airborne dust using time-interval distribution from correlated decay events.

The objective of this study was to investigate the time-interval CUSUM for its applicability towards on-line radiation monitoring. Advantages and disadvantages of the time-interval CUSUM control chart were compared to that of the Poisson CUSUM and the Shewhart control chart. Registering counts in a fixed count time and registering time-intervals provide us with two different data sampling methods. Since the time needed to record a statistically significant number of pulses could be shorter than counting for a fixed count time, time-interval information possesses the potential to reduce the sampling time and respond quickly to abrupt changes in radiation levels. In addition, a robust CUSUM based on time-interval information coupled with a modified runs rule ($mrCUSUM_{ti}$) was proposed to improve the performance of CUSUM schemes for the radiation monitoring. The runs rule applied in this study is the two-in-a-row rule which is similar to that by Lucas and Crosier (1982b). When the runs rule was coupled with time-interval CUSUM, a modification was made to incorporate more previous information into the decision-making.

Theory and Methods

Time-interval Distribution

The random nature of radioactive decay is characterized as a Poisson process when the number of nuclei is large and the observation time is short compared with the half-life of the radioactive species. The probability $P(m)$ for observing m decays (m=0, 1,

2, …) in a time interval t is given by the Poisson distribution,

$$P(m) = \frac{(rt)^m}{m!} e^{-rt} \quad , \tag{4. 1}$$

where r is the mean count rate.

The time-interval density, *f(t)*, is usually employed to characterize the time-interval distribution. The probability of the next event taking place in dt after a delay of time t since the last event is denoted as $f(t)dt$. For the Poisson process, the probability for the next event to occur in dt is:

$$f(t)dt = re^{-rt}dt \quad , \tag{4. 2}$$

where e^{-rt} is the probability of no events from time 0 to t, for $t \geq 0$. The density function expressed in (4.2) is commonly referred to as the exponential distribution (Knoll 2010).

Review of CUSUM Control Charts

The CUSUM control chart is obtained by accumulating the difference between an observed value x_i and a reference value k with a statistic C_i. If the process is in control, the statistic C_i will consist of a random walk around the mean value of the process, but if C_i is continuously increasing or decreasing, a change in the process is indicated. An out-of-control alarm is triggered if the statistic C_i equals or exceeds a preassigned decision interval value h. The most widely used application in radiation detection and monitoring is the detection of an increase in count rate. When count information is used to estimate

the strength of the radiation level, the Poisson CUSUM statistic at the i^{th} observation is determined by

$$C_{cnt,i} = \max(0, x_{cnt,i} - k_{cnt} + C_{cnt,i-1}) , \quad (4.3)$$

where max(*a*,*b*) is the maximum of *a* and *b*, *"cnt"* denotes the observed count data (number of the radiation pulses registered in a fixed count time) which is Poisson distributed. When the count time is set as a unit of time (e.g., 1 second), the reference value k_{cnt} recommended by Lucas (1985) is given by

$$k_{cnt} = (r_d - r_a)/(\ln(r_d) - \ln(r_a)) , \quad (4.4)$$

where r_a is the acceptable mean count rate when the radiation strength is at background level and r_d is the mean count rate when the radiation strength is at the level that the CUSUM scheme is to detect quickly. If the count time, t_c, is not a unit of time, count rate r (r_a and r_d) will be substituted by count data observed in t_c for certain level, and $k'_{cnt} = k_{cnt} \times t_c$. After k_{cnt} is determined, the decision interval value h_{cnt} is chosen on the basis of ARLs in combination with the reference value to provide good ARL performance (Lucas 1985). The value of h_{cnt} should give an appropriately large ARL when the radiation level is at the background level (ARL_0), and give an appropriately small ARL when the radiation level changes to a level that should be detected quickly.

When time-interval information is used to monitor the strength of the radiation level, the most common application is to detect a decrease in time-interval. For this case, the time-interval CUSUM statistic at the i^{th} observation is given by

$$C_{ti,\,i} = \max(0, k_{ti} - x_{ti,\,i} + C_{ti,\,i-1}) , \qquad (4.\ 5)$$

where "*ti*" denotes that the CUSUM control chart is designed for the time-interval information that follows the exponential distribution. The reference value k_{ti} recommended by Lucas (1985) is given by

$$k_{ti} = (\ln(r_d) - \ln(r_a))/(r_d - r_a) \ . \qquad (4.\ 6)$$

Similarly, the decision interval value h_{ti} for the time-interval CUSUM is selected to give appropriate ARLs as designed.

For a standard CUSUM ($CUSUM_{ti}$ or $CUSUM_{cnt}$) control chart, the starting value of the statistic C is typically zero (C_0=0). When the FIR feature is implemented ($FIRCUSUM_{ti}$ or $FIRCUSUM_{cnt}$) to respond rapidly to an initial out-of-control situation, an initial positive "head start" value is used, such as, $C_0=h/2$ (Lucas 1985; Lucas and Crosier 1982a). The decision interval value h_{cnt} or h_{ti} will be substituted for h. In this study, all statistical algorithms for the CUSUM control charts were developed using the statistical software package R (R Development Core Team 2010).

Time-Interval CUSUM with Runs Rules

In this study, a runs rule (called the two-in-a-row rule) is incorporated into the time-interval CUSUM control chart ($rCUSUM_{ti}$) to increase the sensitivity when time-interval information is used to monitor the radiation strength. With the two-in-a-row rule, whenever two successive time-interval observations that could result in an out-of-control

signal are observed, an alarm signal is issued regardless of whether or not the CUSUM statistic $C_{e,i}$ has accumulated strong enough evidence to indicate a change in the background radiation level. A control limit is preassigned to determine if a time-interval observation could trigger an out-of-control signal. The control limit is set based on the background radiation level and the time-interval probability density. For example, when the control limit is set at 10ms, whenever two time-intervals that are both less than 10ms are observed consecutively, an alarm signal is issued. For a background level of 2.0cps, there is about 0.04% probability to observe two consecutive time-intervals that are less than 10ms.

In general, the use of two-in-a-row rule can increase the sensitivity of the CUSUM control chart, but may also produce more false positives when the radiation level is at the background level (Cheng and Chen 2010). To hold the required false positive rate constant, a modified runs rule is proposed for the time-interval CUSUM ($mrCUSUM_{ti}$) in this study. For the modified runs rule, whenever two successive time-intervals that could result in an out-of-control signal are observed, a number of most recent time-intervals including the current one are investigated to see if these measurements are consistent with the background. To quantify the consistency, an instantaneous count rate is calculated based on the most recent time-intervals that are measured. An instantaneous count rate limit, μ_I, is set based on the background count rate and compared with the measured instantaneous count rate. If the measured instantaneous count rate is higher than μ_I, an alarm is issued even though the CUSUM statistic $C_{e,i}$ has not accumulated sufficient evidence to issue an alarm. For example, when two time-

intervals that could result in an out-of-control signal are observed consecutively, an instantaneous count rate is calculated as 5.5cps based on the most recent five time-intervals. If the limit μ_I is set at 4.0cps, an alarm is issued since the instantaneous count rate is higher than μ_I.

According to different settings for the starting value C_0 and the runs rule, there are two types of Poisson CUSUM and four types of time-interval CUSUM that were applied to this study. To help readers differentiate different types of CUSUM analyses applied in this study, Table 4.1 lists the notation for each type of CUSUM analysis and h values for count and time-interval data for the situation with r_a = 2.0cps and r_d =4.0cps. The h_{ti} values were determined based on a given h_{cnt} value: both $CUSUM_{cnt}$ and $CUSUM_{ti}$ gave approximately the same ARL_0 for a given monitoring situation (r_a, r_d). The DL of the Shewhart control chart was determined by using a similar method. DL=8.0 listed in the table is the detection limit of the Shewhart method to give the closest ARL_0 as that of $CUSUM_{cnt}$ for the given h_{cnt}=7. Using this methodology, the three control charts theoretically have the same false positive rate ($1/ARL_0$) at the background level. The same h_{cnt} or h_{ti} values were also used for other CUSUM control charts, $FIRCUSUM_{ti}$ or $FIRCUSUM_{cnt}$, $rCUSUM_{ti}$ and $mrCUSUM_{ti}$.

Table 4.1. Types of CUSUM analyses for count data/time-interval data and h values for the situation of r_a = 2.0cps and r_d =4.0cps.

Methods	Definition	Notation	Count (cnt) data (Poisson CUSUM)	Time-interval (ti) data (Time-interval CUSUM)
Standard CUSUM	$C_0 = 0$	$CUSUM_{ti}$ or $CUSUM_{cnt}$	h_{cnt} = 5, 7, 10	h_{ti}=1.9, 2.7, 3.7
CUSUM with FIR	$C_0 = h/2$	$FIRCUSUM_{ti}$ or $FIRCUSUM_{cnt}$	h_{cnt} = 5, 7, 10	h_{ti}=1.9, 2.7, 3.7
Robust CUSUM	coupled with two-in-a-row rule	$rCUSUM_{ti}$	—	h_{ti} = 2.7
Modified Robust CUSUM	coupled with modified two-in-a-row rule	$mrCUSUM_{ti}$	—	h_{ti}=2.7
Shewhart	a classical method	—	DL =8.0	—

Experimental Instruments and Simulation

Shown in Figure 4.1 is the schematic diagram of the radiation acquisition system used to collect the experimental data. It is the same system that was used for our previous studies on time-interval analyses (Luo et al. 2010, 2011). Gamma radiation (E_γ = 1173.2 keV and 1332.5 keV) from a ^{60}Co source (~14,000 Bq) was detected using a NaI(Tl) scintillation detector. The output from a preamplifier (ORTEC model 113) was digitized by a DGF-4C module (XIA, Inc) which was controlled through a graphical user interface running under IGOR Pro. 4.03 (XIA 2004). Using list mode, a binary output file containing time stamp information was prepared by the DGF-4C module for off-line analyses. The time resolution is 25 ns. A region of interest (ROI) was set to study the radiation pulses from a full energy peak. In this case, the 1332.5 keV peak was studied mostly. By adjusting the distance from the source to the detector, experimental data for low-level radiation (2-10 cps for the 1332.5 keV peak) were acquired. At each level, about 10^5 radiation pulses were registered to provide for a good general comparison among the methods.

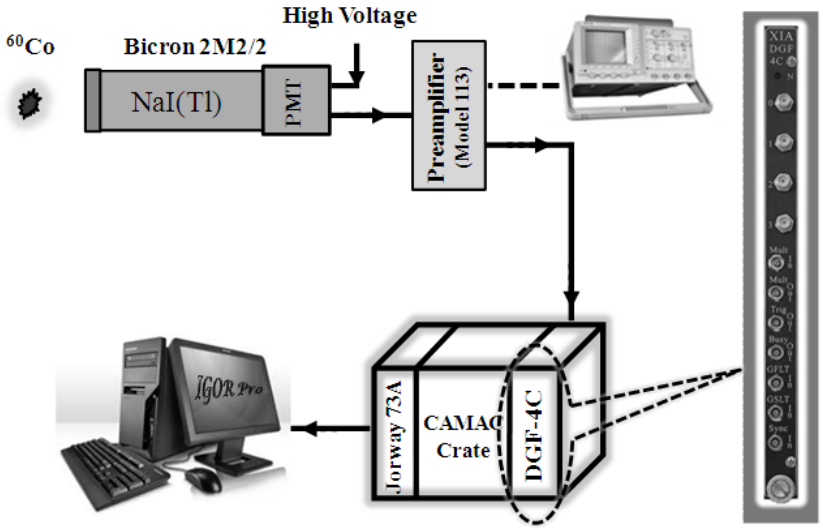

Figure 4.1. Schematic diagram of CAMAC module based time-interval acquisition system.

In addition, a Monte Carlo method was employed to simulate a random radiation sampling based on the time-interval density function given in (4.2). The simulation was conducted in IGOR Pro. At each radiation level, 10^6 random pulses were simulated. To be consistent with the background level of the experimental observation in the 1332.5 keV ROI, the background level of simulated data was set at 2.0cps throughout the study.

The same experimental and simulated data sets were used to evaluate the time-interval CUSUM, the Poisson CUSUM and the Shewhart control charts. A fixed count time (1s) was used for both the Poisson CUSUM and the Shewhart methods which analyzed count data. The performances of the three methods were evaluated in terms of ARL and detection probability (1- β). One thing to be noted is that the detection

probability at the background level is the false positive rate. For radiation levels above the background, a higher detection probability is equivalent to a lower false negative rate. Detection probabilities were calculated for several detection scenarios that were fabricated based on experimental or simulated data. The most used scenario was simulated in the following manner: after a detector system registered 5s of background data, a ^{60}Co source was placed at a predetermined count rate (distance) for 5s, then the source was removed and the detector continued another 5s of background counting. Using the same manner, 10^4 trials were tested at each level. In this study, we provide insight to the advantages and disadvantages of two distinct ways for radiation data analyses – the time-interval CUSUM and the Poisson CUSUM control charts relative to the Shewhart control chart.

Results and Discussion

Performances of $CUSUM_{cnt}$, $CUSUM_{ti}$, $FIRCUSUM_{cnt}$, $FIRCUSUM_{ti}$, $rCUSUM_{ti}$, and $mrCUSUM_{ti}$ were investigated primarily based on simulated radiation data in terms of ARLs and detection probabilities. Experimental data were used to validate the result obtained from simulated data.

Standard CUSUM and CUSUM Charts with FIR

To visually compare ARLs among the three types of control charts, the ratios of the ARL of other types of CUSUM schemes (e.g., $CUSUM_{ti}$ and $rCUSUM_{ti}$) or the

Shewhart control chart versus that of $CUSUM_{cnt}$ were calculated at each radiation level. Figure 4.2 shows the ratios, ARL_{ti}/ARL_{cnt} and $ARL_{Shewhart}/ARL_{cnt}$, for three different h_{cnt} values at the situation with r_a = 2.0cps and r_d =4.0cps. ARL_{ti} is the ARL of any type of the time-interval CUSUM, ARL_{cnt} is the ARL of any type of the Poisson CUSUM, and $ARL_{Shewhart}$ is the ARL of the Shewhart control chart, respectively. Unless otherwise specified, the situation with r_a = 2.0cps and r_d =4.0cps is the same for other results shown in this paper. The h_{cnt} value was chosen for each of 5, 7, 10, and the corresponding h_{ti} values were chosen at h_{ti}=1.9, 2.7 and 3.7, respectively.

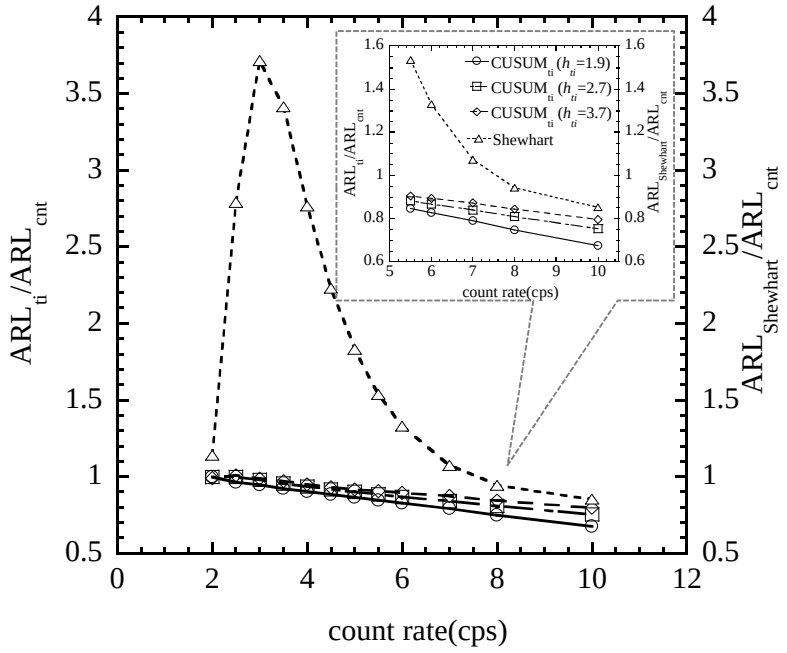

Figure 4.2. ARL_{ti}/ARL_{cnt} for three different h_{cnt} values, 5, 7, and 10, and $ARL_{Shewhart}/ARL_{cnt}$ for h_{cnt}=7. ARL_{ti} is the ARL of any type of the time-interval CUSUM, ARL_{cnt} is the ARL of any type of the Poisson CUSUM, and $ARL_{Shewhart}$ is the ARL of the Shewhart control chart, respectively. ARL ratios for the radiation levels between 5.5cps and 10.0cps are zoomed in the inset. Standard deviations are smaller than the symbols.

Overall, both $CUSUM_{ti}$ and $CUSUM_{cnt}$ have shorter ARLs than that of the Shewhart control chart over the relatively low radiation levels (≤ 8.0cps), especially for the levels from 2.5cps to 5.0cps. Shorter ARLs indicate that both the CUSUM control charts are more sensitive to a small increase in the background radiation level than the Shewhart method. Compared to $CUSUM_{cnt}$, the ARL of $CUSUM_{ti}$ is relatively shorter than that of $CUSUM_{cnt}$, and monotonically decreases with the increase of the radiation level. At 10.0cps, the ARLs of $CUSUM_{ti}$ are 20%-40% shorter than that of $CUSUM_{cnt}$ for the corresponding different *h* values. The comparison implies that the time-interval information can further improve the sensitivity of the CUSUM control chart to detect a change in the background radiation level. Our study shows very similar results for other situations with both higher and lower alarm levels, r_d.

In Figure 4.3, the ARL ratios between $FIRCUSUM_{ti}$ or $FIRCUSUM_{cnt}$ and $CUSUM_{cnt}$ for three different h_{cnt} values are shown. The *h* values for CUSUM control charts with or without the FIR feature were the same as used for the study shown in Figure 4.2. $ARL_{FIR,\ cnt}$ represents the ARL of $FIRCUSUM_{cnt}$, while $ARL_{FIR,ti}$ represents the ARL of $FIRCUSUM_{ti}$.

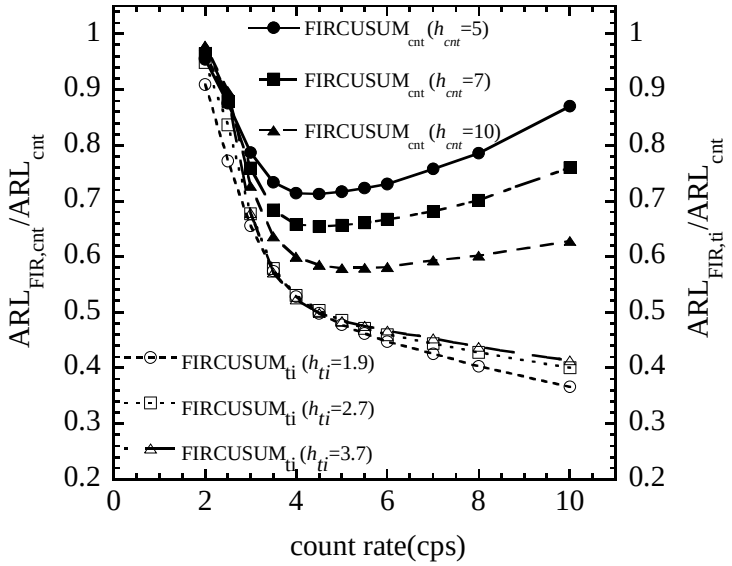

Figure 4.3. ARL Ratios for CUSUM analyses with FIR feature, $FIRCUSUM_{ti}/CUSUM_{cnt}$ and $FIRCUSUM_{cnt}/CUSUM_{cnt}$. $ARL_{FIR,cnt}$ represents the ARL of FIRCUSUMcnt, while $ARL_{FIR,ti}$ represents the ARL of $FIRCUSUM_{ti}$. Standard deviations are smaller than the symbols.

Generally, both $FIRCUSUM_{ti}$ and $FIRCUSUM_{cnt}$ result in a more rapid response to changes in radiation levels than does $CUSUM_{cnt}$. But $FIRCUSUM_{ti}$ and $FIRCUSUM_{cnt}$ show large differences in the patterns of their ARL ratios. First, $FIRCUSUM_{ti}$ has shorter ARLs to detect the change than $FIRCUSUM_{cnt}$. And the difference in their ARL ratios increases with the increase of the radiation levels. Second, the ARL ratio of $FIRCUSUM_{ti}$ continuously decreases with the increase of the radiation levels, while the ARL ratio of $FIRCUSUM_{cnt}$ decreases first, and minimizes around the radiation level of 4.0cps, then increases with the increase of the radiation levels. The third difference lies in the ratios for different *h* values. For different *h* values, the $FIRCUSUM_{cnt}$ shows larger differences in the ratios than does $FIRCUSUM_{ti}$. The large difference indicates that the choice of the

h values has a stronger effect on the performance of the Poisson CUSUM control chart than that of the time-interval CUSUM control chart.

Figure 4.4 illustrates the detection probabilities (1- β) of the CUSUM control charts with or without the FIR feature and the Shewhart control chart for the scenario (5s background + 5s source + 5s background) based on the simulated data. The simulated scenario was explained in the section of experimental instruments and simulation. All the CUSUM control charts show the similar detection probabilities over different radiation levels. But they have higher detection probabilities than that of the Shewhart method for the radiation levels between 2.0cps and 8.0cps. At 4.0cps, the detection probabilities of the CUSUM control charts are 100% higher than that of the Shewhart control chart. For the radiation levels above 8.0cps, all the control charts have almost 100% detection probabilities.

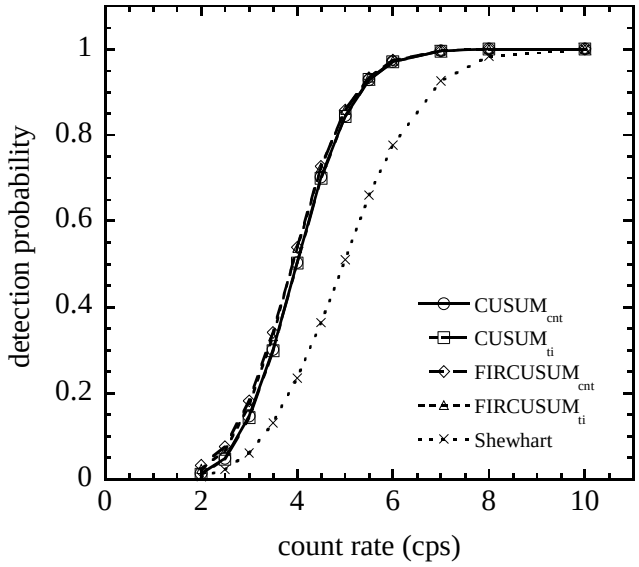

Figure 4.4. Detection probabilities of the CUSUM control charts with or without the FIR feature and the Shewhart method for the scenario (5s background + 5s source + 5s background) based on the simulated data. Standard deviations are smaller than the symbols.

Figure 4.5 shows the detection probabilities for $CUSUM_{cnt}$, $CUSUM_{ti}$ and the Shewhart control chart for four different scenarios in which the radioactive source were presented for different length of time: 2s, 5s, 20s and 50s. The background counts are still 5s before and after the presence of the source. For all the scenarios, both $CUSUM_{cnt}$ and $CUSUM_{ti}$ have greater detection probabilities than the Shewhart method. With the longer time of source presence, the detection probabilities for both the CUSUM and the Shewhart control charts increase. The difference in the detection probabilities between the CUSUM and the Shewhart control charts becomes more apparent, especially over relative low radiation levels from 2.5cps to 6.0cps.

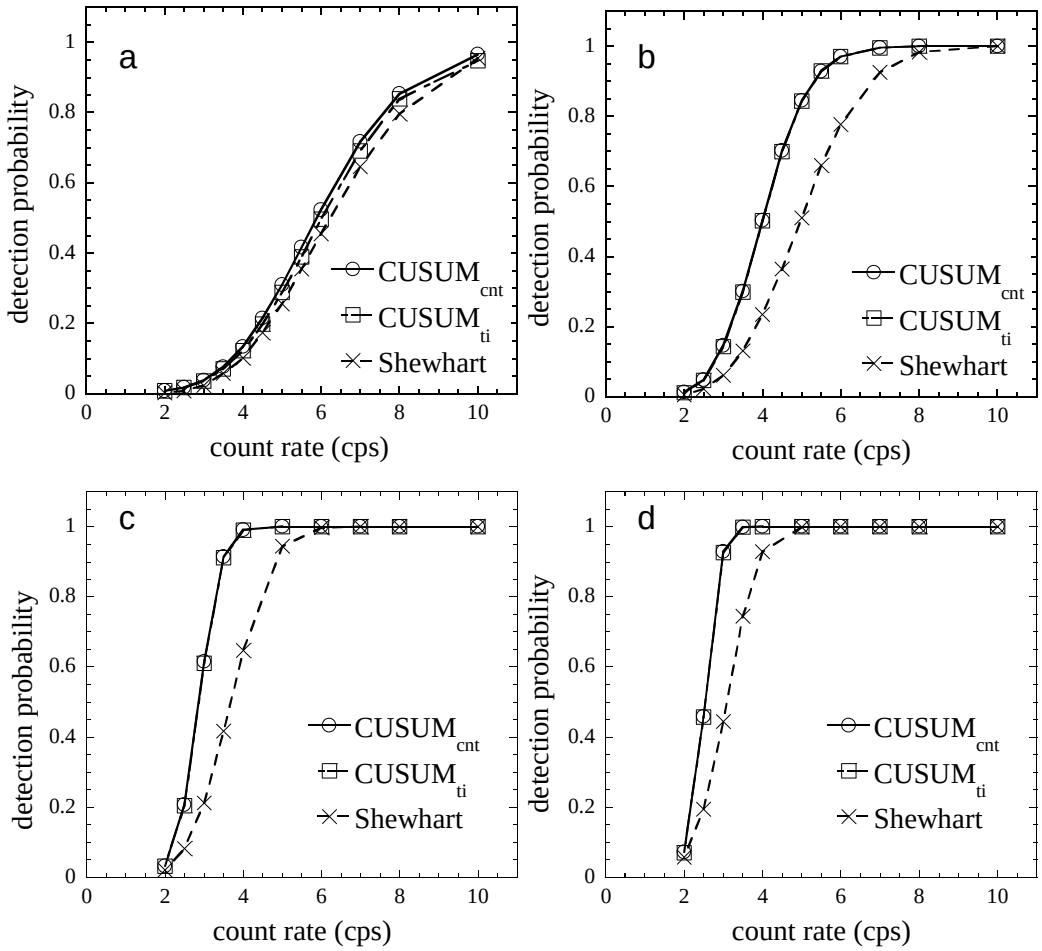

Figure 4.5. Detection probabilities of $CUSUM_{cnt}$, $CUSUM_{ti}$ and the Shewhart control chart for four different scenarios in which the source presented for different length of time: (a) 2s, (b) 5s, (c) 20s, and (d) 50s. Background counts are still 5s before and after the designated time of source presence. Standard deviations are smaller than the symbols.

CUSUM Chart with the Modified Runs Rule

The performance of $rCUSUM_{ti}$ was studied for the cases in which time-interval information was used. Based on a preset control limit (e.g., 50ms), an alarm signal is issued whenever two time-intervals (< 50ms) that are outside of the preset control limit

are observed consecutively. Figure 4.6a illustrates the ARL ratios of between $rCUSUM_{ti}$ (at control limits: 50ms, 20ms and 10ms) and $CUSUM_{cnt}$. The ARL ratio of $CUSUM_{ti}$ to $CUSUM_{cnt}$ is the same as shown in Figure 4.2. The corresponding detection probabilities of $rCUSUM_{ti}$ for the scenario (5s background + 5s source + 5s background) based on the simulated data are shown in Figure 4.6b. The number in the parentheses is the control limit which is used to determine if a time-interval could result in an out-of-control signal or not. The detection probability of $CUSUM_{ti}$ is the same as shown in Figure 4.4.

The $rCUSUM_{ti}$ can reduce the ARLs over the whole range of the radiation levels. Compared to ARLs for the radiation levels above the background level, the ARL_0 is reduced to a larger extent. A short ARL_0 means a high false positive rate at the background level, which is shown in Figure 4.6b. Therefore, $rCUSUM_{ti}$ could improve its performance at the expense of producing more false positives. In addition, with the increase of the control limit, the extent of the reduction of the ARLs for $rCUSUM_{ti}$ is enlarged, and the false positives increase. When the control limit is set at 10ms, the ARLs are just slightly reduced, except for the ARL_0 of $rCUSUM_{ti}$. Therefore, the control limit should be set at an appropriate value (e.g., 50ms) to see an apparent improvement in the performance of $rCUSUM_{ti}$. However, for the purpose of achieving the appropriate improvement, a modification is needed to keep the false positive rate at an acceptable level.

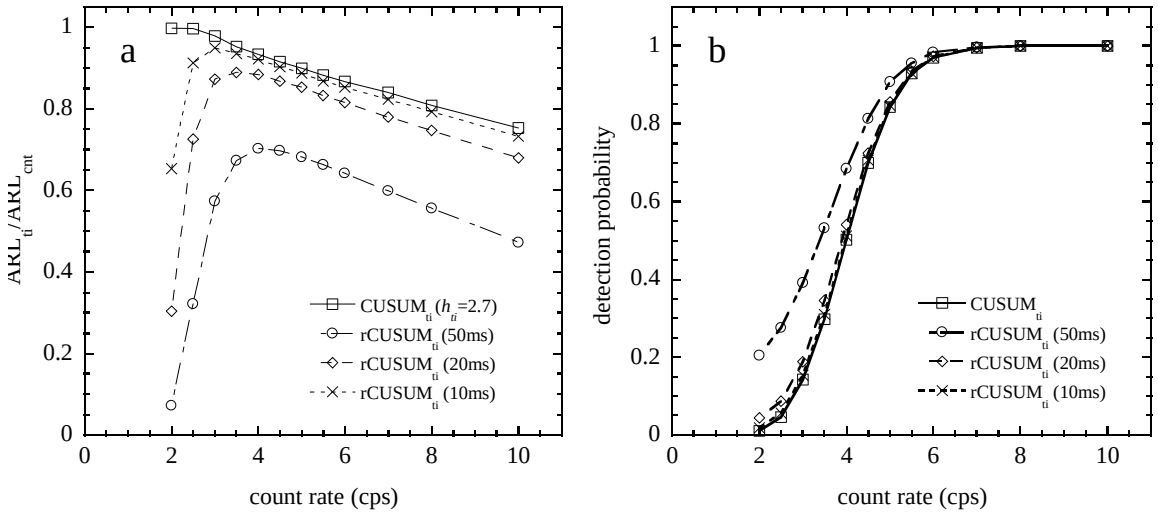

Figure 4.6. ARL ratios of $rCUSUM_{ti}$ to $CUSUM_{cnt}$ (a) and detection probabilities of $rCUSUM_{ti}$ (b). The number in the parentheses is the control limit which is used to determine if a time-interval could result in an out-of-control signal or not. The ARL ratio of $CUSUM_{ti}$ to $CUSUM_{cnt}$ is the same as shown in Figure 4.2. The detection probability of $CUSUM_{ti}$ is the same as shown in Figure 4.4. The detection probabilities were calculated for the scenario (5s background + 5s source + 5s background) based on the simulated data. Standard deviations are smaller than the symbols.

Combined with the modified runs rule proposed in the section of theory and methods, the performance of $mrCUSUM_{ti}$ was investigated. For the modified runs rule, when two successive time-intervals that are both outside the control limit were observed, the instant count rate based on the five most recent time-intervals were calculated and determined if these measurements were consistent with the background based on a predetermined instant count rate limit, μ_I. For the same situation as considered in Figure 4.6, the ARL ratios and detection probabilities of $mrCUSUM_{ti}$ were calculated and presented in Figure 4.7. The control limit was 50ms and μ_I was chosen at 4.0cps, 8.0cps and 12.0cps, respectively.

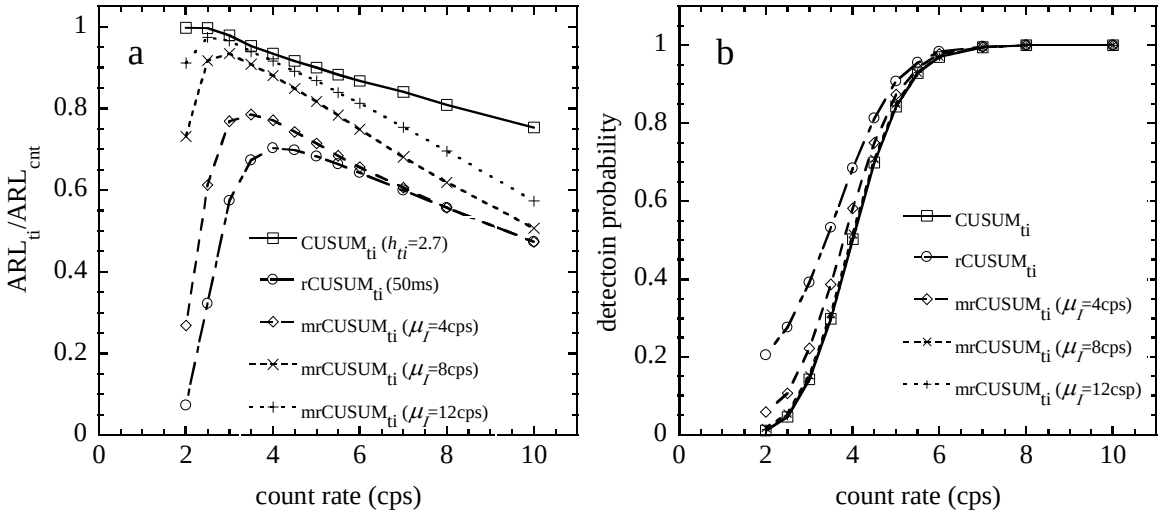

Figure 4.7. ARL ratios of $mrCUSUM_{ti}$ to $CUSUM_{cnt}$ (a) and detection probabilities of $mrCUSUM_{ti}$ (b). The control limit is 50ms. The number in the parentheses is the instant count rate limit which is used to determine if the most recent data are consistent with the background or not. The ARL ratio of $CUSUM_{ti}$ to $CUSUM_{cnt}$ is the same as shown in Figure 4.2. The ARL ratio of $rCUSUM_{ti}$ versus $CUSUM_{cnt}$ is the same as shown in Figure 4.6a. The detection probability of $CUSUM_{ti}$ is the same as shown in Figure 4.4 and the detection probability of $rCUSUM_{ti}$ is the same as shown in Figure 4.6b. The detection probabilities were calculated for the scenario (5s background + 5s source + 5s background) based on the simulated data. Standard deviations are smaller than the symbols.

With the modified runs rule, the ARL_0 of $mrCUSUM_{ti}$ is not reduced as much as that for $rCUSUM_{ti}$. As the result, the false positive rate is reduced. For μ_I =4.0cps, even the ARL_0 is just 26% of ARL_0 of $CUSUM_{cnt}$, the false positive rate is decreased from 20% for $rCUSUM_{ti}$ to 6% for $mrCUSUM_{ti}$. In addition, with the increase of the radiation levels, ARLs for $mrCUSUM_{ti}$ approaches to that of $rCUSUM_{ti}$. Therefore, the modified runs rule has the potential to enable the CUSUM control chart respond quickly to the changes in radiation levels, and hold the false positive rate at an acceptable level.

Experimental Study of CUSUM Charts

Following the aforementioned studies of CUSUM analyses of time-interval information, experimental studies were conducted to validate the result from the simulated data. In the experimental measurements, an ROI was set to look at radiation pulses for the 1332.5 keV full energy peak from the ^{60}Co source. The background radiation level within the 1332.5 keV ROI was about 2.0cps. The *h* values, detection limit of the Shewhart control chart, control limit and instant count rate limit were set using the same way discussed before. Experimental ARLs and experimental detection probabilities were calculated for $CUSUM_{cnt}$, $CUSUM_{ti}$, $mrCUSUM_{ti}$, and the Shewhart control charts. The results are shown in Figure 4.8. The situation is still the same as before: r_a = 2.0cps, r_d =4.0cps, and the simulated scenario are 5s background + 5s source + 5s background.

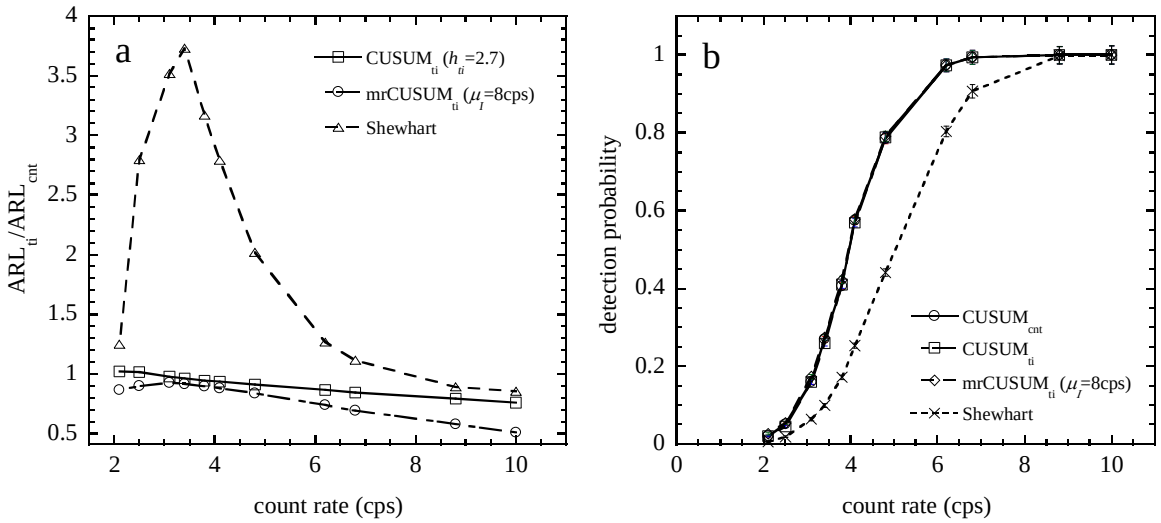

Figure 4.8. Experimental ARL ratios (a) and detection probabilities (b) of the CUSUM control charts: $CUSUM_{cnt}$, $CUSUM_{ti}$, $mrCUSUM_{ti}$, and the Shewhart control chart. The control limit is 50ms. The detection probabilities were calculated for the scenario (5s background + 5s source + 5s background) based on the experimental data. Standard deviations are smaller than the symbols in (a).

Overall, the experimental results are consistent with the results from the simulated data. Time-interval information is beneficial for the CUSUM control chart to detect changes in radiation levels and the modified runs rule can further improve the performance of the CUSUM control chart.

Conclusion

The CUSUM control chart has the ability to incorporate previous information into radiation detection decisions, which results in a quicker response to changes in radiation levels than the Shewhart control chart, and has higher detection probabilities than the Shewhart method for relatively low radiation levels. The special features of time-intervals

provide an alternative for low-level radiation monitoring. When the CUSUM control chart is applied for on-line time series data, time-interval information shows a similar detection probability to the count information, and is capable of detecting changes in radiation levels with the shortest ARL. Without considering other factors (e.g. detection system and analyzing process) that could affect the time needed for detection decision, time-interval information has the potential to respond quickly at relatively higher radiation levels. Use of the modified runs rule, $mrCUSUM_{ti}$ could further improve the performance of the CUSUM control chart by holding the false positive rate at an acceptable level. When the FIR feature is implemented, $FIRCUSUM_{ti}$ outperforms $FIRCUSUM_{cnt}$. Radiation monitoring based on time-interval analysis is preferred if other factors are the same since registering time-intervals could reduce the sampling time required to obtain sufficient information to detect changes in radiation levels.

References

Arandjelovic, V., A. Koturovic, and R. Vukanovic. 2002. A software method for suppressing statistical fluctuations in preset count digital-rate meter algorithms. *IEEE Transactions on Nuclear Science* 49, (5 Part 3): 2561-6.

Cheng, C. S., and P. W. Chen. 2010. An ARL-unbiased design of time-between-events control charts with runs rules. *Journal of Statistical Computation and Simulation* 81, (7): 857-871.

DeVol, T. A., A. A. Gohres, and C. L. Williams. 2009. Application of classical versus Bayesian statistical control charts to on-line radiological monitoring. *Journal of Radioanalytical and Nuclear Chemistry* 282, (3) (DEC): 933-8.

Dowdy, E. J., C. N. Henry, R. D. Hastings, and S. W. France. 1978. Neutron detector suitcase for the nuclear emergency search team. *Los Alamos Scientific Lab. Report LA*-7108.

Hughes, L. D., and T. A. DeVol. 2008. Evaluation of statistical control charts for on-line radiation monitoring. *Journal of Radioanalytical and Nuclear Chemistry* 277, (1): 227-34.

Jarman, K. D., L. E. Smith, and D. K. Carlson. 2004. Sequential probability ratio test for long-term radiation monitoring. *IEEE Transactions on Nuclear Science* 51, (4) (AUG): 1662-6.

Kenett, R., and S. Zacks. 1998. *Modern industrial statistics: Design and control of quality and reliability.* California: Duxbury Press.

Knoll, G. F. 2010. *Radiation detection and measurement*. 4th ed. New Jersey: John Wiley & Sons Inc.

Laedermann, J. P., J. F. Valley, and F. O. Bochud. 2005. Measurement of radioactive samples: Application of the Bayesian statistical decision theory. *Metrologia* 42, (5) (OCT): 442-8.

Liu, J. Y, M. Xie, TN Goh, and PR Sharma. 2006. A comparative study of exponential time between events charts. *Quality Technology & Quantitative Management* 3, (3): 347-59.

Lucas, J. M. 1985. Counted data cusums. *Technometrics* 27, (2): 129-44.

Lucas, J. M., and R. B. Crosier. 1982. Fast initial response for cusum quality-control schemes - give your cusum a head-start. *Technometrics* 24, (3): 199-205.

———. 1982. Robust cusum - a robustness study for cusum quality-control schemes. *Communications in Statistics Part A-Theory and Methods* 11, (23): 2669-87.

Luo, P., T. A. DeVol, and J. L. Sharp. 2010. Sequential probability ratio test using scaled time-intervals for environmental radiation monitoring. *IEEE Transaction on Nuclear Science* 57, (3): 1556-62.

Luo, P., J. L. Sharp, and T. A. DeVol. 2011. Bayesian analysis of time-interval data for environmental radiation monitoring. *IEEE Transactions on Nuclear Science*. under review.

Marshall, R. A. G. 1977. Cumulative sum charts for monitoring of radioactivity background count rates. *Analytical Chemistry* 49, (14): 2193-6.

Montgomery, D. C. 2001. *Introduction to statistical quality control.* New York: John Wiley & Sons.

Page, E. S. 1954. Continuous inspection schemes. *Biometrika* 41, (1-2): 100-15.

R Development Core Team. 2010. The R project for statistical computing. http://www.r-project.org/.

Sakaue, H., H. Fujimaki, S. Tonouchi, S. Itou, and T. Hashimoto. 2007. A new time interval analysis system for the on-line monitoring of artificial radionuclides in airborne dust using a phosfitch type alpha/beta detector. *Journal of Radioanalytical and Nuclear Chemistry* 274, (3): 449-54.

U.S. Department of Energy. 2004. *Transport of contaminants in subsurface environments at DOE sites.* DE-FG01-05ER05-12.

Vardeman, S., and D. Ray. 1985. Average run lengths for CUSUM schemes when observations are exponentially distributed. *Technometrics* 27, (2): 145-50.

XIA. 2004. *User's manual digital gamma finder (DGF) DGF-4C*. Newark, CA: X-Ray Instrumentation Associates.

Xie, Y. J., K. L. Tsui, M. Xie, and T. N. Goh. 2010. Monitoring time-between-events for health management. Paper presented at Prognostics and Health Management Conference, PHM'10.

CHAPTER 5

CLOSURE

Summary

This research presents the study of the time-interval analysis based on three statistical methods for radiation monitoring with experimental and simulated data. The experimental data were acquired with a DGF-4C (XIA, Inc) system in list mode. Simulated data were obtained by using Monte Carlo techniques to obtain a random sampling of a Poisson process. All statistical algorithms were developed using R (R Core Development Team, 2010). The three statistical methods that were specifically applied to time-interval analyses are sequential probability ratio test (SPRT), Bayesian statistics, and cumulative sum (CUSUM) control chart. The results from this study show that the special features of time-intervals provide a good alternative for on-line low-level radiation monitoring. When time-interval data were used, all three methods resulted in a similar detection probability as that of count data registered in a fixed count time, and a faster response to changes in radiation levels than count data. To improve the performance of time-interval based on-line radiation monitoring, modifications were proposed for each of the three standard statistical methods.

For SPRT method, the effects of the thresholds (*A* and *B*) and truncation strategy on the detection probability and the average time to make a detection decision were investigated based on scaled time-interval information. With a smaller *A* value, the actual false negative rate β is reduced while the actual false positive rate α is increased. On the

other hand, when a larger B value is used, the actual β is increased while the actual α is reduced. The truncation strategy applied to SPRT reduced the average time to make a detection decision, which resulted in a similar detection probability as that for SPRT without the truncation strategy. The adjustment to the preset background level r_0 in the SPRT algorithm showed the ability to increase the detection probability at relatively low radiation levels and reduce the average time to trigger an alarm when scaled time-interval data were used for radiation monitoring.

For the Bayesian analyses of time-interval information, effects of factors such as source time, detection limit and change point were studied to find possible effective ways to improve detection decisions for on-line radiation monitoring. When source time is limited (< count time), Bayesian analysis of time-interval information could result in a higher detection probability than Bayesian analysis of count information since the overall count information obtained in the entire fixed count time could be averaged out by background counts. The change point determines the amount of background data that are incorporated into the prior. When a large amount of background data is included into the Bayesian inference, the detection decision would be deteriorated or delayed. To reduce the effect of the change point, the enhanced reset modification and moving prior were introduced. The results showed that both modified Bayesian analysis methods had higher detection probabilities than the Bayesian analyses without modifications. The performances of the two modified methods are independent of the change point.

The study of the time-interval CUSUM control chart showed that time-interval information had the shortest ARL compared to the Poisson CUSUM and Shewhart

control charts. Both the time-interval CUSUM and the Poisson CUSUM are more sensitive to small changes in radiation levels than the Shewhart control chart. When the FIR feature was incorporated, the time-interval CUSUM was superior to the Poisson CUSUM since the ARL of the time-interval CUSUM continuously decreased with the increase of radiation levels and is insensitive to the decision interval values. When time-interval CUSUM is coupled with a modified two-in-a-row rule, it has the potential to further reduce the time to detect changes in radiation levels and hold the false positive rate at a required level.

The time-interval analyses based on the three chosen statistical methods show that time-interval information results in a quicker detection than count information, while providing a similar detection probability. The sensitivity of time-interval based statistical methods could be beneficial to the applications in which a fast detection of radioactive sources is essential, such as portal monitoring and locating a lost radioactive source.

By using time-interval information, all the three statistical methods can be operated in a continuous mode in which a detection decision is sequentially updated whenever new radiation pulses are registered. Both Bayesian statistics and CUSUM can update their statistics and detection decisions by incorporating one radiation pulse at a time; while SPRT can only start its updating until N (digital scaler) pulses have been registered. Compared to SPRT and Bayesian statistics, CUSUM is the easiest one to implement because it is conceptually easy to understand and it has the least computational load for statistics updating. On the contrary, Bayesian techniques are relatively more difficult to understand and it has the most computational load for its

complex posterior calculation, but resulted in much longer ARL_0 than the other techniques investigated in this dissertation.

The SPRT, Bayesian, and CUSUM (without modifications) time-interval methods were compared with the Shewhart control chart under similar conditions and revealed that the time-interval methods resulted in approximately the same false positive rate, but a lower false negative rate (higher detection probability) with shorter average run lengths. Compared to the Shewhart control chart in which only the information contained in the latest data point is exploited, all the three statistical methods proposed for time-interval analyses have the ability to incorporate additional information contained in previous data points. When time-interval data are analyzed one-at-a-time, it will take less time to collect statistically sufficient information to reach the same detection decision than that for count data analyses. The comparison among the three methods (SPRT, Bayesian, and CUSUM) relative to the Shewhart control chart was conducted for a simulated scenario (5s background + 5s source + 5s background). The detection probability and ARL (or average time) for each standard method (without modifications) were investigated. For each method, the parameters were adjusted to have approximately the same false positive rate at the background level. According to the results (shown in Figure 5.1 and 5.2), all the three methods are superior to the Shewhart method in terms of the detection probably and ARL. When time-interval information is used, CUSUM has the highest detection probability (e.g. 25% higher than that for SPRT and Bayesian statistics at the level of 4.0cps). SPRT and Bayesian statistics have similar detection probabilities. For the ARLs of the three methods, CUSUM has the longest ARL for levels above background relative

to SPRT and Bayesian statistics, especially over the low radiation range from 2.0cps to 4.0cps (e.g. two times the ARL of Bayesian statistics at the level of 2.5cps). One thing to be noted is that the average time of SPRT is confined by the parameter N_{max}. On the contrary, there is no constraint on the number of data points that are utilized to update the detection decision. In practice, which method is used to analyze time-interval information for on-line monitoring should be determined based on investigator's knowledge about the three methods, the difficulty to implement the method, and requirements on detection probability or ARL.

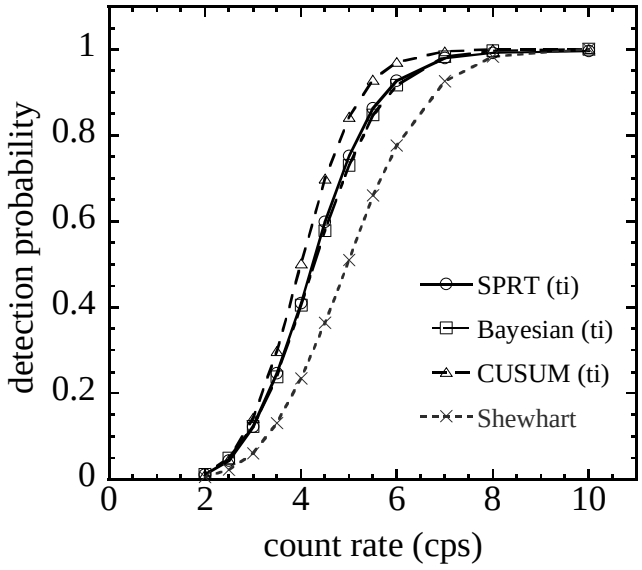

Figure 5.1. Detection probabilities of the three time-interval analyses by SPRT, Bayesian statistics and CUSUM relative to the analysis by Shewhart control chart. The simulated scenario is 5s background + 5s source +5s background based on simulated data. Standard deviations are smaller than symbols.

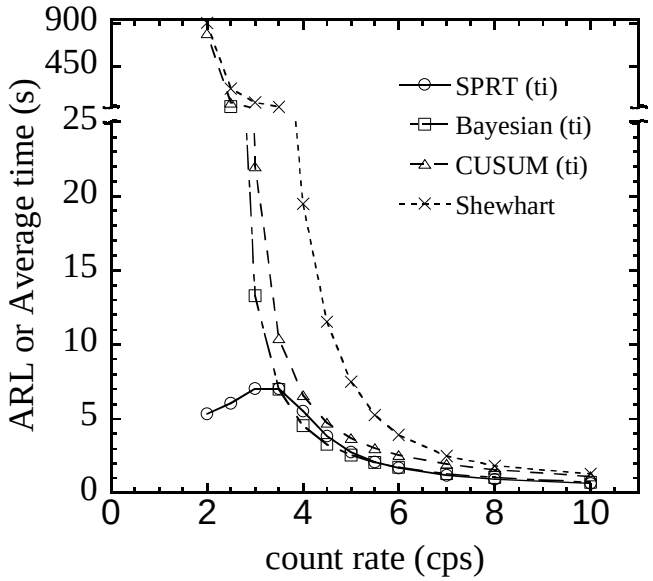

Figure 5.2. ARLs of the three time-interval analyses by SPRT, Bayesian statistics and CUSUM relative to the analysis by Shewhart control chart. The simulated scenario is 5s background + 5s source +5s background based on simulated data. Standard deviations are smaller than symbols.

Recommendations for Future Work

For a potential application in portal monitoring and searching for lost radioactive sources, one may design a laboratory experiment on these practical applications to further exploit the benefits of time-interval data for radiation monitoring. For the design of the laboratory experiment, one needs to specify the background level, alarm level to be detected quickly, fixed count time, and full energy peak from the radioactive source that is monitored, etc.

The radiation detection for the situation in which a radioactive source is present for very short time (< count time) has been conducted based on Bayesian inference. The

results showed that time-interval information had higher detection probability than count information. This interesting finding is a potential advantage to detect a radioactive source contained in a moving media. An extended study on the situations in which source time is extremely short relative to the count time is needed to check the feasibility and sensitivity to use time-interval data for radiation monitoring. The study will focus on the detection probabilities at a variety of combinations of source strength, the time length of the source presence, and fixed count time.

A further study can be conducted to investigate the effects from different prior probabilities on the Bayesian inference. In this study, a natural conjugate prior was used as the initial prior which was assigned based on previous background measurements. A prior that is given based on a measurement with the presence of a radioactive source could improve the detection probability when a source is present, while it could increase the false positive rate at the background level. In addition, the effects from a "noninformative" or "empirical" prior should be examined and compared to a conjugate prior.

Derived from Bayesian statistics, Shiryayev-Roberts (S-R) control chart (Kenett and Zacks 1998) has been applied by DeVol et al. (2009) for reducing false positive rates in low-level radioactivity monitoring based on count information. One may develop a new algorithm based on S-R control chart to analyze time-interval information and compare the performance of S-R control chart with the Bayesian approach used in this study which is based on the fundamental Bayes' theorem.

For the time-interval CUSUM control chart, a modified runs rule was proposed to increase the sensitivity of the control chart. This runs rule could also be applicable in combination with SPRT and Bayesian methods. It is worthwhile to investigate the advantages/disadvantages of SPRT and Bayesian statistics or other methods by coupling with the runs rule to detect changes in radiation levels.

For the situation in which the sample size is n=1, individual moving range (IMR) control chart has been used to help identifying where or when a process shift has occurred (Montgomery 2001). A study on the time-interval analysis combining an IMR control chart with the CUSUM control chart or other statistical methods should be a worthwhile endeavor.

In this study, the detection probabilities of Bayesian and CUSUM methods were calculated based on a series of simulated scenarios. In these scenarios, an abrupt change in radiation strengths was assumed. In a real application, the change in radiation strength varies with time and distance. An experiment or a simulated scenario based on a real application could be designed to further study the sensitivity of time-interval data for radiation monitoring.

An extended study is needed for the situations in which background level is different from the level utilized in this study. This dissertation presents significant data and analyses for a detection system with a background count rate of 2.0 cps. With that information it is problematic to extrapolate these findings to detection systems with higher or lower background count rates. For the extended study, ARLs and detection probabilities of the three time-interval methods could be calculated for a series of

situations with different count rates from very low level (e.g., 0.01cps) to very high level (e.g., 100cps). If it is possible, the preassigned false positive rate should be set at the same level. A good solution for these situations is to provide a general table of ARL and detection probability by scaling other levels to a background level for different situations.

APPENDICES

Appendix A

Other Related Results Obtained from This Study

Experimental Time-Interval Distribution

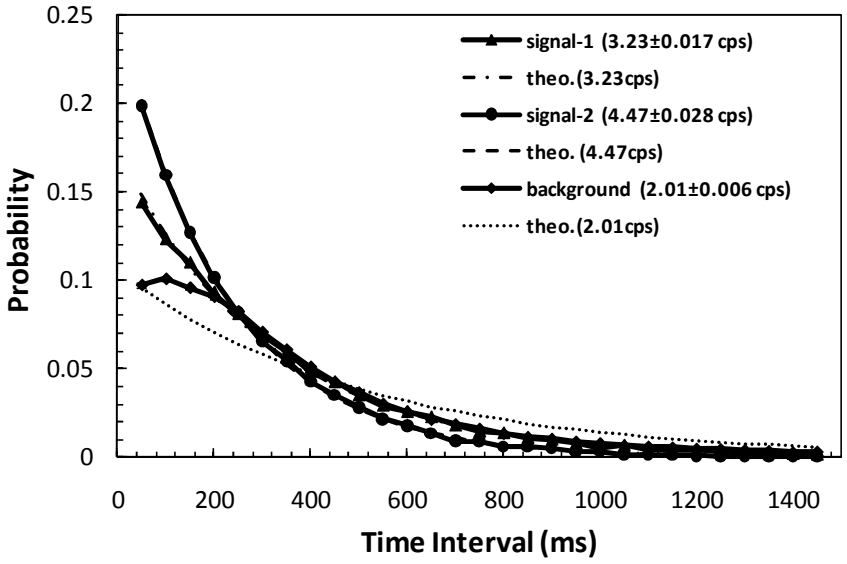

Figure A.3. Experimental and theoretical time-interval probability distributions. In the parentheses are the mean count rates. Standard deviations of experimental data are smaller than the symbols.

Currie's Detection Limit (L_D) Based on Time-Interval Data

In the course of radiation monitoring for the possible presence of radioactive contaminants, an *a priori* limit of detection, L_D, introduced by Currie (1968) is given by

$$L_D = L_C + k_\beta \sigma_{N_D} \quad , \tag{A. 1}$$

where $L_C = k_\alpha \sigma_0$, σ_{N_D} is the standard deviation of the net signal when a radioactive source is present, and k_β is the critical value of the standard normal distribution that has the probability of β. k_α is the 1-α percentile of the standardized normal distribution

corresponding to the probability of α, and σ_0 is the standard deviation of the net signal when the radioactive source is not present. For radiation monitoring, L_D can be interpreted as the minimum number of radiation counts needed from the radioactive source such that the false negative rate is not larger than β and the false positive rate is not larger than α. For a case with a 5% false positive rate and a 5% false negative rate that are commonly used, L_D is appropriately given as following (Currie 1968),

$$L_D = 2.706 + 4.653\sigma_0 \quad . \tag{A. 2}$$

The time-interval distribution shown in Figure A-1indicates that a change of time-interval distribution in the shorter time-interval range will be observed if the mean count rate increases as the result of the presence of a radioactive source. Based on the property of the time-interval distribution, a new *a priori* detection limit, L_D', can be determined from the number of time-intervals. For a radiation detection process with a mean count rate *r*, the number of time-intervals that are shorter than a given length of time, t_0, is calculated by

$$N_{t \le t_0} = (N_{total} - 1)(1 - e^{-rt_0}) \ , \tag{A. 3}$$

where N_{total} is the total number of pulses registered in the background measurement. Accordingly, the limit of detection, L_D', for the time-intervals $N_{t \le t_0}$ is

$$L_D' = 2.706 + 4.65\sqrt{N_{t \le t_0}} \quad . \tag{A. 4}$$

Therefore, the count rate at the alarm level, r_1', can be calculated based the L_D' using the follow relationship,

$$(r_1't_c - 1)(1 - e^{-r_1't_0}) = N_{t \le t_0} + L_D' \quad , \tag{A. 5}$$

where t_c is the count time. The improvement of the new detection limit is defined as,

$$\frac{r_1 - r_1'}{r_1} \times 100\% \quad , \tag{A. 6}$$

where $r_1 = r_0 + L_D/t_c$ is the count rate at the alarm level based on count information, and r_0 is the mean count rate of the background level. Using the Solver function in the Microsoft Office Excel, the detection limits with different parts of time-intervals for the mean background count rates of 2.0cps and 20 cps are calculated and shown in Figure A.2 and Figure A.3, respectively. The results show that the detection limit based on time-interval information are lowered in most range of values of time-interval length, and minimized at certain value. For the 2.0cps background, the detection limit is lowest at the value around 0.5s. And the minimum detection limit for the 20.0cps background happens at about 0.05s. So, a value that is close to the average time-interval value can result in a minimum detection limit.

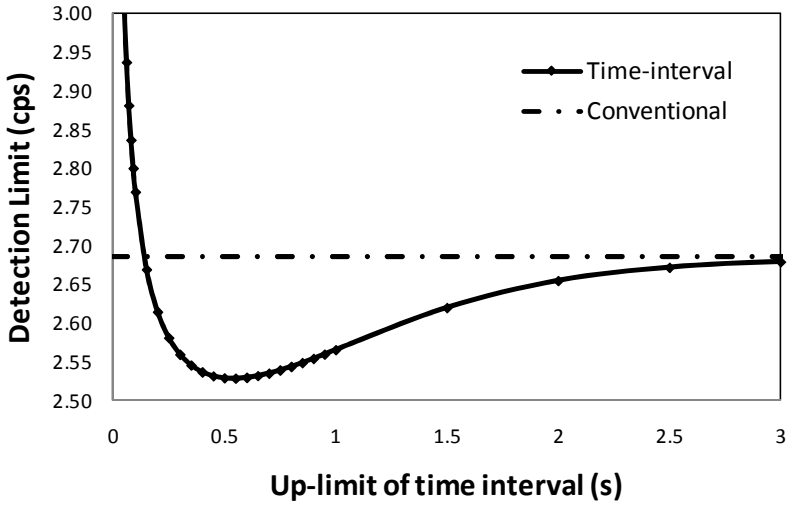

Figure A.4. The detection limit based on the number of time-intervals less than preassigned value, t_0, for the background mean of 2.0cps. The count time, t_c, is 100s.

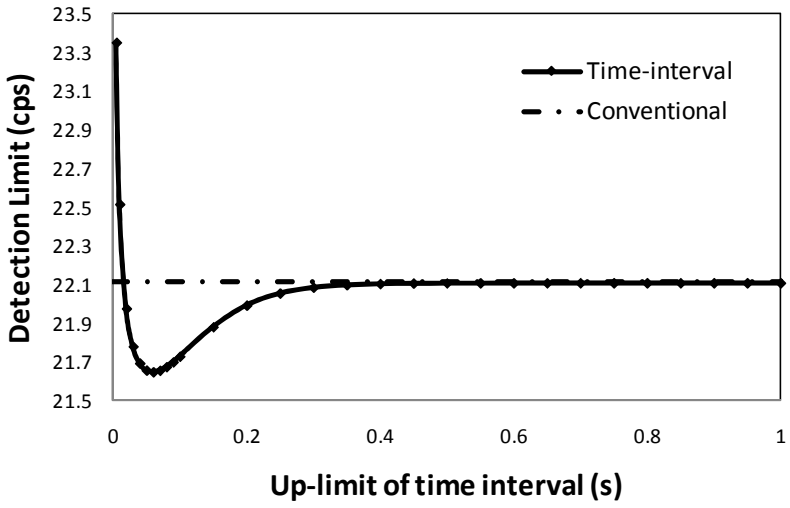

Figure A.5. The detection limit based on the number of time-intervals less than preassigned value, t_0, for the background mean of 20.0cps. The count time, t_c, is 100s.

Figure A.4 shows the effect of the background count time to the minimum detection limit. It implies that the improvement is independent of the background count time except for the short count time. At the shorter count time range, the improvement decreases with the count time increases. In practice, short count time will result in a large uncertainty in the results. A proper count time should be chosen within a reasonable range depending on the strength of radiation, detection system, expected uncertainty, and other factors.

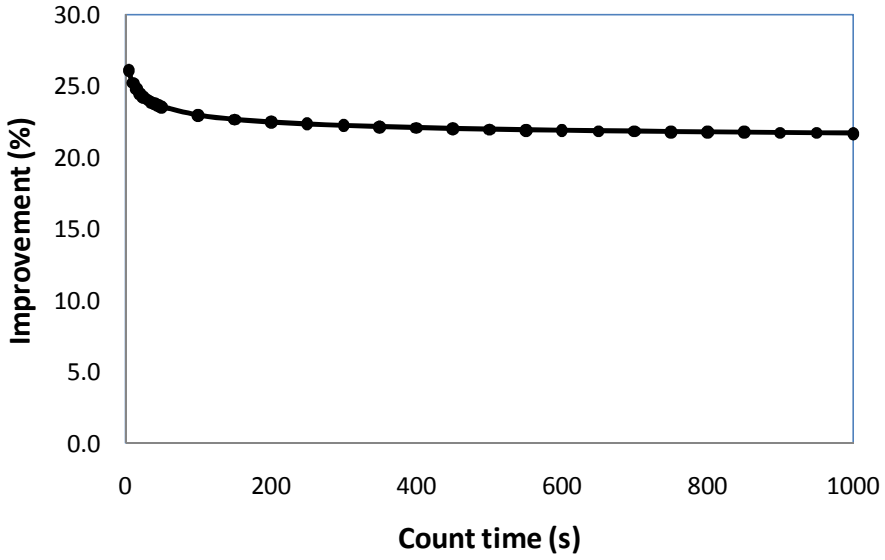

Figure A.6. The effect of the count time to the detection limit based on time-interval information.

Detection Probabilities of SPRT for Different Error Rates (α,β)

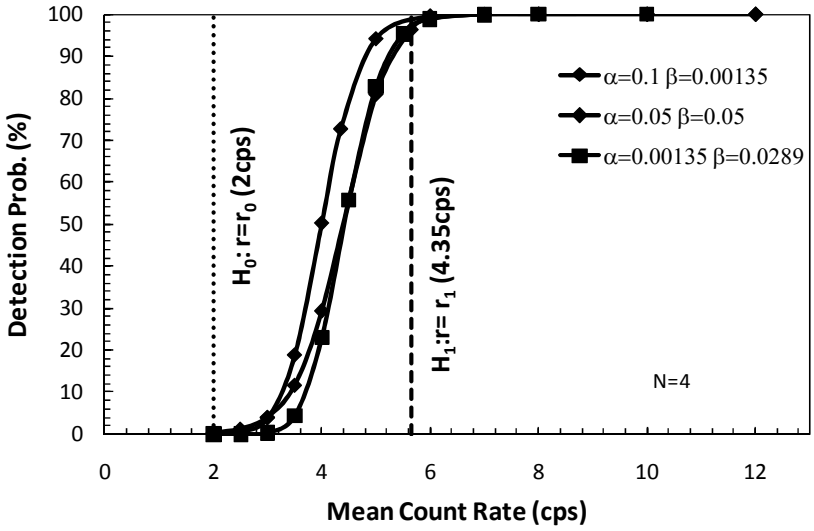

Figure A.7. Detection probabilities of SPRT for three different error rate pairs (α,β).

Experimental Average Run Length of Bayesian Analyses for
1173.2keV ROI

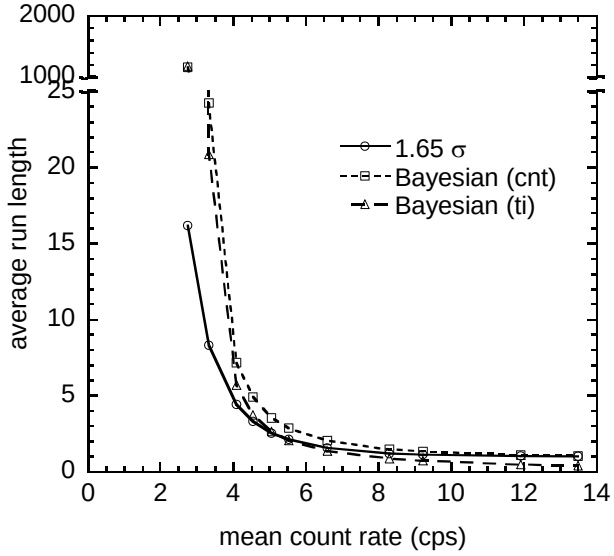

Figure A.8. Experimental average run lengths of Bayesian analyses for the radiation pulses within the 1173.2keV ROI of ^{60}Co.

Experimental Average Run Length of Bayesian Analyses for Sum Peak of ^{60}Co

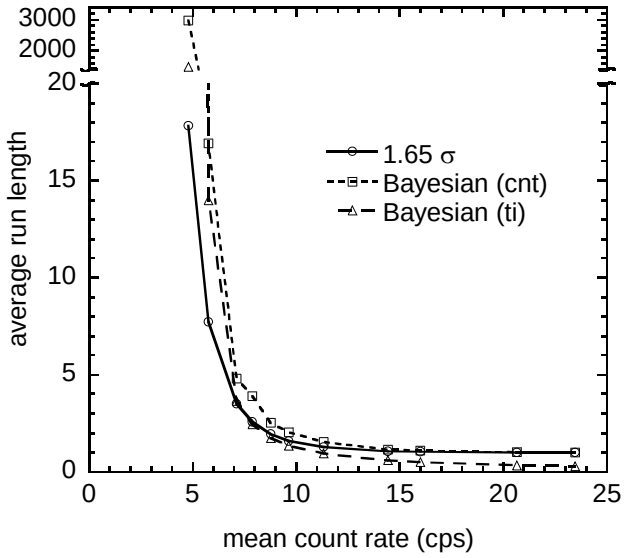

Figure A.9. Experimental average run lengths of Bayesian analyses for the radiation pulses within the ROI containing 1173.2keV and 1332.5keV of ^{60}Co.

Average Run Length of Bayesian Analyses for 60% Detection Limit

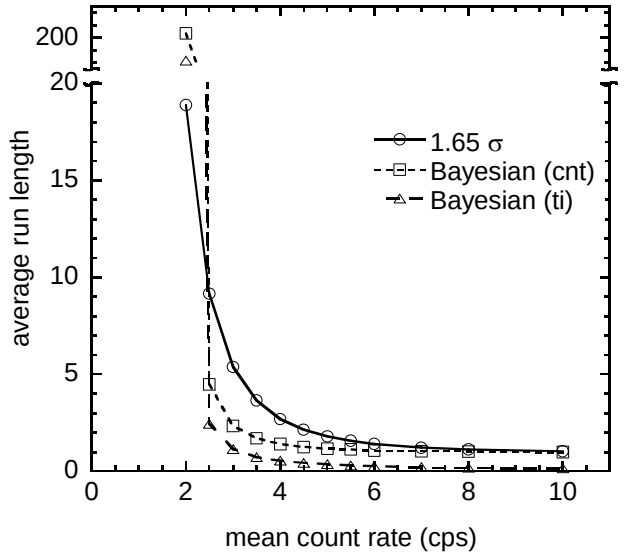

Figure A.10. Average run lengths of Bayesian analyses when the detection limit is set at 60%.

Effect on the Bayesian Analyses from the Initial Prior

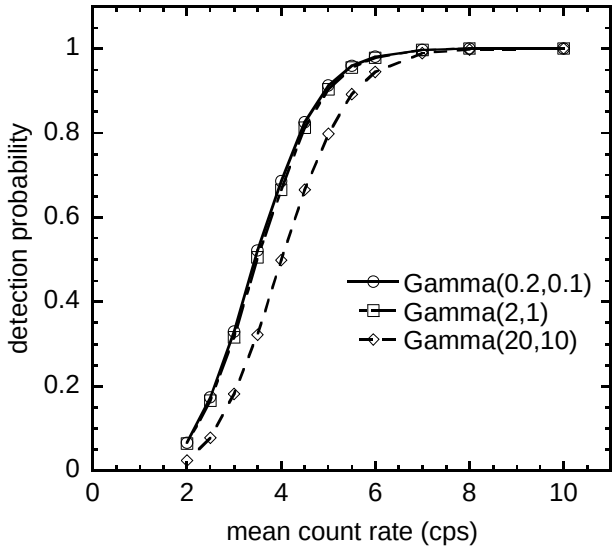

Figure A.11. Effect on the Bayesian analyses from the initial prior.

Average Run Length for Situations with Different r_d

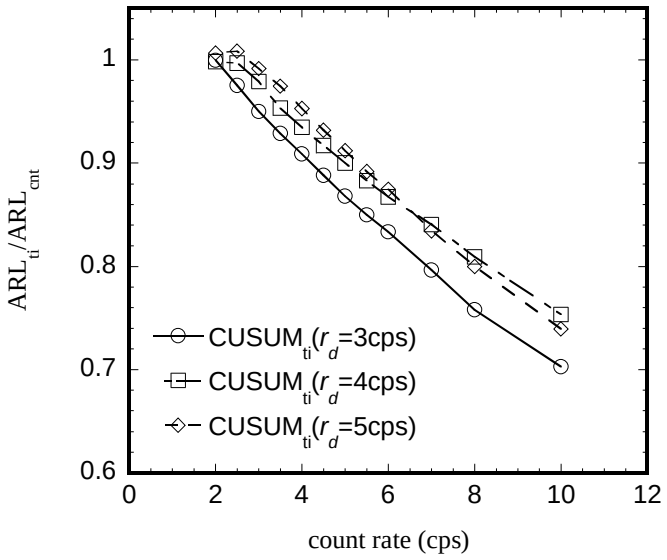

Figure A.12. Average run length of CUSUM for different situations with different r_d.

Detection Probabilities of CUSUM for Different h_{ti}

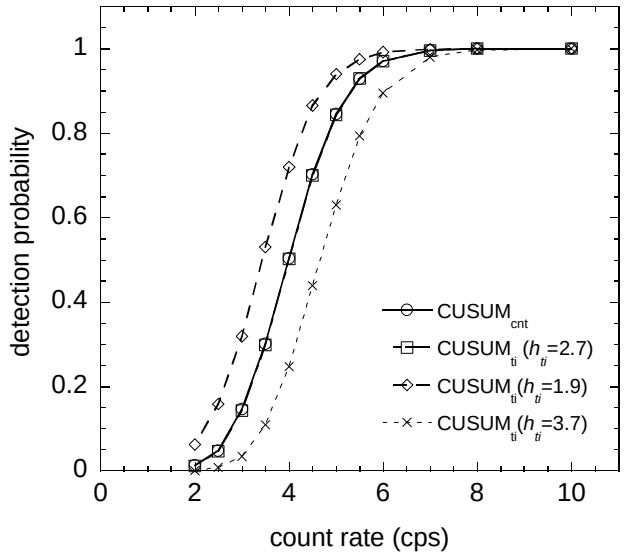

Figure A.13. Detection probabilities of CUSUM for different h_{ti} values when time-interval data are used.

Appendix B

Development of the Igor Pro. Codes and R Programming

Igor Pro. Code for Experimental Time-Intervals

```
#pragma rtGlobals=1                    // Use modern global access method.
//For 101 runs, extracting real time and energy of each event for arbitrary number of events in a run//
//get rid of the time-interval between two runs//

Function Time_Int()
//declare variables
        variable energyindex, trigtimeindex, n, i, j, k, t_low, t_high, real_high, w, m, m1
// energyindex is the index for energy array
 //trigtimeindex is the index for Trigtime array, n is the index of new waves//
 // i is the index of wave0 for inner loop condition, j is the index of wave0 for another new run.
// k is the index for the total number of spills, h is used to control the inner loop
// t_low is the index for EVT_TIMELO word, t_high is the index for EVT_TIMEHI
// real_high is the index for CHAN_REALTIMEHI
//w, m, and m1 are the indexes for waves used to extract time stamps and time-intervals
        wave Event_No   // this wave is created by loading the general text file (.dat )
        variable num_wave=numpnts(Event_No), num_spills=600
// ***these two values have to be input before run***//
        variable E_low= 39200, E_high=45350         //*** set the ROI region for the first peak//
// create waves in which information of each event is stored
        wave wave0  // this wave is generated by loading the general binary file (.bin)
//ENERGY, TRIGTIME, TIMELO, TIMEHI, REALTIMEHI, REALTIME, TIMEINTERVAL,
INTERREALT, ENERGYI are contained in wave0//
// High word is REALTIMEHI, middle word is TIMEHI, low word is TIMELO or TRIGTIME
        make/R/O/N=(num_wave)  ENERGY1, TRIGTIME, TIMELO, TIMEHI,  REALTIMEHI,
                                    REALTIME, INTERREALT
//Above waves are used to extract time stamps for each radiation pulse and time-intervals
        make/R/O/N=(num_wave) TIMEINTERVAL= -10, ENERGY2= -10
        Redimension/D/N= (num_wave)  ENERGY1, TRIGTIME, TIMELO, TIMEHI, REALTIMEHI,
                                        REALTIME, INTERREALT, TIMEINTERVAL, ENERGY2
        energyindex=11
        trigtimeindex=10
        t_low=8
        t_high=7
        real_high=17
        i=0
        k=0
        j=wave0(0)
    W=0
    m1=0
        Do
                n=0
                m=0
```

```
		Do
			ENERGY1[n]=wave0[energyindex]
			TRIGTIME[n]=wave0[trigtimeindex]
			TIMELO[n]=wave0[t_low]
			TIMEHI[n]=wave0[t_high]
			REALTIMEHI[n]=wave0[real_high]
	REALTIME[n]=(TIMELO[n]+TIMEHI[n]*(2^16)+REALTIMEHI[n]*(2^32))*25/(10^6) //ms
			if ((ENERGY1[n]>= E_low) &&  (ENERGY1[n]<= E_high))
// for interest energy range, the low limit and upper limit of energy need to input before run this code!!!! //
			INTERREALT[m]=REALTIME[n]
			ENERGY2[m1]=ENERGY1[n]
			  if (m>=1)
			  TIMEINTERVAL[w]=INTERREALT[m]-INTERREALT[m-1]
			    w+=1
			  endif
			m+=1
			m1+=1
			endif
			energyindex+=12
			trigtimeindex+=12
			t_high+=12
			real_high+=12
			t_low+=12
			n+=1
		while (n<(wave0[i]-6)/12)
		energyindex=j+11
		i=j
		trigtimeindex=j+10
		t_high=j+7
		real_high=j+17
		t_low=j+8
		j+=wave0(i)
		k+=1
	while (k<num_spills)
// the following progamming removes the non-positive values in the timeinterval wave//
	variable i1, t1, i2
	i1=0
	t1=0
	i2=0
	Do
		if  (TIMEINTERVAL[i1]>0)
			i2+=1
			t1+=TIMEINTERVAL[i1]
		endif
		i1+=1
	while (i1<num_wave)
	make/R/O/N=(i2) selectedti
	variable j1
	j1=0
	Do
		selectedti[j1]=TIMEINTERVAL[j1]
		j1+=1
	while (j1<i2)
```

```
        variable cr   //count rate (cps)
        cr=(i2+1)/t1*1000
        print "count rate=", cr, "live time= ", t1
        print "total timeintervals=", i2
        print E_low, E_high
End
```

SPRT Analyses of Simulated Data

```
#pragma rtGlobals=1                    // Use modern global access method.
Function pulse_generate()
// generate a time series containing time information of each registered pulse //
        setrandomseed 0.05
        variable n1, CR
        CR= 2       //***the count rate in 'cps' of the simulated  counting process ***//
        n1=10^6    // ***number of pulses that are simulated ***//
        make/R/D/O/N=(n1) radomnum=enoise(0.5)+0.5    // generate random numbers between 0 and 1 //
        make/R/D/O/N=(n1) timeinterval=0, timestamp=0
        variable n2
        n2=0
        Do
                timeinterval[n2]=(-LN(1-radomnum[n2])/CR)*1000          // in unit of ms//
                if (n2==0)
                timestamp[n2]=timeinterval[n2]
                else
                timestamp[n2]=timestamp[n2-1]+timeinterval[n2]
                endif
                n2+=1
        while (n2<n1)
end

////////////  SIT test using counts in single count time ////////////////////
Function SIT_test()
        variable delta_t = 6       // *** in unit of 's', this is the fixed counting interval for SIT test ***//
        variable m1=10^6         // *** the number of simulated pulses ***//
        variable LC=17.70         // *** Discriminator level for SIT test ***//
        variable pulse_num       // use this index to shorten the runing time
        variable m2, m3, m4      // m2 is the number of data point for SIT test//
        wave timestamp           // this wave is generated by the above function //
        m2=floor(timestamp[m1-1]/1000/delta_t)          // number  of SIT counting time intervals //
        make/R/D/O/N=(m2) SIT_counts=0                // counts in each SIT counting time //
        m3=0
        pulse_num=0
        Do
                m4=pulse_num
                Do
                if (timestamp[m4]>(m3*delta_t*1000) && timestamp[m4]<=((m3+1)*delta_t*1000))
```

```
                SIT_counts[m3]+=1
            endif
            m4+=1
            while(timestamp[m4]<=(m3+1)*delta_t*1000)
            pulse_num=m4-1
            m3+=1
        while(m3<m2)
        variable m5, alarm, alarm_ratio
        m5=0
        alarm=0
        Do
            if (SIT_counts[m5]>=LC)
                alarm+=1
            endif
            m5+=1
        while (m5<m2)
        alarm_ratio=100*alarm/m2
        print alarm_ratio


////////////////////////// SPRT test using counts in fixed counting time ////////////////////////////////////////////////
Function SPRTF_test()
        variable fixed_t= 1          // *** in unit of s, this is the fixed counting interval for SPRT test ***//
        variable k1=10^6             // *** the number of simulated pulses ***//
        variable R0=2, R1=4.35   //***  background level and alarm level ***//
        variable LA=2.9444, LB=-2.9444    // *** two test thresholds ***//
        variable  Nmax=16                  // *** the maximum steps for the test ***//
        variable pulse_numF                // use this index to shorten the runing time
        variable k2, k3, k4                // m2 is the number of data point for sit test//
        wave timestamp                     // this wave is generated by the above function //
        k2=floor(timestamp[k1-1]/1000/fixed_t)
        make/R/D/O/N=(k2) fixed_counts=0
        k3=0
        pulse_numF=0
        Do
            k4=pulse_numF
            Do
            if (timestamp[k4]>(k3*fixed_t*1000) && timestamp[k4]<=((k3+1)*fixed_t*1000))
               fixed_counts[k3]+=1
            endif
            k4+=1
            while(timestamp[k4]<=(k3+1)*fixed_t*1000)
            pulse_numF=k4-1
            k3+=1
        while(k3<k2)
// check the number of pulses that are used for this test
        variable totalcounts=0, k5
        k5=0
        do
            totalcounts+=fixed_counts[k5]
```

```
                k5+=1
        while (k5<k2)
        print totalcounts
//ratio calculation and decision making
        variable x, zi, k6, stepn
        make/R/O/D/N=(k2) sigalarm=0, backg=0, forces=0, forceb=0
        k6=0
        zi=0
        stepn=0
        Do
                stepn+=1
                x=fixed_counts[k6]
                zi+=(LN(R1/R0))*x+(R0-R1)*fixed_t
                if (zi>= LA)
                        sigalarm[k6]=stepn
                        zi=0
                        stepn=0
                elseif (zi<=LB)
                        backg[k6]=stepn
                        zi=0
                        stepn=0
                elseif (stepn==Nmax)
                        if (zi>0)
                                forces[k6]=Nmax
                                zi=0
                                stepn=0
                        else
                                forceb[k6]=Nmax
                                zi=0
                                stepn=0
                        endif
                endif
                k6+=1
        while (k6<k2)
//decision results analyses
        variable  gg1, gg2, gg3, gg4, detp, N_alarm=0, N_clear=0, N_fs=0, N_fb=0, Totalsteps_a=0,
                Totalsteps_b=0
        variable  avgstep_a=0, avgstep_b=0, totalavg_step=0
        gg1=0
        Do
                If (sigalarm[gg1]>=1)
                        N_alarm+=1
                        Totalsteps_a+=sigalarm[gg1]
                endif
                gg1+=1
        while (gg1<k2)
        gg2=0
        Do
                If (backg[gg2]>=1)
                        N_clear+=1
```

```
                Totalsteps_b+=backg[gg2]
            endif
            gg2+=1
        while (gg2<k2)
        gg3=0
        Do
            If (forces[gg3]>=1)
                N_fs+=1
            endif
            gg3+=1
        while (gg3<k2)
        gg4=0
        Do
            If (forceb[gg4]>=1)
                N_fb +=1
            endif
            gg4+=1
        while (gg4<k2)
        avgstep_a = (totalsteps_a + N_fs*NMax)/(N_alarm + N_fs)
        avgstep_b = (totalsteps_b + N_fb*NMax)/(N_clear + N_fb)
    totalavg_step=(totalsteps_a+totalsteps_b+N_fs*NMax+N_fb*NMax)/(N_alarm+N_clear+N_fs+N_fb)
        detp= (N_alarm+N_fs)/(N_alarm+N_fs+N_clear+N_fb)*100
//statistical anlayses
        print detp, N_alarm, N_clear, N_fs, N_fb, avgstep_a, avgstep_b, totalavg_step
        make/R/O/D/N=(k2) total_Fwave=0, total_Falarm, total_Fclear
        total_Fwave=sigalarm+backg+forces+forceb
        total_Falarm=sigalarm+forces
        total_Fclear=backg+forceb
        variable total_Fdecision=N_alarm+N_clear+N_fs+N_fb
        variable total_FNalarm=N_alarm+N_fs
        variable total_FNclear=N_clear+N_fb
        make/R/O/D/N=(total_Fdecision) F_decision=0
        make/R/O/D/N=(total_FNalarm) F_Dalarm=0
        make/R/O/D/N=(total_FNclear) F_Dclear=0
        variable th5, th6
        th5=0
        th6=0
        Do
            if(total_Fwave[th5]!=0)
                F_decision[th6]=total_Fwave[th5]
                th6+=1
            endif
            th5+=1
        while (th5<k2)
        wavestats/Q F_decision
        variable F_stddev=V_SDev, F_meanT=V_avg
        print "Ftddev=", F_stddev
        print "F_meanT=", F_meanT

        variable th7, th8
```

```
	th7=0
	th8=0
	Do
		if(total_Falarm[th7]!=0)
			F_Dalarm[th8]=total_Falarm[th7]
			th8+=1
		endif
		th7+=1
	while(th7<k2)

	variable alarm_std, alarm_mean
	if (total_FNalarm<2)
		alarm_std=0
		alarm_mean=0
	else
		wavestats/q F_Dalarm
		alarm_std=V_SDev
		alarm_mean=V_avg
	endif
	print "alarm_std=", alarm_std
	print "alarm_mean=", alarm_mean
	variable th9, th10
	th9=0
	th10=0
	Do
		if(total_Fclear[th9]!=0)
			F_Dclear[th10]=total_Fclear[th9]
			th10+=1
		endif
		th9+=1
	while(th9<k2)

	variable clear_std, clear_mean
	if(total_FNclear<=1)
		clear_std=0
		clear_mean=0
	else
		wavestats/q F_Dclear
		clear_std=V_SDev
		clear_mean=V_avg
	endif
	print "clear_std=", clear_std
	print "clear_mean=", clear_mean
End


//////////////////////////SPRT using scaled time-intervals ////////////////////////////////////
Function SPRTS_test()
	variable num_pulses= 10^6		//*** num of simulated pulses ***//
	variable scale_N = 4			// *** num of scaled pulses ***//
```

```
	variable B0, B1, LLA, LLB, SNMax
	B0=2 //***  background level ***//
	B1=4.35 //***  alarm level ***//
	LLA=2.9444
	LLB=-2.9444
	SNmax=16
	variable s1, scaled_num
	scaled_num=floor(num_pulses/scale_N)
	make/R/O/D/N=(scaled_num) scaled_TI=0, S_alarm=0, S_backg=0, S_forceS=0, S_forceB=0 ,
	                          T_alarm=0, T_backg=0, T_forceS=0, T_forceB=0
	wave timestamp  // this wave is generated by the function, pulse_generate() //
	s1=0
	Do
		if (s1==0)
			scaled_TI[s1]=timestamp[(s1+1)*scale_N-1]
		else
			scaled_TI[s1]=timestamp[(s1+1)*scale_N-1]-timestamp[s1*scale_N-1]
		endif
		s1+=1
	while (s1<scaled_num)
// ratio calculation and decision making
	variable x1, zzi, Sstepn, s2, sti
	s2=0
	sti=0
	zzi=0
	Sstepn=0
	Do
		Sstepn+=1
		x1=scaled_TI[s2]
		sti+=x1 // record the the time needed to make a decision//
		zzi+=LN(B1/B0)*(scale_N-1)+(B0-B1)*x1/1000
		if (zzi>=LLA)
			S_alarm[s2]=Sstepn
			T_alarm[s2]=sti
			sti=0
			zzi=0
			Sstepn=0
		elseif (zzi<=LLB)
			S_backg[s2]=Sstepn
			T_backg[s2]=sti
			sti=0
			zzi=0
			Sstepn=0
		elseif (Sstepn==SNmax)
			if (zzi>0)
				S_forceS[s2]=SNmax
				T_forceS[s2]=sti
				sti=0
				zzi=0
				Sstepn=0
```

```
                    else
                        S_forceB[s2]=SNmax
                        T_forceB[s2]=sti
                        sti=0
                        zzi=0
                        Sstepn=0
                    endif
                endif
                s2+=1
            while(s2<scaled_num)
//Decision results analyses
            variable hh1, hh2, hh3, hh4, SN_alarm=0, SN_clear=0, SN_fs=0, SN_fb=0, STotalsteps_a=0,
                STotalsteps_b=0
            variable Savgstep_a=0, Savgstep_b=0, S_det=0, Stotalavg_step=0
            hh1=0
            Do
                If (S_alarm[hh1]>=1)
                    SN_alarm+=1
                    STotalsteps_a+=S_alarm[hh1]
                endif
                hh1+=1
            while (hh1<scaled_num)
            hh2=0
            Do
                If (S_backg[hh2]>=1)
                    SN_clear+=1
                    STotalsteps_b+=S_backg[hh2]
                endif
                hh2+=1
            while (hh2<scaled_num)
            hh3=0
            Do
                If (S_forceS[hh3]>=1)
                    SN_fs+=1
                endif
                hh3+=1
            while (hh3<scaled_num)
            hh4=0
            Do
                If (S_forceB[hh4]>=1)
                    SN_fb +=1
                endif
                hh4+=1
            while (hh4<scaled_num)
            Savgstep_a = (Stotalsteps_a + SN_fs*SNMax)/(SN_alarm + SN_fs)
            Savgstep_b = (Stotalsteps_b + SN_fb*SNMax)/(SN_clear + SN_fb)
            Stotalavg_step=(Stotalsteps_a+Stotalsteps_b+SN_fs*SNMax+SN_fb*SNMax)/(SN_alarm+SN_fs
                    +SN_clear+SN_fb)
            S_det=100*(SN_alarm+SN_fs)/(SN_alarm+SN_fs+SN_clear+SN_fb)
            print SN_alarm, SN_clear, SN_fs, SN_fb, Savgstep_a, Savgstep_b, Stotalavg_step
```

```
        print s_det
        variable ST_alarm=0, ST_backg=0, ST_forceS=0, ST_forceB=0
        variable th1, th2, th3, th4, AvgT_alarm=0, AvgT_backg=0, Stotalavg_t=0
        th1=0
        Do
                If (T_alarm[th1]!=0)
                        ST_alarm+=T_alarm[th1]
                endif
                th1+=1
        while (th1<scaled_num)
        th2=0
        Do
                If (T_backg[th2]!=0)
                         ST_backg+=T_backg[th2]
                endif
                th2+=1
        while (th2<scaled_num)
        th3=0
        Do
                If (T_forceS[th3]!=0)
                        ST_forceS+=T_forceS[th3]
                endif
                th3+=1
        while (th3<scaled_num)
        th4=0
        Do
                If (T_forceB[th4]!=0)
                        ST_forceB+=T_forceB[th4]
                endif
                th4+=1
        while (th4<scaled_num)

        AvgT_alarm= (ST_alarm+ST_forceS)/(SN_alarm+SN_fs)/1000
        Stotalavg_t=(ST_alarm+ST_forceS+ST_backg+ST_forceB)/(SN_alarm+SN_fs+SN_clear
                +SN_fb)/1000
print AvgT_alarm, AvgT_backg, Stotalavg_t
//statistics calculation
        make/R/O/D/N=(scaled_num) total_Twave=0, total_Talarm, total_Tclear
        total_Twave=T_alarm+T_backg+T_forceS+T_forceB
        total_Talarm=T_alarm+T_forceS
        total_Tclear=T_backg+T_forceB
        variable total_Tdecision=SN_alarm+SN_clear+SN_fs+SN_fb
        variable total_Dalarm=SN_alarm+SN_fs
        variable total_Dclear=SN_clear+SN_fb
        make/R/O/D/N=(total_Tdecision) T_decision=0
        make/R/O/D/N=(total_Dalarm) T_Dalarm=0
        make/R/O/D/N=(total_Dclear) T_Dclear=0
        variable th5, th6
        th5=0
        th6=0
```

```
Do
	if(total_Twave[th5]!=0)
		T_decision[th6]=total_Twave[th5]
		th6+=1
	endif
	th5+=1
while (th5<scaled_num)
wavestats/Q T_decision
variable S_stddev=V_SDev, S_meanT=V_avg
print "Stddev=", S_stddev
print "S_meanT=", S_meanT
variable th7, th8
th7=0
th8=0
Do
	if(total_Talarm[th7]!=0)
		T_Dalarm[th8]=total_Talarm[th7]
		th8+=1
	endif
	th7+=1
while(th7<scaled_num)
variable alarm_std, alarm_mean
if (total_Dalarm<2)
	alarm_std=0
	alarm_mean=0
else
	wavestats/q T_Dalarm
	alarm_std=V_SDev
	alarm_mean=V_avg
endif
print "alarm_std=", alarm_std
print "alarm_mean=", alarm_mean
variable th9, th10
th9=0
th10=0
Do
	if(total_Tclear[th9]!=0)
		T_Dclear[th10]=total_Tclear[th9]
		th10+=1
	endif
	th9+=1
while(th9<scaled_num)
variable clear_std, clear_mean
if(total_Dclear<=1)
	clear_std=0
	clear_mean=0
else
	wavestats/q T_Dclear
	clear_std=V_SDev
	clear_mean=V_avg
```

```
        endif
        print "clear_std=", clear_std
        print "clear_mean=", clear_mean
End
```

Igor Pro. Code for SPRT with Scaled Time-Intervals for Experimental Data

```
#pragma rtGlobals=1                    // Use modern global access method.
// This function is designated for SPRT analysis using simulated scaled time-intervals//
Function pulses_analysis()
      variable max_num= 209, spill_num= 120          //*** input these two value before run ***//
      variable ScaledN=4                             //***number of pulsed that are scaled***//
      variable  t_low, t_high, real_high, i, h, k, j, n, start_hi, start_mi, start_lo
// t_low, t_high, real_high are the low word, middle word and high word for the realtime of each pulse;
// start_lo, start_mi, start_hi are the low word, middle word and high word for the start time of each run for
data acquisition;
// i is the index to check the number of words in the 'BUF_NDATA' of the list mode data;
// h is used to control the inner "do... while" loop, and k is used to control the outer "do... while" loop;
// n is index for the realtime waves, timelo, timehi, realtimehi;
//j is the index of wave0, which is a temporary index that is used to transfer values for 'i'.
      wave wave0   // wave0 is data wave from the command ' GBLoadWave' function in IGOR.//
// create waves and arrays that are going to be used for obtaining the timestamp of each signal.
      make/R/O/D/N=(max_num*spill_num) timelo, timehi, realtimehi
      make/R/D/O/N=(max_num, spill_num) timestamp =0
//timestamp contains the absolute time information of each pulse that is registered.
     make/R/O/D/N=(spill_num) start_time=0  //the start point of each run//
     t_low=8
     t_high=7
     real_high=17
    start_hi=3
    start_mi=4
    start_lo=5
    i=0
    k=0
    n=0
    j=wave0(0)
   Do
  start_time[k]=(wave0[start_lo] + wave0[start_mi]*(2^16) + wave0[start_hi]*(2^32))*25/(10^6)
// run start time
  h=0

       Do
       If (wave0[i] <18)
       break
       endif
```

```
            timelo[n]=wave0[t_low]
        timehi[n]=wave0[t_high]
        realtimehi[n]=wave0[real_high]
        timestamp[h][k]=(timelo[n]+timehi[n]*(2^16)+realtimehi[n]*(2^32))*25/(10^6)   // in unit of ms
// timestamp is the array that contains the realtime information for each signal.
        t_high+=12
        t_low+=12
        real_high+=12
        n+=1
        h+=1
       while (h<(wave0[i]-6)/12)
        i=j
        t_high=j+7
        t_low=j+8
        real_high=j+17
        start_hi=j+3
        start_mi=j+4
        start_lo=j+5
        j+=wave0[i]
        k+=1
       while (k<spill_num)
       Duplicate/D/O timestamp realtime_stamp
       killwaves timestamp
// 'Duplicate' and 'killwaves' commands are used to make sure that contents in each arrays are cleared
 before a new operation.
//This part produce time-intervals of scaled pulses
       variable n1, n2
//used for do... while loops control.
      variable num_scale
      num_scale=max_num/ScaledN
      make/R/O/D/N=(num_scale, spill_num) relativetime=0, scaledTI=0
      n1=0
      Do
        n2=0
        Do
            relativetime[n2][n1]=realtime_stamp[(n2+1)*scaledN-1][n1]-start_time[n1]
             n2 +=1
        while (n2+1 <= num_scale)
     n1+=1
    while (n1<spill_num)
     variable n3, n4
     n3=0
     DO
       n4=0
       Do
          if (n4==0)
           scaledTI[n4][n3]=relativetime[n4][n3]
          else
            scaledTI[n4][n3]=relativetime[n4][n3]-relativetime[n4-1][n3]
          endif
```

```
            n4+=1
          while (n4<num_scale)
      n3+=1
      while (n3<spill_num)
     variable n5, n6, scaleindex
     make/R/O/D/N=(num_scale*spill_num) scale_selected=0
     scaleindex=0
     n5=0
     Do
       n6=0
       Do
          if (scaledTI[n6][n5]>0)
          scale_selected[scaleindex]=scaledTI[n6][n5]
          endif
          scaleindex+=1
          n6+=1
        while (n6<=num_scale-1)
       n5+=1
  while (n5<spill_num)
End
```

///////After this step, a similar programming code as that for simulated scaled time-intervals is used for experimental scaled time-intervals contained in the wave scale_selected//////

Igor Pro. Code for SPRT with a Fixed Count Time for Experimental Data

```
#pragma rtGlobals=1                    // Use modern global access method.
Function Poisson_analysis()
         variable max_num= 209, spill_num= 120  //*** input these two value before run ***//
         variable delta_t=1   //&&&&& in unit of 's', the fixed time interval, input this value &&&&&//
         variable  t_low, t_high, real_high, i, h, k, j, n, start_hi, start_mi, start_lo
// t_low, t_high, real_high are the low word, middle word and high word for the realtime of each signal;
// start_lo, start_mi, start_hi are the low word, middle word and high word for the start time of each run for data collection;
// i is the index to check the number of words in the 'BUF_NDATA' of the list mode data;
// h is used to control the inner do... while loop, and k is used to control the outer do... while loop;
// n is index for the realtime waves, timelo, timehi, realtimehi;
//j is the index of wave0, which is a temporary index this is used to transfer values for 'i'.
        wave wave0      // wave0 is data wave from the command ' GBLoadWave' function in IGOR.
// create waves and arrays that are going to be used for obtaining the relative timestamp of each signal.
        make/R/O/D/N=(max_num*spill_num) timelo, timehi, realtimehi
        make/R/D/O/N=(max_num, spill_num) timestamp, r_timestamp
//timestamp contains the absolute time information that each event is registered; r_timestamp is the time information
//relative to the start point of the corresponding run.
       make/R/O/D/N=(spill_num) start_time  //the start point of each run
       make/R/O/D/N=(spill_num) signal_num // the number of registered events for each run.
       t_low=8
```

```
      t_high=7
      real_high=17
      start_hi=3
      start_mi=4
      start_lo=5
      i=0
      k=0
      n=0
      j=wave0(0)
     Do
         start_time[k]=(wave0[start_lo] + wave0[start_mi]*(2^16) + wave0[start_hi]*(2^32))*25/(10^9)
         signal_num[k]=(wave0[i]-6)/12
         h=0
        Do
           If (wave0[i] <18)
           break
          endif
          timelo[n]=wave0[t_low]
          timehi[n]=wave0[t_high]
          realtimehi[n]=wave0[real_high]
          timestamp[h][k]=(timelo[n]+timehi[n]*(2^16)+realtimehi[n]*(2^32))*25/(10^9)
          r_timestamp[h][k]=timestamp[h][k]-start_time[k]
// time is in unit of s
// timestamp is the array that contains the realtime information for each signal;
//r_timestamp is the array that contains the relative time information to its run start time.
          t_high+=12
          t_low+=12
          real_high+=12
          n+=1
          h+=1
      while (h<(wave0[i]-6)/12)
      i=j
      t_high=j+7
      t_low=j+8
      real_high=j+17
      start_hi=j+3
      start_mi=j+4
      start_lo=j+5
      j+=wave0[i]
      k+=1
      while (k<spill_num)
      WaveStats/q signal_num
      print V_avg, V_min, V_max, V_sdev   // statistics for the number of events in a fixed time interval.
      Duplicate/D/O timestamp realtime_stamp
      Duplicate/D/O r_timestamp relativetime
      killwaves timestamp, r_timestamp

 // 'Duplicate' and 'killwaves' commands are used to make sure that contents in each arrays are cleared
 // before the next new operation
////////////// This part is used to analyze the num of signals that are observed in a fixed count time //////////
```

```
          variable n1, n2, n3, lastp, t_n2
/// used for do... while loops control, lastp is index for the last event for each run in the wave signal_num.
          wave countswave // output wave
          variable runtime=180, rownum //&&&& in unit of 's' &&&&&&&//
          rownum=runtime/delta_t + 10
         make/R/O/N=(rownum, spill_num) countswave=0
         make/R/O/N=(spill_num) deltat_num=0
        n1=0
        Do
          n2=0
          Do
            n3=0
            Do
            if (relativetime[n3][n1]>(n2*delta_t)  && relativetime[n3][n1]<=((n2+1)*delta_t))
            countswave[n2][n1] +=1
            endif
            n3+=1
           while (n3<signal_num[n1])
//controlled by the number of events for each run.
           n2 +=1
           lastp=signal_num[n1]-1
          T_n2=n2*delta_t
          while (T_n2 <= relativetime[lastp][n1])
 //controlled by the relative time of the last event for each run
       deltat_num[n1]=n2-1   /// the number of fixed time intervals for each run
       n1+=1
      while (n1<spill_num)
      Duplicate/D/O countswave, countobserve
      Killwaves countswave
      End
```

///////After this step, a similar programming code as that for simulated data is used for experimental data contained in the wave countobserve//////

R Code for Average Run Length Calculation for Bayesian Analysis with Time-Interval Data

```
#R code for Bayesian analysis. Posterior distribution is created by "rgamma" function
#This code is used for time-interval information

setwd("C:/Peng's Bayesian/Bugs tests")  #set working directory

alpha1 <- 2     #prior parameter

beta1 <- 1      #prior parameter
```

```
nnn<-10000        #number of simulation sampling from the posterior distribution

theta0 <- 2       #the background count rate
DL<-0.95          #the detection limit

timeint <- read.table("C:/Peng's Bayesian/runlength data/timeinterval-8.0cps-2.txt", head=T)
x<-timeint$timeinterval
J<-nrow(timeint)    #total number of data points

runlength<-c()
decisiontime<-c()
n1<-1          #data point index
n2<-1          # index to record the number of data points for a decision making
timetodecision<-0  #to record the time to make a decision
while (n1<=J) {
          x.r=x[n1]/1000
          timetodecision<-timetodecision+x.r
          if (n2==1) {
                    alpha2<-alpha1+1
                    beta2<-beta1+x.r

                    post.gam<-rgamma(nnn,alpha2,beta2)     #posterior calculation
                    mean.theta<-mean(post.gam)            #mean of the posterior
                    probtheta<-round(sum(post.gam>=theta0)/nnn,3)      #the probability that the posterior is
above the background
                    if (probtheta>=DL) {
                              runlength<-c(runlength,n2)
                              decisiontime<-c(decisiontime,timetodecision)
                              n2<-1
                              timetodecision<-0
                              } else {

                              n2<-n2+1
                              }
                     } else {
                     alpha2<-alpha2+1
                     beta2<-beta2+x.r
                    post.gam<-rgamma(nnn,alpha2,beta2)     #posterior calculation
                    mean.theta<-mean(post.gam)            #mean of the posterior
                    probtheta<-round(sum(post.gam>=theta0)/nnn,3)      #the probability that the posterior is
above the background
                    if (probtheta>=DL) {
                              runlength<-c(runlength,n2)
                              decisiontime<-c(decisiontime,timetodecision)
                              n2<-1
                              timetodecision<-0
                              } else {

                              n2<-n2+1
                              }
```

```
                }
        n1<-n1+1
        }


#summary of the runlength
runlength<-as.matrix(runlength)
totaldecision<-nrow(runlength)
averageRL<-mean(runlength)
RL.std<-(var(runlength))^(1/2)
totaldecision
averageRL
RL.std

#summary of the decisiontime
J
n1
n2
probtheta
decisiontime<-as.matrix(decisiontime)
totaldecision2<-nrow(decisiontime)
averageDT<-mean(decisiontime)
DT.std<-(var(decisiontime))^(1/2)
totaldecision2
averageDT
DT.std
summary(decisiontime)
```

R Code for Detection Probability Calculation for Bayesian Analysis with Time-Interval Data

```
#R code for Bayesian analysis. Posterior distribution is created by "rgamma" function
#This code is used for the detection probability of time-interval information
#The data are simulated for different conditions, bkg1+source+bkg2
setwd("C:/Peng's Bayesian/Bugs tests")  #set working directory
alpha1 <- 2          #prior parameter
beta1 <- 1           #prior parameter
nnn<-10000           #number of simulation sampling from the posterior distribution
theta0 <- 2          #the background count rate
DL<-0.95             #the detection limit
bkg1<-5         #the counting time of the background before the presence of the source
timeint <- read.table("C:/Peng's Bayesian/simulated conditions-5-5-5/simulatedtimeinterval-4.0cps-
2.txt",head=F)          #data
J1<-nrow(timeint)    #total number of sub-data sets
```

```
decmatrix<-rep(-1,J1)
tmat<-rep(0,J1)
J2<-ncol(timeint)
i1<-1 #indext for the number of sub-dat sets
while(i1<=J1) {
      x<-timeint[i1,]
      n1<-1         #data point index
      n2<-1         # index to record the number of data points for a decision making
     timetodecision<-0  #to record the time to make a decision
      probtheta<-0
          while (n1<=J2) {
          if(probtheta>=DL && timetodecision>=bkg1) break
          x.r=x[n1]/1000
          x.r=as.numeric(x.r)
          if((1000*x.r)==-100) break
          timetodecision<-timetodecision+x.r
          if (n2==1) {
                  alpha2<-alpha1+1
                  beta2<-beta1+x.r
                  post.gam<-rgamma(nnn,alpha2,beta2)    #posterior calculation
                  mean.theta<-mean(post.gam)            #mean of the posterior
                  probtheta<-round(sum(post.gam>=theta0)/nnn,3)
#the probability that the posterior is above the background
                  if (probtheta>=DL) {
                                  n2<-1
                                  } else {
                                  n2<-n2+1
                                  }
                   } else {
                   alpha2<-alpha2+1
                   beta2<-beta2+x.r
                  post.gam<-rgamma(nnn,alpha2,beta2)    #posterior calculation
                  mean.theta<-mean(post.gam)            #mean of the posterior
                  probtheta<-round(sum(post.gam>=theta0)/nnn,3)
 #the probability that the posterior is above the background
                  if (probtheta>=DL) {
                                  # runlength<-c(runlength,n2)
                                  # decisiontime<-c(decisiontime,timetodecision)
                                   n2<-1
                                  # timetodecision<-0
                                   } else {
                                   n2<-n2+1
                                   }
                           }
                          n1<-n1+1
              }
 decmatrix[i1]<-probtheta
 tmat[i1]<-timetodecision
i1<-i1+1
}
```

```
detectionpro<-(sum(decmatrix>=DL))/J1
std.dectpro<-sqrt(sum(decmatrix>=DL))/J1
print(detectionpro,digits=3)
std.dectpro
```

R Code for Average Run Length Calculation for CUSUM Analysis with Time-Interval Data

```
# CUSUM analysis of time-interval information
setwd("d:/profile.cu/My Documents/CUSUM")          #set working directory
cr_b<-2            #the mean count rate of the background
cr_d<-5            #the mean count rate that is needed to detect quickly
k<-(log(cr_d)-log(cr_b))/(cr_d-cr_b)          #the reference value, nature log function
DL<-3.32           #the detection limit wether an alarm should be issued
radti <- read.table("C:/Peng's Research/CUSUM analysis/Simulated data/runlength data/timeinterval-
10.0cps.txt",head=T)        #data
x<-radti$timeinterval
J<-nrow(radti)              #total number of data points
ci<-rep(-1,J)               #matrix to contain the cusum value for each data point
runlength<-c()              #create an maxtrix to contain rungth values
ci_value<-c()               #matrix to contain ci values
decisiontime<-c()           #matrix to contain time to make a detection
C0<-0                       #the starting ci value
n1<-1
n2<-1
timetodecision<-0
while (n1<=J) {
    x.r<-x[n1]/1000 # in unit of second (s)
    timetodecision<-timetodecision+x.r
    if (n2==1)  {
      c_sum<-k-x.r+C0
            } else {
              c_sum<-k-x.r+ci[n1-1]
                  }
     ci[n1]<-max(0,c_sum)
     if (ci[n1]>=DL) {
                runlength<-c(runlength,n2)
                ci_value<-c(ci_value, ci[n1])
                decisiontime<-c(decisiontime,timetodecision)
                n2<-1
                timetodecision<-0

                } else {
                     n2<-n2+1
                      }
  n1<-n1+1
```

```
        }
#summary of the runlength
runlength<-as.matrix(runlength)
totaldecision<-nrow(runlength)
ARL<-mean(runlength)
RL.std<-(var(runlength))^(1/2)
totaldecision
ARL
RL.std
summary(runlength)
#summary of the decisiontime
decisiontime<-as.matrix(decisiontime)
totaldecision2<-nrow(decisiontime)
averageDT<-mean(decisiontime)
DT.std<-(var(decisiontime))^(1/2)
totaldecision2
averageDT
DT.std
k
DL
cr_b
cr_d
```

R Code for Detection Probability Calculation for CUSUM Analysis with Time-Interval Data

```
# R code for CUSUM analysis to check the detection efficiency when time-interval information is used
setwd("C:/Peng's Research/CUSUM analysis/R codes")  #set working directory
cr_b<-2  #the mean count rate of the background
cr_d<-4  #the mean count rate that is needed to detect quickly
k<-(log(cr_d)-log(cr_b))/(cr_d-cr_b)   #the reference value, nature log function
DL<-2.66    #the detection limit whether an alarm should be issued
bkg1=5   #the background measurement before the presence of the source
timeint <- read.table("C:/Peng's Research/CUSUM analysis/Simulated data/simulated conditions-5-20-5/simulatedtimeinterval-5.0cps.txt",head=F) #data
J1<-nrow(timeint) #total number of sub data sets
ci_value<-rep(-1,J1)
decisiontime<-rep(0,J1)
J2<-ncol(timeint)
i1<-1 #index for the number of sub data sets
while (i1<=J1) {

    x<-timeint[i1,]
    n1<-1  # index to record the number of data points for a decision
    timetodecision<-0  # to record the time to make a decision
    C0<-0       #the starting ci value
```

```
      ci<-rep(-1,J2)
      while (n1<=J2) {
        if (ci[n1-1]>=DL && timetodecision>=bkg1) break
        x.r<-x[n1]/1000
        x.r<-as.numeric(x.r)
        if ((1000*x.r)==-100) break
        timetodecision<-timetodecision+x.r
        if (n1==1)  {
                c_sum<-k-x.r+C0
              } else {
                c_sum<-k-x.r+ci[n1-1]
                    }
       ci[n1]<-max(0,c_sum)
       n1<-n1+1
                  }
ci_value[i1]<-ci[n1-1]
if (ci_value[i1]>=DL) {
            decisiontime[i1]<-timetodecision
                  } else {
             decisiontime[i1]<--1
                        }
i1<-i1+1
             }
decisiontime<-decisiontime[decisiontime>0]
decisiontime<-as.matrix(decisiontime)
summary(decisiontime)
detectionpro<-(sum(ci_value>=DL))/J1
std.detectpro<-sqrt(sum(ci_value>=DL))/J1
print (detectionpro, digits=3)
std.detectpro
```

Appendix C

Data Relative to Experimental Results

Table C.1. Experimental detection probabilities of the three methods: SIT, SPRT_scaled and SPRT_scaled.

CR (cps)	Detection Probability (%)			
	SIT (6s)	SPRT_fixed (1s)	SPRT_scaled N=4	SPRT_scaled N=6
1.87	10.19	2.14	0.09	0.06
2.02	11.97	3.31	0.04	0.32
2.07	7.65	1.74	0.00	0.00
2.25	16.74	5.94	0.09	0.53
2.38	23.03	7.86	0.05	0.39
2.52	26.18	13.73	0.11	0.85
3.08	58.36	52.27	3.51	11.00
3.39	77.97	77.40	7.14	26.68
4.90	99.62	99.37	95.07	98.37
5.51	99.96	99.85	99.28	99.78
7.42	100.00	100.00	100.00	100.00
9.23	100.00	100.00	100.00	100.00

Table C.2. Experimental average time for SIT, SPRT_fixed and SPRT_scaled.

CR (cps)	Average Time (s)		
	SPRT_fixed (1s)	SPRT_scaled N=4	SPRT_scaled N=6
1.87	3.83	5.27	6.91
2.02	4.29	5.07	6.54
2.07	4.66	4.52	5.78
2.25	5.26	4.93	6.37
2.38	5.86	5.10	6.70
2.52	6.44	5.28	6.87
3.08	7.51	6.95	9.73
3.39	7.27	8.76	12.75
4.90	2.90	6.12	4.54
5.51	2.27	4.05	3.24
7.42	1.49	1.83	1.70
9.23	1.20	1.21	1.22

Table C.3. Experimental average run length of Bayesian analyses for radiation pulses within the 1332.5keV ROI of ^{60}Co.

CR (cps)	Average Run Length (s)		
	1.65 σ	Bayesian (cnt)	Bayesian (ti)
2.08	16.56	28657	28650
2.46	9.69	39.89	34.83
3.06	5.19	9.32	7.64
3.36	3.98	6.49	5.16
3.75	3.11	4.61	3.54
4.12	2.5	3.61	2.68
4.77	1.92	2.68	1.86
6.16	1.36	1.8	1.1
6.82	1.23	1.6	0.92
8.77	1.07	1.25	0.61
9.99	1.03	1.14	0.51

Table C.4. Experimental detection probabilities of Bayesian analyses for the scenario (5s background + 5s source + 5s background) using the radiation pulses within the 1332.5 keV ROI.

CR (cps)	Detection Probability					
	1.65 σ	std.	Bayesian (cnt)	std.	Bayesian (ti)	std.
2.08	0.266	0.007	0.0782	0.0039	0.0626	0.0035
2.46	0.419	0.009	0.139	0.0053	0.123	0.005
3.06	0.66	0.012	0.32	0.0086	0.303	0.0084
3.36	0.76	0.012	0.415	0.0091	0.394	0.0088
3.75	0.861	0.013	0.554	0.0105	0.543	0.0104
4.12	0.922	0.014	0.682	0.0117	0.671	0.0116
4.77	0.976	0.014	0.843	0.0131	0.844	0.0131
6.16	0.999	0.016	0.979	0.0156	0.975	0.0155
6.82	1	0.018	0.993	0.0178	0.992	0.0178
8.77	1	0.022	1	0.0217	1	0.0217
9.99	1	0.023	1	0.0231	1	0.0231

Table C.5. Experimental ARL ratios of CUSUM analyses for radiation pulses within the 1332.5keV ROI of ^{60}Co.

CR (cps)	ARL ratios		
	$CUSUM_{ti}$	$mrCUSUM_{ti}$ (μ_I=8cps)	Shewhart
2.10	1.00	0.86	1.20
2.50	1.00	0.90	2.80
3.10	0.98	0.93	3.50
3.40	0.96	0.91	3.70
3.80	0.94	0.90	3.20
4.10	0.93	0.88	2.80
4.80	0.91	0.84	2.00
6.20	0.86	0.74	1.30
6.80	0.84	0.69	1.10
8.80	0.79	0.58	0.89
10.00	0.76	0.51	0.85

Table C.6. Experimental ARLs of CUSUM analyses for radiation pulses within the 1332.5keV ROI of ^{60}Co.

CR (cps)	ARL (s)			
	$CUSUM_{cnt}$	$CUSUM_{ti}$	mrCUSUM	Shewhart
2.1	559.6	570.8	483.7	697.6
2.5	92.2	93.5	82.7	257.6
3.1	20.1	19.6	18.6	70.7
3.4	12.8	12.3	11.7	47.6
3.8	8.6	8.1	7.7	27.1
4.1	6.4	6.0	5.7	18.0
4.8	4.5	4.1	3.8	9.1
6.2	2.8	2.4	2.1	3.6
6.8	2.4	2.0	1.7	2.7
8.8	1.7	1.4	1.0	1.5
10.0	1.5	1.1	0.8	1.3

Table C.7. Experimental detection probabilities of CUSUM analyses for radiation pulses within the 1332.5keV ROI of ^{60}Co.

CR (cps)	Detection Probability							
	$CUSUM_{cnt}$	std.	$CUSUM_{ti}$	std.	$mrCUSUM_{ti}$ (μ_I=8cps)	std.	Shewhart	std.
2.10	0.02	0.002	0.02	0.002	0.03	0.002	0.01	0.001
2.50	0.05	0.003	0.05	0.003	0.05	0.003	0.02	0.002
3.10	0.16	0.006	0.16	0.006	0.17	0.006	0.06	0.004
3.40	0.27	0.007	0.26	0.007	0.27	0.007	0.10	0.005
3.80	0.41	0.009	0.41	0.009	0.42	0.009	0.17	0.006
4.10	0.58	0.010	0.57	0.011	0.58	0.011	0.25	0.007
4.80	0.79	0.013	0.79	0.013	0.79	0.013	0.44	0.009
6.20	0.97	0.016	0.97	0.016	0.97	0.016	0.80	0.014
6.80	0.99	0.018	0.99	0.018	0.99	0.018	0.91	0.017
8.80	1.00	0.022	1.00	0.022	1.00	0.022	1.00	0.022
10.00	1.00	0.023	1.00	0.023	1.00	0.023	1.00	0.023

Table C.8. Experimental time-interval distributions.

time-interval (ms)	Time-Interval Probability					
	2.01cps	std.	3.23cps	std.	4.47cps	std.
50	0.097	0.0010	0.144	0.0022	0.198	0.0031
100	0.101	0.0010	0.123	0.0020	0.160	0.0027
150	0.096	0.0010	0.110	0.0019	0.127	0.0024
200	0.091	0.0010	0.093	0.0017	0.102	0.0021
250	0.082	0.0009	0.081	0.0016	0.082	0.0019
300	0.071	0.0008	0.069	0.0015	0.066	0.0017
350	0.061	0.0008	0.059	0.0013	0.055	0.0015
400	0.051	0.0007	0.048	0.0012	0.043	0.0013
450	0.043	0.0006	0.042	0.0011	0.035	0.0012
500	0.037	0.0006	0.035	0.0010	0.028	0.0011
550	0.030	0.0005	0.029	0.0009	0.022	0.0009
600	0.026	0.0005	0.026	0.0009	0.018	0.0009
650	0.022	0.0005	0.023	0.0008	0.014	0.0007
700	0.019	0.0004	0.018	0.0007	0.009	0.0006
750	0.016	0.0004	0.015	0.0006	0.009	0.0006
800	0.014	0.0004	0.014	0.0006	0.006	0.0005
850	0.012	0.0003	0.011	0.0006	0.006	0.0005
900	0.011	0.0003	0.010	0.0005	0.005	0.0004
950	0.009	0.0003	0.008	0.0005	0.003	0.0004
1000	0.008	0.0003	0.005	0.0004	0.003	0.0004
1050	0.007	0.0003	0.007	0.0004	0.002	0.0003
1100	0.006	0.0002	0.004	0.0003	0.002	0.0003
1150	0.006	0.0002	0.004	0.0003	0.001	0.0002
1200	0.005	0.0002	0.004	0.0003	0.001	0.0002
1250	0.005	0.0002	0.003	0.0003	0.001	0.0002
1300	0.004	0.0002	0.002	0.0003	0.001	0.0002
1350	0.004	0.0002	0.003	0.0003	0.000	0.0001
1400	0.003	0.0002	0.002	0.0002	0.001	0.0002
1450	0.003	0.0002	0.001	0.0002	0.000	0.0001

BIBLIOGRAPHY

Apostolopoulos, G. 2008. On-line statistical processing of radiation detector pulse trains with time-varying count rates. *Nuclear Instruments & Methods in Physics Research Section A-Accelerators Spectrometers Detectors and Associated Equipment* 595, (2) (OCT): 464-73.

Arandjelovic, V., A. Koturovic, and R. Vukanovic. 2002. A software method for suppressing statistical fluctuations in preset count digital-rate meter algorithms. *IEEE Transactions on Nuclear Science* 49, (5 Part 3): 2561-6.

Attardo, A. M. 2007. Application of classical versus Bayesian statistical methods to on-line radiological monitoring. M.S., Clemson University.

Baeten, P., M. Bruggeman, R. Carchon, and W. De Boeck. 1998. Neutron multiplicity measurements on 2201 waste drums containing Pu in the range 0.1-1 g Pu-240(eff) with the time interval analysis method. *Nuclear Instruments & Methods in Physics Research Section A-Accelerators Spectrometers Detectors and Associated Equipment* 413, (2-3) (AUG): 333-40.

Bergin, M. S., and J. B. Milford. 2000. Application of Bayesian Monte Carlo analysis to a lagrangian photochemical air quality model. *Atmospheric Environment* 34, (5): 781-92.

Bochud, F. O., C. J. Bailat, and J. P. Laedermann. 2007. Bayesian statistics in radionuclide metrology: Measurement of a decaying source. *Metrologia* 44, (4) (AUG): S95-S101.

Bolstad, W. M. 2007. *Introduction to Bayesian statistics.* New Jersey: Wiley-IEEE.

Chandrikamohan, P., and T. A. DeVol. 2007. Comparison of pulse shape discrimination methods for phoswich and CsI :T1 detectors. *IEEE Transactions on Nuclear Science* 54, (2) (APR): 398-403.

Cheng, C. S., and P. W. Chen. 2010. An ARL-unbiased design of time-between-events control charts with runs rules. *Journal of Statistical Computation and Simulation* 81, (7): 857-71.

Cherry, S., M. A. Haroldson, J. Robison-Cox, and C. C. Schwartz. 2002. Estimating total human-caused mortality from reported mortality using data from radio-instrumented grizzly bears. *Ursus* 13: 175-84.

Coop, K. L. 1985. Monte-carlo simulation of the sequential probability ratio test for radiation monitoring. *IEEE Transactions on Nuclear Science* 32, (1): 934-8.

Currie, L. A. 1968. Limits for qualitative detection and quantitative determination - application to radiochemistry. *Analytical Chemistry* 40, (3): 586-93.

DeVol, T. A., A. A. Gohres, and C. L. Williams. 2009. Application of classical versus Bayesian statistical control charts to on-line radiological monitoring. *Journal of Radioanalytical and Nuclear Chemistry* 282, (3) (DEC): 933-8.

Dowdy, E. J., C. N. Henry, R. D. Hastings, and S. W. France. 1978. Neutron detector suitcase for the nuclear emergency search team. *Los Alamos Scientific Lab. Report LA*-7108.

Ellison, A. M. 1996. An introduction to Bayesian inference for ecological research and environmental decision-making. *Ecological Applications* 6, (4) (NOV): 1036-46.

Evans, R. D. 1955. *The atomic nucleus.* New York: McGraw-Hill.

Fehlau, P. E., J. C. Pratt, J. T. Markin, and T. Scurry Jr. 1983. Smarter radiation monitors for safeguards and security. Proceedings of the 24th Annual Meeting of the Institute of Nuclear Materials Management, Vail, Colorado, 1983, pp. 122-8.

Fehlau, P. E. 1993. Comparing a recursive digital-filter with the moving-average and sequential probability-ratio detection methods for snm portal monitors. *IEEE Transactions on Nuclear Science* 40, (2) (APR): 143-6.

Gelman, A. 2004. *Bayesian data analysis.* New York: CRC press.

Ghosh, B. K., and P. K. Sen. 1991. *Handbook of sequential analysis.* New York: Marcel Dekker.

Gibbons, R. D. 1999. Use of combined shewhart-CUSUM control charts for ground water monitoring applications. *Ground Water* 37, (5) (SEP-OCT): 682-91.

Groer, P. G., and Y. Lo. 1996. Measurement of airborne Po-218 - A Bayesian approach. *Health Physics* 71, (6) (DEC): 951-5.

Gross, K. C., and K. E. Humenik. 1991. Sequential probability ratio test for nuclear-plant component surveillance. *Nuclear Technology* 93, (2) (FEB): 131-7.

Holdbrook, F. K. A. 2001. Modified cumulative sum procedures for count data with application to early detection of morbidity in radio frequency-monitored animals. Bozeman (MT): Montana State University.

Hughes, L. D., and T. A. DeVol. 2008. Evaluation of statistical control charts for on-line radiation monitoring. *Journal of Radioanalytical and Nuclear Chemistry* 277, (1): 227-34.

Humenik, K., and K. C. Gross. 1990. Sequential probability ratio tests for reactor signal validation and sensor surveillance applications. *Nuclear Science and Engineering* 105, (4) (AUG): 383-90.

ICRU report 52. 1994. *Particle counting in radioactivity measurements.*

Jarman, K. D., L. E. Smith, and D. K. Carlson. 2004. Sequential probability ratio test for long-term radiation monitoring. *IEEE Transactions on Nuclear Science* 51, (4) (AUG): 1662-6.

Kaeker, R., and A. Jones. 2003. On use of Bayesian statistics to make the guide to the expression of uncertainty in measurement consistent. *Metrologia* 40, (5): 235-48.

Kenett, R., and S. Zacks. 1998. *Modern industrial statistics: Design and control of quality and reliability.* California: Duxbury Press.

Kenett, R. S., and M. Pollak. 1996. Data-analytic aspects of the shiryayev-roberts control chart: Surveillance of a non-homogeneous poisson process. *Journal of Applied Statistics* 23, (1): 125-38.

Knoll, G. F. 2010. *Radiation detection and measurement*. 4th ed. New Jersey: John Wiley & Sons Inc.

Laedermann, J. P., J. F. Valley, and F. O. Bochud. 2005. Measurement of radioactive samples: Application of the Bayesian statistical decision theory. *Metrologia* 42, (5) (OCT): 442-8.

Lee, Hung-Ho. 2004. Bayesian theory based probability estimation for model predictive monitoring. M.S., University of South Alabama.

Little, R. J. A. 1982. The statistical-analysis of low-level radioactivity in the presence of background counts. *Health Physics* 43, (5): 693-703.

Liu, J. Y, M. Xie, TN Goh, and PR Sharma. 2006. A comparative study of exponential time between events charts. *Quality Technology & Quantitative Management* 3, (3): 347-59.

Lucas, J. M. 1985. Counted data cusums. *Technometrics* 27, (2): 129-44.

Lucas, J. M., and R. B. Crosier. 1982a. Fast initial response for cusum quality-control schemes - give your cusum a head-start. *Technometrics* 24, (3): 199-205.

———. 1982b. Robust cusum - a robustness study for cusum quality-control schemes. *Communications in Statistics Part A-Theory and Methods* 11, (23): 2669-87.

Luo, P., T. A. DeVol, and J. L. Sharp. 2010. Sequential probability ratio test using scaled time-intervals for environmental radiation monitoring. *IEEE Transactions on Nuclear Science* 57, (3): 1556-62.

Luo, P., J. L. Sharp, and T. A. DeVol. 2011. Bayesian analysis of time-interval data for environmental radiation monitoring. *IEEE transactions on Nuclear Science*, under review.

Malakoff, D. 1999. Bayes offers a 'new' way to make sense of numbers. *Science* 286, (5444) (NOV): 1460-4.

Manly, B. F. J., and D. MacKenzie. 2000. A cumulative sum type of method for environmental monitoring. *Environmetrics* 11, (2) (MAR-APR): 151-66.

Marshall, R. A. G. 1977. Cumulative sum charts for monitoring of radioactivity background count rates. *Analytical Chemistry* 49, (14): 2193-6.

Miller, G., W. C. Inkret, T. T. Little, H. F. Martz, and M. E. Schillaci. 2001. Bayesian prior probability distributions for internal dosimetry. *Radiation Protection Dosimetry* 94, (4): 347-52.

Miller, G., W. C. Inkret, and H. F. Martz. 1993. Bayesian detection analysis for radiation exposure. *Radiation Protection Dosimetry* 48, (3): 251-6.

Miller, G., H. F. Martz, T. T. Little, and R. Guilmette. 2002. Using exact poisson likelihood functions in Bayesian interpretation of counting measurements. *Health Physics* 83, (4) (OCT): 512-8.

Montgomery, D. C. 2001. *Introduction to statistical quality control.* New York: John Wiley & Sons.

Morelande, M. R., and B. Ristic. 2009. Radiological source detection and localization using Bayesian techniques. *IEEE Transactions on Signal Processing* 57, (11) (NOV): 4220-31.

Moshirpour, A. A. 1997. A general statistical approach to engineering problem solving. Morgantown (WV): West Virginia University.

Page, E. S. 1954. Continuous inspection schemes. *Biometrika* 41, (1-2): 100-15.

Palmisano, A., and T. Hazen. 2003. *Bioremediation of metals and radionuclides: What it is and how it works (2nd edition).* LBNL-42595.

Panofsky, W. K. H. 2003. Nuclear proliferation risks, new and old. *Issues in Science and Technology* 19, (4): 73-4.

Pomme, S. 1999. Time-interval distributions and counting statistics with a non-paralysable spectrometer. *Nuclear Instruments & Methods in Physics Research Section A-Accelerators Spectrometers Detectors and Associated Equipment* 437, (2-3) (NOV): 481-9.

R Development Core Team. 2010. The R project for statistical computing. http://www.r-project.org/.

Sakaue, H., H. Fujimaki, S. Tonouchi, S. Itou, and T. Hashimoto. 2007. A new time interval analysis system for the on-line monitoring of artificial radionuclides in airborne dust using a phosfitch type alpha/beta detector. *Journal of Radioanalytical and Nuclear Chemistry* 274, (3): 449-54.

Skulski, W., and M. Momayezi. 2001. Particle identification in CsI(tl) using digital pulse shape analysis. *Nuclear Instruments & Methods in Physics Research Section A-Accelerators Spectrometers Detectors and Associated Equipment* 458, (3) (FEB): 759-71.

Strom, D. J. 1998. False alarms, true alarms, and statistics: Correct usage of decision level and minimum detectable amount. *Health Physics Society, Continuing Education Lecture, Minneapolis, Minnesota*.

Strom, D. J., and J. A. MacLellan. 2001. Evaluation of eight decision rules for low-level radioactivity counting. *Health Physics* 81, (1) (JUL): 27-34.

U.S. Department of Energy. January 1997. *Linking legacies.* DOE/EM-0319. http://www.em.doe.gov/Publications/linklegacy.aspx

———. 2004. *Transport of contaminants in subsurface environments at DOE sites.* DE-FG01-05ER05-12.

———. 2000. *Research needs in subsurface science.* ISBN: 0-309-51437-1. http://www.nap.edu/catalog/9793.html.

Vardeman, S., and D. Ray. 1985. Average run lengths for CUSUM schemes when observations are exponentially distributed. *Technometrics* 27, (2): 145-50.

Wald, A. 1952. *Sequential analysis.* New York: John Wiley & Sons.

Walpole, R. E., and R. H. Myers. 1997. *Probability & statistics for engineers & scientists*. 6th ed. Prentice Hall College Div.

Weise, K., K. Huebel, E. Rose, M. Schlaeger, D. Schrammel, M. Taeschner, and R. Michel. 2006. Bayesian decision threshold, detection limit and confidence limits in ionizing-radiation measurement. *Radiation Protection Dosimetry* 121, (1) (DEC): 52-63.

XIA. 2004. *User's manual digital gamma finder (DGF) DGF-4C*. Newark, CA: X-Ray Instrumentation Associates.

Xie, Y. J., K. L. Tsui, M. Xie, and T. N. Goh. 2010. Monitoring time-between-events for health management. Paper presented at Prognostics and Health Management Conference, PHM'10.

York, R. L., and P. E. Fehlau. 1997. *1997 update for the applications guide to vehicle SNM monitors.* LA-13247-MS.

Young, A., and M. MacDonell. 1999. Facing the environmental risk issues of the cold war legacy. *Environmental Science and Pollution Research* 6, (4): 186-7.

Yuan, D., and W. Kernan. 2006. Sequential probability ratio test (SPRT) for dynamic radiation level Determination–Preliminary assessment. *Computational Science–ICCS 2006*: 179-87.